

**THE ROLE OF MDM2 IN MOUSE DEVELOPMENT AND ITS  
IMPLICATION IN THE PATHOGENESIS OF CANCER AND  
DEVELOPMENTAL DISEASES**

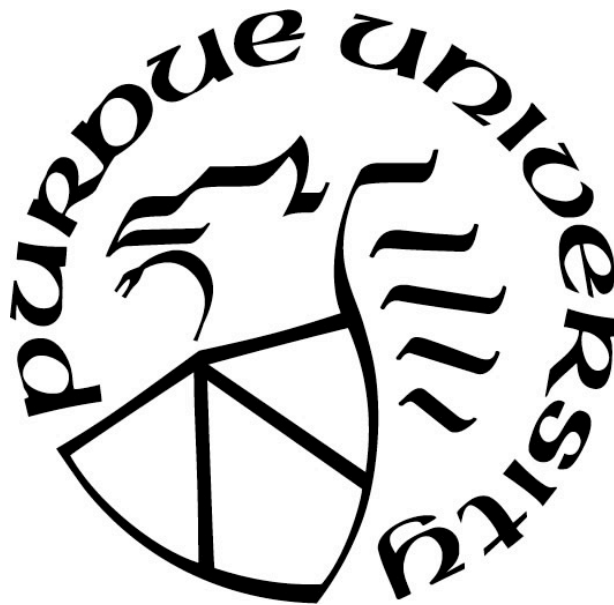
by  
**Joselyn Cruz Cruz**

**A Dissertation**

*Submitted to the Faculty of Purdue University*

*In Partial Fulfillment of the Requirements for the degree of*

**Doctor of Philosophy**



Basic Medical Sciences, Purdue University College of Veterinary Medicine  
West Lafayette, Indiana

May 2019

**THE PURDUE UNIVERSITY GRADUATE SCHOOL**  
**STATEMENT OF COMMITTEE APPROVAL**

Dr. Susan M. Mendrysa

Department of Basic Medical Sciences

Dr. Jer-Yen Yang

Department of Basic Medical Sciences

Dr. R. Claudio Aguilar

Department of Biological Sciences

Dr. Andrea Kasinski

Department of Biological Sciences

**Approved by:**

Dr. Jason R. Cannon

Head of the Graduate Program

*I would like to dedicate this dissertation to my older sister Madeline Ubiles Cruz. She lost her battle to cancer when she was only 29 years old. Because of her, I decided to study biology and do research in cancer. I still remember my last conversation with her in the hospital. She told me I was the role model of my family. Now, it is my goal to serve as a role model to all first-generation students with similar backgrounds as myself.*

*“Success is going from failure to failure without loss of enthusiasm”*

*- Winston Churchill*

## ACKNOWLEDGMENTS

I would like to thank my advisor Dr. Susan M. Mendrysa for giving me the opportunity to join her lab back in June 2014. She taught me how to think and work independently as a scientist. Thanks to her mentorship and guidance I was able to obtain multiple fellowships and awards which have opened many doors in my career.

I am also very grateful for the lab mates that at some point shared with me and helped me in the lab. Special thanks to Dr. Erin Wissing, a former postdoc in my lab that taught me how to work with mice. I will always be thankful to Stasa Tumpa and Benjamin R. Fields, two of my mentees that helped me greatly in my research projects.

My sincere thanks to my committee members: Dr. R. Claudio Aguilar, Dr. Andrea Kasinski, and Dr. Jer-Yen Yang for their constructive advice in every committee reunion.

Last but not least, I would like to thank my mom, Wanda T. Cruz Torres, for always being there supporting me. She always made me know that I had the necessary potential to complete my doctorate degree. Thank you, mom!

## TABLE OF CONTENTS

LIST OF TABLES .....	7
LIST OF FIGURES .....	8
LIST OF ABBREVIATIONS.....	12
ABSTRACT.....	15
CHAPTER 1: INTRODUCTION .....	1
1.1 The p53 Tumor Suppressor .....	1
1.1.1 Discovery of p53 .....	1
1.1.2 Structure and functional domains of p53 protein .....	2
1.1.3 Mutations in p53 .....	3
1.1.4 The role of p53 in cell cycle arrest and apoptosis .....	3
1.1.5 p53 in cell differentiation .....	8
1.1.6 Regulation of p53 .....	10
1.2 Mdm2: the main negative regulator of p53 .....	12
1.2.1 Regulation of Mdm2 .....	13
1.2.2 Mdm2 amplification and overexpression in cancer .....	14
1.2.3 Small molecules to inhibit Mdm2-p53 interaction.....	16
1.2.4 Mouse Models to study Mdm2-p53 pathway.....	17
1.3 The Rationale of this Study .....	19
CHAPTER 2: MATERIALS AND METHODS .....	21
2.1 Animal husbandry .....	21
2.2 Mouse strains.....	21
2.3 Mouse genotyping .....	21
2.4 Tamoxifen preparation, delivery and cerebellum dissection.....	22
2.5 Timed Matings.....	22
2.6 Embryo collection, processing and cryosectioning .....	22
2.7 Phenotype scoring .....	23
2.8 Haematoxylin and Eosin staining.....	23
2.9 TUNEL staining .....	23
2.10 Alcian and Alizarin staining in whole-mount mouse skeletons .....	24
2.11 RNA Isolation, cDNA preparation and real-time PCR .....	25
2.12 Protein Isolation.....	26

2.13 Western Blot.....	27
2.14 Statistical methods.....	27
CHAPTER 3: THE ROLE OF MDM2 IN GRANULE NEURON PRECURSOR CELLS	
DURING POSTNATAL CEREBELLAR DEVELOPMENT .....	
3.1 Cerebellum: function and development.....	28
3.2 Medulloblastoma .....	29
3.2.1 Wnt subtype .....	30
3.2.2 Shh subtype .....	31
3.2.3 Group 3 subtype .....	32
3.2.4 Group 4 subtype .....	32
3.3 p53-Mdm2 pathway in Medulloblastoma.....	33
3.4 Mouse model to study the effect of Mdm2 inhibition on GNPs of the cerebellum .....	35
3.5 <i>Mdm2</i> recombination is detected in <i>Mdm2<sup>lox/lox</sup>; Cre (+)</i> mice injected with tamoxifen at P0/P1 or P1/P2.....	36
3.6 Deletion of <i>Mdm2</i> in GNPs decreased cerebellar size and disrupted lobules morphology.	38
3.7 Deletion of <i>Mdm2</i> did not significantly increase apoptosis of GNPs in the External Granule Layer of mice.....	43
3.8 Loss of function of Mdm2 in GNPs does not affect mice behavior .....	43
3.9 Discussion.....	44
CHAPTER 4: THE ROLE OF MDM2 IN CRANIOFACIAL DEVELOPMENT .....	
4.1 Craniofacial development.....	47
4.1.1 The contribution of neural crest cells (NCCs) in embryo development .....	48
4.2 The role of p53 in craniofacial malformations .....	49
4.2.1 Congenital syndromes that exhibit heightened activation of p53 .....	50
4.3 Mouse model to study activation of wild-type p53 during development .....	53
4.4 Perinatal lethality of C57BL/6 <i>Mdm2</i> hypomorphic embryos .....	54
4.5 Loss of Mdm2 results in craniofacial malformations in C57BL/6 mice .....	55
4.6 Bone ossification is decreased in <i>Mdm2</i> hypomorphic embryos .....	56
4.7 Palate development is delayed due to low levels of Mdm2 .....	59
4.8 Abnormal eye development due to low levels of Mdm2 .....	61
4.9 p53 targets gene expression is increased in embryos expressing a low level of Mdm2.....	63
4.10 Discussion.....	66
REFERENCES .....	70
VITA.....	90

## LIST OF TABLES

Table 1.1 Genetic background and phenotypes of selected <i>Mdm2</i> mouse models.....	19
Table 2.1 Primers used to genotype mice .....	22
Table 2.2 Primers used for real-time PCR .....	26
Table 2.3 Antibodies used for Western Blot.....	27
Table 3.1 The four main Medulloblastoma subtypes.....	33
Table 4.1 Activation of p53 is involved in the pathology of a variety of congenital syndromes .....	53
Table 4.2 Expected and observed genotype of offspring from C57BL/6 <i>Mdm2</i> <sup><i>purol</i>/+</sup> and <i>Mdm2</i> <sup>+/<math>\Delta</math>7-9</sup> intercrosses at different embryonic days .....	55
Table 4.3 Incidence of phenotypes observed in embryos dissected at E15.5 .....	56
Table 4.4 Summary of percentage of the long bone ossification.....	58
Table 4.5 Phenotypes shared among CHARGE syndrome patients and mouse models	66

## LIST OF FIGURES

**Figure 1.1 Schematic of p53 protein functional domains.** The p53 N-terminus contains 2 domains: TAD1 and TAD2, important for its transactivation activity as a transcription factor. In addition, p53 N-terminus has a proline rich region. At the center of the protein there is a DNA Binding Domain (DBD) that allows p53 to bind to specific DNA sequences and which is commonly mutated in cancer. At the C-terminus, a Nuclear Localization Signal (NLS), a Tetramerization (TET) domain, and a basic domain that are important for p53 localization, ability to form a homotetramer, and regulation, respectively. ....2

**Figure 1.2 The role of p53 in the cell cycle during cellular stress.** p53 is involved in the transcription of genes that can stop the cell cycle in stressed cells at Growth Phase I (G1) or Growth Phase 2 (G2). The p53-mediated transcription of p21<sup>WAF1/CIP1</sup> stop the cell cycle at G1. In addition, p53 has been reported to repress the expression of *c-Myc* by recruiting histone deacetylases to *c-Myc* promoter and silencing *c-Myc*. During G2 checkpoint, p53 induces the genes *YWHAS* and *Gadd45*. ....5

**Figure 1.3 The role of p53 in the extrinsic and intrinsic apoptotic pathways.** The protein p53 regulates both the intrinsic and extrinsic apoptotic pathways. In the extrinsic apoptosis pathway, p53 increases the expression of the death receptor genes *Fas*, *Dr5* and *Perp*. In addition, cytosolic p53 increases Fas trafficking from the golgi apparatus to the plasma membrane sensitizing the cell to incoming apoptotic signals. The activation of death receptors results in the activation of caspase 8 and the cleavages of caspases 3, 6 and 7 resulting in apoptosis. In the intrinsic apoptosis pathway, p53 induces the transcription of pro-apoptotic genes *Bax*, *Puma*, and *Noxa*. The pro-apoptotic protein Puma helps Bax to translocate to the mitochondria outer membrane where Bax forms pores releasing the cytochrome C (Cyt-C) to the cytosol. Additionally, Puma, Noxa and cytosolic p53 inhibit anti-apoptotic proteins Bcl-2, Bcl-Xl, and Mcl-1. The cytosolic Cyt-C binds to Apaf-1 and pro-caspase 9 to form the apoptosome that initiates the cleavage of caspases 3, 6, and 7 causing apoptosis. ....7

**Figure 1.4 Schematic of Mdm2 protein functional domains.** The Mdm2 N-terminus contains the p53 binding domain followed by a nuclear localization signal (NLS) and nuclear export signal (NES) domains that control Mdm2 transport to and from the nucleus. The central acidic and Zn domains of Mdm2 are important for the regulation of Mdm2 by the binding of other factors, including many ribosomal proteins. A RING domain contains the E3 ubiquitin ligase activity is localized at the C-terminus of Mdm2.12

**Figure 1.5 p53 – Mdm2 negative feedback loop.** The tumor suppressor p53 is a transcription factor that regulates expression of genes involve in cell cycle arrest, apoptosis, differentiation and/or senescence when cells are under stress conditions. In addition, p53 activates the transcription of its main negative regulator *Mdm2*, creating an autoregulatory feedback loop. Mdm2 is an ubiquitin ligase that negatively regulates p53 by targeting it for proteasomal degradation or blocking its transcriptional activity. ....13

**Figure 3.1 Schematic representation of postnatal cerebellar development in mice. A)** Shh mitogen released from Purkinje cells induces GNPs proliferation in the External Granule Layer (EGL). Following expansion of the EGL, GNPs differentiate and migrate through the Purkinje Cell Layer (PCL) to make the Granule Layer (GL). The mature cerebellum consists of three layers: Molecular Layer (ML), PCL and GL. Picture taken and modified from Marzban et al., *Frontiers in Cellular Neuroscience*, 2015. **B)** The gross anatomy of the cerebellum consists of 4 lobes: anterior, central, posterior and nodular; each containing folds called lobules (I to X). The lobularization or foliation pattern is tightly controlled during cerebellar development by Shh signaling and GNP expansion in the EGL. Figure taken from White & Sillitoe, *Developmental Biology*, 2013. ....29

**Figure 3.2  $Mdm2^{flox/flox}$  and  $Math1-CreER^{TM}$  mouse models used to spatiotemporally knockdown  $Mdm2$  in postnatal GNPs. A)** Schematic representation of the  $Mdm2^{flox}$  allele.  $Mdm2$  loxP sites flanking exons 7 and 9 are recombined by tamoxifen-activated  $CreER^{TM}$  recombinase to generate a  $Mdm2^{\Delta7-9}$  null allele. **B)** The expression of  $CreER^{TM}$  is controlled by the  $Math1$  promoter, which is activated in postnatal proliferating GNPs.36

**Figure 3.3  $Mdm2$  recombination in  $Mdm2^{flox/flox}$ ;  $Cre (+)$  mice injected with tamoxifen.** Mice from lanes #1 through #4 were injected with tamoxifen (lanes #1 and #3 at P0/P1; lanes #2 and #4 at P1/P2). All these mice were euthanized at P6 and cerebellar DNA isolated for PCR.  $Mdm2^{flox/flox}$ ;  $Cre (+)$  (lanes #3 and #4) have bands for  $Mdm2^{flox/flox}$ ,  $Mdm2^{\Delta7-9}$  alleles, and  $CreER^{TM}$  alleles. In contrasts,  $Mdm2^{flox/flox}$ ;  $Cre (-)$  (lanes #1 and #2) only have bands for  $Mdm2^{flox/flox}$  alleles. ....37

**Figure 3.4 Decreased cerebellar size and disrupted morphology of anterior cerebellar lobules in  $Mdm2^{flox/flox}$ ;  $Cre (+)$  cerebellum due to tamoxifen activated  $Cre$  recombination of  $Mdm2$  at P0/P1. A)** H&E stained sections taken at 4X show that  $Mdm2$  deletion results in small cerebellum and disrupted morphology of anterior lobules II and III. B) H&E stained sections of lobule II EGL at 40X showing thinner EGL due to  $Mdm2$  deletion. ....39

**Figure 3.5  $Mdm2^{flox/flox}$ ;  $Cre (+)$  mice injected at P1/P2 have smaller cerebella and disrupted morphology of anterior lobules II and III. A)** H&E stained sections at 4X show small cerebellum and abnormal morphology of anterior lobules II and III in  $Mdm2^{flox/flox}$ ;  $Cre (+)$ . B) H&E stained sections of lobule II at 40X shows thinner EGL in  $Mdm2^{flox/flox}$ ;  $Cre (+)$ . ....40

**Figure 3.6 Cerebellar area is significant smaller in  $Mdm2^{flox/flox}$ ;  $Cre (+)$  mice injected with tamoxifen at P0/P1. A)** Average cerebellar area of P0/P1  $Mdm2^{flox/flox}$ ;  $Cre (-)$  (n=7) and  $Mdm2^{flox/flox}$ ;  $Cre (+)$  (n=9) tamoxifen-injected mice. \*  $p < 0.05$  **B)** Average cerebellar area of P1/P2  $Mdm2^{flox/flox}$ ;  $Cre (-)$  (n=4) and  $Mdm2^{flox/flox}$ ;  $Cre (+)$  (n=4) tamoxifen-injected mice. ns = not significant,  $p = 0.92$ . ....41

**Figure 3.7 EGL thickness is not significantly reduced in mice after acute deletion of  $Mdm2$ .** The thickness of first lobule was measured in mice with and without  $Mdm2$  deletion in GNPs. The results show there is no significant reduction in the thickness of EGL in  $Mdm2^{flox/flox}$ ;  $Cre (+)$  compared to  $Mdm2^{flox/flox}$ ;  $Cre (-)$  ns = not significant,  $p = 0.73$ . ....41

**Figure 3.8 Deletion of Mdm2 in GNP's disrupts the morphology of anterior cerebellar lobules of three-week-old Mdm2<sup>flx/flx</sup>; Cre (+) mice.** A) Smaller anterior lobules II and III of three-week-old Mdm2<sup>flx/flx</sup>; Cre (+) mice that had been injected with tamoxifen at P0/P1 B) Mdm2<sup>flx/flx</sup>; Cre (+) mice injected with tamoxifen at P1/P2 have smaller anterior cerebellar lobules. ....42

**Figure 3.9 Deletion of Mdm2 in GNP's does not increase GNP's apoptosis in the EGL.** A) TUNEL stained sections of lobule II at 40X of mice injected with tamoxifen at P0/P1. TUNEL positive or apoptotic cells (brown nuclei) are indicated with black arrows. B) Percentage of apoptotic area in the cerebellar EGL of Mdm2<sup>flx/flx</sup>; Cre (-) (n=3) and Mdm2<sup>flx/flx</sup>; Cre (+) (n=3) mice. ns, p = 0.49 .....43

**Figure 4.1 Similarities between murine and human craniofacial development.** A) Human craniofacial development from 4 to 10 weeks. B) Murine craniofacial development from embryonic days 9.5 to 14.5. (Figure taken and modified from Suzuki et al., 2015.) .....48

**Figure 4.2 Schematic of Mdm2 hypomorphic and null alleles.** (A) The Mdm2<sup>puro</sup> hypomorphic allele was created by insertion of a puromycin resistance cassette (PURO) after exon 6. LoxP sites are present flanking the puromycin resistance cassette and after exon 9. Cre-mediated recombination deleted the puromycin resistance cassette resulting in the generation of the Mdm2<sup>Δ7-9</sup> null allele (Mendrysa et al., 2003).....54

**Figure 4.3 C57BL/6 inbred mice hypomorphic for Mdm2 exhibit craniofacial malformations.** In contrast to wild-type controls (A), E15.5 Mdm2<sup>puro/Δ7-9</sup> embryos (B, C) show an array of craniofacial deformations including squared faces, tongue protrusion, coloboma (black arrows), and exencephaly (yellow arrow).....56

**Figure 4.4 Small size of embryos expressing a low level of Mdm2.** The crown to rump length measurement of E15.5 embryos were taken with an electronic caliper after embryo dissection and before processing tissues for histology. The results show a significant reduction in length of Mdm2<sup>puro/Δ7-9</sup> (n=5) as compared wild-type (n=11) embryos (\*p<0.05).....57

**Figure 4.5 Loss of Mdm2 impairs bone ossification.** Alcian and Alizarin staining was performed on wild-type (A-C) and Mdm2<sup>puro/Δ7-9</sup> (D-F) embryos at E17.5 to detect bone and cartilage formation. Examination of the whole skeleton shows decreases in bone ossification in Mdm2<sup>puro/Δ7-9</sup> embryo (D) compared with their wild-type counterpart (A). Higher magnification of Mdm2<sup>puro/Δ7-9</sup> embryo in (A) show delayed ossification of parietal and frontal bone (B versus E) and vertebrae (C versus F) as shown as lack of alizarin staining. Black arrows in (B) and (E) pointed to parietal and frontal bones. Yellow arrows in (C) and (F) pointed to ossification centers in the vertebrae. Embryos were stained by Stasa Tumpa and photographed by JCC and Stasa Tumpa.....58

**Figure 4.6 Decreased ossification in Mdm2<sup>puro/Δ7-9</sup> embryos.** Graphed is the percentage of bone ossification in long bones of wild-type (n=5) and Mdm2<sup>puro/Δ7-9</sup> (n=5) embryos at E17. Quantification was performed using ImageJ software. Ossification in Mdm2<sup>puro/Δ7-9</sup> embryos is significantly decreased as compared with wild-type controls (\*p<0.05).....59

- Figure 4.7 Delayed palatal fusion due to low levels of Mdm2.** **A-I)** H&E staining on coronal palate of E15.5 wild-type embryos (A-C, n=9) and *Mdm2*<sup>puro/ $\Delta$ 7-9</sup> (D-I, n=8) and. Black arrows point to MEE structure in pictures D through H. Red arrow points to cleft palate in picture I. Pictures were taken at 10X. Scale bar 20  $\mu$ m. **J-K)** TUNEL staining slides on coronal palate of E15.5 wild-type (J, n=4) and *Mdm2*<sup>puro/ $\Delta$ 7-9</sup> (K, n=5) palates. Pictures were taken at 40X. Scale bar 50  $\mu$ m. ....60
- Figure 4.8 Mice deficient for Mdm2 exhibit microphthalmia, coloboma and increased apoptosis in the retina.** **A-C)** H&E staining in coronal eye of Wild-type (n=3) and *Mdm2* hypomorphic (n=6) embryos. Black arrows (B and C) point to the retina and red arrow (C) points to a rupture in the retina. **D-E)** TUNEL staining in coronal eye of Wild-type (n=4) and *Mdm2* hypomorphic (n=6) embryos. **F)** Quantification of eye area of 3 Wild-type and 6 *Mdm2* hypomorphic eyes. \*p<0.05. ....62
- Figure 4.9 Increased levels of Mdm2 in *Mdm2*<sup>puro/ $\Delta$ 7-9</sup> embryos.** **A)** WB analysis of p53 levels in E10.5 embryos of indicated genotype and genetic background.  $\beta$ -Actin was used as a loading control. **B)** Densitometry analysis of two independent WB using  $\beta$ -Actin as a loading control. ns=not significance. ....63
- Figure 4.10 p53 signaling is increased in B6 and F1 embryos expressing low levels of Mdm2.** Expression of p53 target genes *p21*, *Bax*, *CyclinG1*, *Noxa*, and *Perp* and Shh target gene *Gli1* in whole E10.5 embryos was determined by real-time PCR and normalized to *Tubb5*. Graphed is the average fold change in gene expression of p53- and Shh-target genes on the indicated mouse genetic background (B6 = C57BL/6; F1= 129S6/C57BL/6 F1) and *Mdm2*<sup>puro/ $\Delta$ 7-9</sup> relative to *Mdm2*<sup>+/+</sup> controls (n = 6, \*p<0.05, ANOVA, \*\* p<0.05, ANOVA with Tukey Test). ....65

## LIST OF ABBREVIATIONS

ANOVA	Analysis of Variance
APC	Adenomatous polyposis coli
C	Celsius
CBP	Creb-binding protein
CDKs	Cyclin Dependent Kinases
CHARGE	<b>C</b> oloboma, <b>H</b> earth, <b>A</b> tresia choanae, growth <b>R</b> etardation, <b>G</b> enital and <b>E</b> ar abnormalities
CHD	Congenital Heart Defect
CNC	Cranial Neural Crest cells
CNS	Central Nervous System
CreER	Tamoxifen-dependent Cre recombinase
CT	Computed Tomography
DBA	Diamond-Blackfan Anemia
DEPC	Diethyl pyrocarbonate
DGS	DiGeorge Syndrome
DNA	Deoxyribose Nucleic Acid
E	Embryonic day
EDTA	Ethylenediaminetetraacetic acid
EGL	External Granule Layer
g	gravitational force relative to centrifugal force
GNPs	Granule Neuron Precursor cells
H&E	Haematoxylin and Eosin
HCl	Hydrogen chloride
IGL	Internal Granule Layer
IR	Irradiation
KOH	Potassium Hydroxide
LSA	Life Sciences Animal building
MB	Medulloblastoma
Mdm2	Mouse Double Minute 2

MEE	Medial Edge Epithelia
MES	Midline Epithelial Seam
μl	microliter
μm	micrometer
ml	milliliter
mM	milimolar
mg/ml	milligram per milliliter
ML	Molecular Layer
MRI	Magnetic Resonance Imaging
NaCl	Sodium Chloride
NCC	Neural Crest Cells
NCP	Neurocristopathies
OCT	Optimal Cutting Temperature compound
OFT	Outflow Tract
P	Postnatal day
PACUC	Purdue University Animal Case and Use Committee
PCR	Polymerase Chain Reaction
PCNA	Poliferating Cell Nuclear Antigen
PET	Positron Emission Tomography
PCL	Purkinje Cell Layer
PRR	Proline-rich-region
Ptch	Patched
RB	Retinoblastoma
RING	Really Interesting New Gene Domain
RIPA	Radioimmunoprecipitation assay buffer
RNA	Ribonuclei Acid
rRNA	ribosomal Ribonuclei Acid
SDS	Sodium Dodecyl Sulphate
SHF	Second Heart Field
Shh	Sonic Hedgehog
shRNA	short hair Ribonuclei Acid

Smo	Smoothened
Sufu	Suppressor of fused homolog
TAD	Transactivation Domain
Tbx1	T-box transcription factor 1
TUNEL	Terminal deoxynucleotidyl transferase dUTP nick end labeling
UBF	Upstream Binding Factor
UV	Ultraviolet
WB	Western Blot
Wnt	Wingless
WHO	World Health Organization

## ABSTRACT

Author: Cruz Cruz, Joselyn. PhD

Institution: Purdue University

Degree Received: May 2019

Title: The Role of Mdm2 in Mouse Development and its Implication in the Pathogenesis of Cancer and Congenital Syndromes.

Committee Chair: Susan M. Mendrysa

The tumor suppressor protein p53, encoded by *Tp53* gene, is a transcription factor that regulates cell cycle arrest and apoptosis following cellular stresses that compromise DNA integrity and normal cellular function. *Tp53* is mutated in approximately 50% of human cancers, thereby allowing cancer cells to replicate uncontrollably. In cancers in which *Tp53* is not mutated, p53 is frequently functionally inactivated through other mechanisms. For example, Mdm2, a proximal negative regulator p53 is often overexpressed in cancers in which *p53* is wild-type. Mdm2 is E3 ubiquitin ligase that binds to and targets p53 for proteasomal degradation and as well as inhibits p53 transcriptional activity. Pharmacological disruption of the Mdm2-p53 interaction in cancer cells with wild-type *p53* is currently being explored as a strategy to enhance p53-mediated cell death in response to conventional chemotherapeutics. Nutlin-3, an Mdm2 inhibitor, promotes cell death in cultured cells from human medulloblastoma (MB), a common cerebellar pediatric cancer, suggesting that Mdm2 is a promising target to treat this tumor type. Consistent with this idea, studies in a mouse model of MB have shown that loss of Mdm2 limits the development of preneoplastic lesion in the cerebellum. The developing nature of the cerebellum in the youngest of MB patients is a major contributing factor to the side-effects resulting from current MB therapies. Studies in adult rodents suggest that nutlin-3 is non-genotoxic in normal homeostatic tissues; however the effects of nutlin-3 have not been evaluated in developing tissues. To gain insight into the potential side effects of p53 activation on the developing cerebellum, the pharmacological effects of Mdm2 inhibition in Granule Neuron Precursor cells (GNPs) was mimicked genetically using a mouse model in which *Mdm2* could be selectively deleted in postnatal GNPs. My studies revealed that deletion of *Mdm2* in GNPs led to a reduction in cerebellum size but did not negatively impact gross motor coordination.

These results suggest that Mdm2 inhibitors may promote the killing of MB tumor cells of pediatric patients without minimal side effects on normal cerebellum development

In addition to cancer, p53 has an important role guarding proliferating cells during development. Activation of p53 has been implicated in the pathology of several human congenital syndromes, and mice lacking *Mdm2* die in utero due to p53-mediated apoptosis. These studies highlight the need for p53 function to be tightly regulated as even modest decreases or increases in p53 function can promote cancer or disrupt normal development, respectively. During the course of my studies on Mdm2 inhibition in MB, it was serendipitously discovered that in the absence of a wild-type level of Mdm2, the phenotypic consequences of p53 activation on the developing mouse embryo were strongly influenced by the genetic background. On a 129S6/B6 F1 hybrid genetic background, mice expressing ~30% the wild-type level of Mdm2 were viable, while mice on an inbred C57BL/6 genetic background died at birth and exhibited an array of craniofacial abnormalities including coloboma, exencephaly, and cleft palate. This is the first demonstration of a role for Mdm2 in craniofacial development. The genotype-dependence, further, indicates the presence of additional genes affecting craniofacial dysmorphology. In human pleiotropic malformation syndromes, there is often clinical variability amongst individuals with an identical underlying mutation at the major effect locus. Currently, the modifier genes that influence craniofacial dysmorphology are unknown. The allelic variants encoded by the divergent genetic backgrounds that increase the penetrance and expressivity of craniofacial malformations in the *Mdm2* hypomorphic mice identify the gene and protein networks governing craniofacial development. In the future, it will be important to determine the genes that are differentially expressed between mice that express low levels of Mdm2 in C57BL/6 and 129S6/B6 F1 genetic backgrounds. The results from this comparison are predicted to lead to the identification of candidate genes that influence craniofacial development through the modulation of p53 function.

## CHAPTER 1: INTRODUCTION

### 1.1 The p53 Tumor Suppressor

The p53 tumor suppressor protein is mutated or inactivated in approximately 50% of human malignancies (Hollstein et al., 1991). In healthy cells, p53 is unstable and targeted rapidly for proteasomal degradation by several ubiquitin ligases including Mdm2, Pirh2, COP-1, and CHIP (Haupt et al., 1997; Honda et al., 1997; Leng et al., 2003; Dornan et al., 2004; Esser et al., 2005). Cellular stresses that compromise cell normal function and DNA integrity promote stabilization of p53 by post-translational modifications. Upon stabilization and activation, wild-type p53 functions to limit the growth of cells under stress, allowing cells time to repair damage to their DNA. Due to this important function of p53, p53 is known as the “guardian of the genome”. In cases when DNA damage of the cell cannot be repaired, p53 induces programmed cell death or apoptosis to prevent cell replication, thereby eliminating cells that could become neoplastic. In addition to growth arrest and apoptosis, p53 has been implicated in the regulation of other essential cellular functions including senescence, differentiation, metabolism, DNA repair, and ribosome biogenesis (Golomba et al., 2014; Kung and Murphy, 2016; Williams and Schumacher, 2016).

#### 1.1.1 Discovery of p53

The p53 protein was discovered in 1979 by several research groups that were identifying proteins that interacted with SV40 virus large T antigen (Kress et al., 1979; Lane & Crawford, 1979; Linzer & Levine, 1979; Melero et al., 1979; Smith et al., 1979). The *TP53* gene was initially cloned from transformed cells and its knockout cause cellular arrest, consistent with the role of p53 as an oncogene (Eliyahu et al., 1984; Jenkins et al., 1984; Parada et al, 1984). This *TP53* gene cloned from transformed cells was later determined to have a mutation that allowed p53 to function as an oncogene. The status of p53 as an oncogene was changed in 1989 when wild-type *TP53* was cloned and its anti-proliferative properties demonstrated (Baker et al, 1989; Takahashi et al., 1989).

Wild-type p53 is now widely recognized as an important tumor suppressor that induces cell cycle arrest or apoptosis during cellular stresses that compromise DNA integrity.

### 1.1.2 Structure and functional domains of p53 protein

The *TP53* gene is located on chromosome 17 in humans and chromosome 11 in mice (*Trp53*). This gene encodes a transcription factor that forms a homotetramer that binds to specific DNA-sequences called response elements (RE) on target genes (Zambetti et al., 1992; McLure et al., 1998). Each p53 monomer consists of two N-terminal transactivation domains (TAD1 and TAD2), a conserved Proline-Rich Region (PRR), a central DNA binding domain, a nuclear localization signal, a tetramerization (TET) domain, and a carboxy-terminal basic regulatory domain (Figure 1.1). The frequent mutation of residues in the p53 DNA binding domain in cancer highlights the importance of the transcriptional activity of p53 to tumor suppression (Cho et al., 1994; Walker et al., 1999). While many mutations lead to loss of p53 function, some mutations in p53 result in a gain of function or dominant negative effect on wild-type p53, thereby inactivating the p53 homotetramer and changing its transcriptional gene profile (Ko & Prives, 1996; O'Farrell et al., 2004).

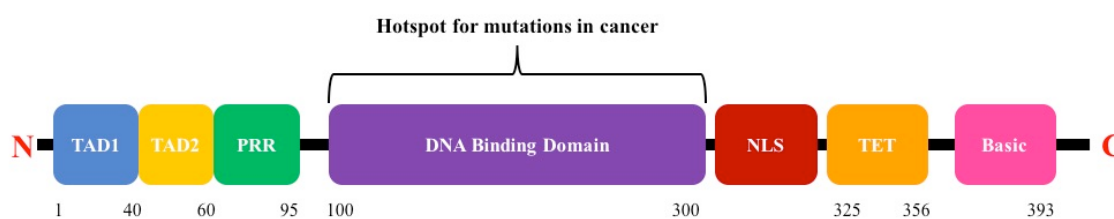


**Figure 1.1 Schematic of p53 protein functional domains.** The p53 N-terminus contains 2 domains: TAD1 and TAD2, important for its transactivation activity as a transcription factor. In addition, p53 N-terminus has a proline rich region. At the center of the protein there is a DNA Binding Domain (DBD) that allows p53 to bind to specific DNA sequences and which is commonly mutated in cancer. At the C-terminus, a Nuclear Localization Signal (NLS), a Tetramerization (TET) domain, and a basic domain that are important for p53 localization, ability to form a homotetramer, and regulation, respectively.

### 1.1.3 Mutations in p53

Mutations in p53 can abrogate its tumor suppressive activities and in some cases, confer new functions that promote tumor progression (Oren & Rotter, 2010). In tumors, the DNA binding domain of p53 is the most common site for mutations, abrogating p53's ability to bind its target genes (Willis et al., 2004). Moreover, p53 mutations in cancer can also have dominant negative effects that result in inactivation of wild-type p53, transactivation of new gene targets, and inappropriate binding to other cellular proteins (Roemer, 1999; Kim & Deppert, 2004). Mutation of p53 is highly correlated with an increased risk of tumorigenesis, as seen in people affected with Li-Fraumeni syndrome and p53 knockout mouse models (Srivastava et al., 1990; Donehower, 1996). Despite the prevalence of p53 mutations in the majority of human cancers, mutations in the *TP53* gene are not frequently detected in pediatric cancers, suggesting that in these types of cancers, p53 is functionally inactivated through other mechanisms (Van Maerken et al, 2014).

### 1.1.4 The role of p53 in cell cycle arrest and apoptosis

The tumor suppressing activity of p53 stems from its ability to induce cellular protective responses including growth arrest and apoptosis. Cellular stresses including ionizing or UV irradiation, DNA damage, hypoxia, oncogene activation, and nutrient deprivation lead to p53 stabilization and activation (Ko & Prives; 1996). Activated p53 transcriptionally regulates numerous genes involved in cell cycle arrest or apoptosis with the cellular outcome dependent on the nature of the stimulus and the cell type affected.

The cell cycle has two major checkpoints denoted as G1 and G2 to ensure proper cell growth, DNA replication and division of the genetic material. This process is regulated by complexes of Cyclin Dependent Kinases (CDKs) and Cyclins. A major p53 gene target is the CDK inhibitor *Cdkn1a* that encodes the protein p21<sup>WAF1/CIP1</sup> (El-Deiry et al., 1994) (See Figure 1.2). p21<sup>WAF1/CIP1</sup> inhibits CyclinA-Cdk2 and CyclinE-Cdk2 complexes at the G1 cell cycle checkpoint (Dulic et al., 1994). Inhibition of Cdk2 and Cdk4 kinases promotes pRb-mediated inhibition of E2F1, a transcription factor that

positively regulates DNA replication and cell cycle progression genes (Harper et al., 1993). In addition, p21<sup>WAF1/CIP1</sup> can form a complex with the proliferating cell nuclear antigen (PCNA) to inhibit DNA replication (Waga et al., 1994). The role of p21<sup>WAF1/CIP1</sup> in cell cycle arrest was confirmed in a mouse model lacking this protein in which cells were unable to arrest the cell cycle after DNA damage (Deng et al., 1995). Cell cycle arrest at G1 can also be induced by repression of *c-Myc*, an oncogene involved in cell growth and proliferation. p53 binds to the *c-Myc* promoter and recruits histone deacetylases to repress *c-Myc* transcription (Ho et al., 2005).

Activation of p53 can induce cell cycle arrest at G2/M by increasing the expression of target genes such as *YWHAS* and *Gadd45* (Hermeking et al., 1997; Xiao et al., 2000) (See Figure 1.2). *YWHAS* encodes the protein 14-3-3 $\sigma$  that sequesters the Cdc2/CyclinB1 complex in the cytoplasm during G2 checkpoint (Hermeking et al., 1997). In addition, *Gadd45* encodes the Gadd45 protein that binds to Cdc2 dissociating it from the Cdc2/CyclinB1 complex (Jin et al., 2000; Zhan et al., 1999). By stopping cell cycle progression, p53 allows cells time to repair DNA damage caused by stress. However, when cells have had severe damage compromising DNA integrity, p53 induces apoptosis.

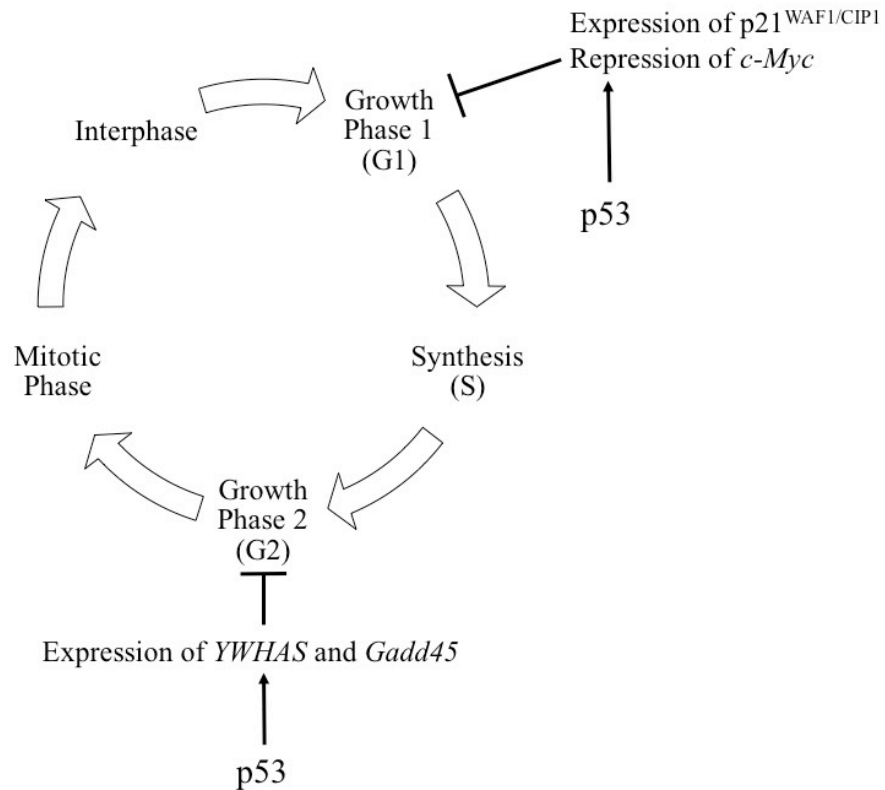


**Figure 1.2 The role of p53 in the cell cycle during cellular stress.** p53 is involved in the transcription of genes that can stop the cell cycle in stressed cells at Growth Phase I (G1) or Growth Phase 2 (G2). The p53-mediated transcription of p21<sup>WAF1/CIP1</sup> stop the cell cycle at G1. In addition, p53 has been reported to repress the expression of *c-Myc* by recruiting histone deacetylases to *c-Myc* promoter and silencing *c-Myc*. During G2 checkpoint, p53 induces the genes *YWHAS* and *Gadd45*.

Apoptosis is a controlled process in which a cell destructs itself. This process, also known as programmed cell death, occurs normally during growth and development and as part of tissue homeostasis to get rid of unneeded or damaged cells. Apoptosis is also induced following cellular stress that severely compromises DNA integrity or normal cell function. The p53 protein plays an important role in apoptosis by activating the transcription of multiple pro-apoptotic genes involved in both intrinsic and extrinsic apoptotic pathways (See Figure 1.3).

The intrinsic apoptotic pathway is characterized by mitochondrial outer member permeabilization (MOMP) which releases cytochrome C from the mitochondrial intermembrane (Liu et al., 1996). Bcl-2 family members regulate MOMP in the intrinsic

apoptotic pathway (Vaseva & Moll, 2009). Anti-apoptotic proteins including Bcl-2, Bcl-XL, and Mcl-1 protect the mitochondrial membrane from MOMP. In contrast, pro-apoptotic proteins including Bax, Noxa and Puma are involved in forming pores in the mitochondrial outer membrane, inhibiting anti-apoptotic proteins and releasing cytochrome C. The balance among anti-apoptotic and pro-apoptotic Bcl-2 family members determines the cellular outcome. After cellular stresses, for example UV irradiation, p53-mediated transcription of *Bax*, *Noxa* and *Puma* shifts the balance toward apoptosis by inducing MOMP (Miyashita & Reed, 1995; Oda et al., 2000; Nakano et al., 2001; Yu et al., 2001). Puma and Noxa function similarly, binding to and translocating Bax from cytosol to the mitochondria outer membrane. Puma and Noxa also inhibit anti-apoptotic Bcl-2 family members found in the mitochondrial outer membrane (Yu et al., 2003, Haupt et al., 2003). Activated Bax oligomerizes in the mitochondrial outer membrane creating pores where cytochrome C is released (Korsmeyer et al., 2000). Cytochrome C can then interact with Apaf-1 and pro-caspase 9 to form the apoptosome, thereby activating the caspase cascade that leads to apoptosis (Chari et al., 2009). In addition to transcriptional activation of multiple pro-apoptotic target genes, p53 can physically interact with and inhibit the anti-apoptotic proteins Bcl-2, Bcl-XL, and Mcl-1 in the mitochondria outer membrane, thereby inducing apoptosis (Wolff et al., 2008). Thus, p53 has both transcription-dependent and -independent functions in the intrinsic apoptotic pathway.

In the extrinsic apoptotic pathway, activation of death receptors through ligand binding induces the cleavage of caspase 8 initiating a cascade of signals that results in apoptosis (Haupt et al., 2003). p53 contributes to the regulation of extrinsic apoptosis by promoting the transcription of *Fas*, *Dr5* and *Perp* (Muller et al., 1998; Wu et al., 1997; Attardi et al., 2000). Fas is a transmembrane receptor from the TNF-R family that is activated through the binding of FasL ligand, predominantly expressed in T cells (Muzio, 1998). Activation of p53 by  $\gamma$ -irradiation induces the transcription of *Fas* in a tissue-specific manner, being highly expressed in the spleen, thymus, kidney and lungs (Bouvard et al., 2000). Additionally, p53 increases trafficking of Fas from the Golgi apparatus, thereby sensitizing the cell to incoming apoptotic signals (Bennett et al., 1998). The Dr5 receptor contains a death-domain which is activated through the TNF-

related apoptosis-inducing ligand (TRAIL) (Haupt et al., 2003). Similar to *Fas*, the expression of *Dr5* is tissue-specific during  $\gamma$ -irradiation, being highly expressed in the spleen, thymus and small intestine (Burns et al., 2001). These studies highlight the tissue-specificity of p53-mediated extrinsic apoptotic pathway during cellular stresses.

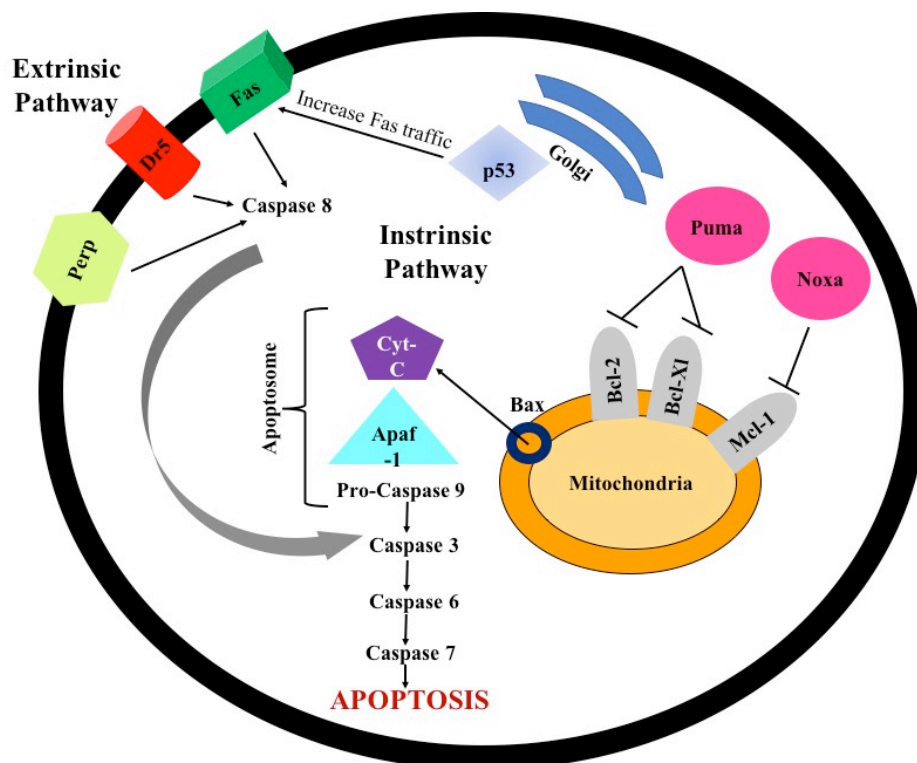


**Figure 1.3 The role of p53 in the extrinsic and intrinsic apoptotic pathways.** The protein p53 regulates both the intrinsic and extrinsic apoptotic pathways. In the extrinsic apoptosis pathway, p53 increases the expression of the death receptor genes *Fas*, *Dr5* and *Perp*. In addition, cytosolic p53 increases Fas trafficking from the golgi apparatus to the plasma membrane sensitizing the cell to incoming apoptotic signals. The activation of death receptors results in the activation of caspase 8 and the cleavages of caspases 3, 6 and 7 resulting in apoptosis. In the intrinsic apoptosis pathway, p53 induces the transcription of pro-apoptotic genes *Bax*, *Puma*, and *Noxa*. The pro-apoptotic protein Puma helps Bax to translocate to the mitochondria outer membrane where Bax forms pores releasing the cytochrome C (Cyt-C) to the cytosol. Additionally, Puma, Noxa and cytosolic p53 inhibit anti-apoptotic proteins Bcl-2, Bcl-Xl, and Mcl-1. The cytosolic Cyt-C binds to Apaf-1 and pro-caspase 9 to form the apoptosome that initiates the cleavage of caspases 3, 6, and 7 causing apoptosis.

### 1.1.5 p53 in cell differentiation

Cell differentiation is a process in which a cell becomes specialized to carry out a particular function within a tissue. The role of p53 in cell differentiation is not well understood, with studies supporting a role for p53 both in the promotion and inhibition of cell differentiation. Among the first studies of p53 in cell differentiation, Shaulsky et al demonstrated that introduction of wild-type p53 in L12 pre-B cells increased expression of immunoglobulin  $\mu$  and the cell surface marker B220 and accelerated differentiation of L12 pre-B cells compared to cells that did not expressed p53 (Shaulsky et al, 1991). However, this study failed to determine whether the p53 transcriptional activity was directly involved in the expression of L12 pre-B cells differentiation markers (Shaulsky et al, 1991). *In vivo* studies using p53 in situ hybridization have inversely correlated p53 mRNA levels with cell differentiation during embryogenesis. During mouse development, high p53 mRNA and protein levels are observed ubiquitously in the mouse embryo during early stages of development where undifferentiated cells are actively proliferating suggesting that p53 is guarding the developing embryo and proliferating cells from possible cellular stresses. After midgestation (E11), p53 levels decrease when organogenesis and differentiation process begins. At this stage, p53 become more tissue-specific and detected in cells undergoing early differentiation events, for example postmitotic neurons (Schmid et al., 1991). The localization of p53 in the nucleus was observed in oligodendrocytes and PC12 cells (rat pheochromocytoma) that were undergoing differentiation (Eizenberg et al., 1996). However, terminally differentiated oligodendrocytes and PC12 cells had p53 in their cytoplasm suggesting that in terminally differentiated cells p53 is exported from the nucleus (Eizenberg et al., 1996). Consistent with the idea that p53 promotes cell differentiation, inhibition of p53 in oligodendrocytes and PC12 cells inhibited cell differentiation and spontaneous apoptosis normally seen in these cell types (Eizenberg et al., 1996). p53 can promote growth arrest and differentiation of PC12 cells by inducing the expression of Trk2 receptor, thereby sensitizing cells Nerve Growth Factor (NGF) signaling (Zhang et al., 2006). Genome-wide ChIP analyses in PC12 cells treated with NGF demonstrated that p53 regulates the pro-differentiation genes *Wnt7b* and *Grhl3*, which are implicated in dendritic extension and ectodermal development, respectively (Brynczka et al., 2007). Together, the studies

suggest that p53 is involved in the early stages of cell differentiation. However, more studies are needed to clarify the tissue-specific role of p53 in cell differentiation.

There is growing interest into the role of p53 in cell differentiation due to potential implications in regenerative medicine for stem-cell based therapies. Adult somatic cells can be reprogrammed using dedifferentiation factors to generate induced pluripotent stem cells (iPS) (Jain & Barton, 2018). The derivation of iPS from adult somatic cells offers a new system to potentially modulate diseases and discover new drugs and circumvents issues regarding the ethical use of Embryonic Stem Cells (ESCs) for studies in regenerative medicine (Singh et al., 2015). The abrogation of p53 function in iPS increases their reprogramming efficiency (Hong et al., 2009; Kawamura et al., 2009; Marion et al., 2009; Utikal et al., 2009). However, the loss of p53 function in iPS also increases their genomic instability, making them susceptible to malignant transformation (Marion et al., 2009). In addition to increased genomic instability, iPS share other traits with malignant cells including uncontrolled proliferation and transcription of pluripotency factors (*e.g.* Myc), which raises concerns as to whether iPS should be used for therapeutic purposes (Semi et al., 2013). The reintroduction of p53 into iPS causes them to activate differentiation pathways that counteract their reprogramming (Yi et al., 2012). Among the p53-target genes that counteract iPS reprogramming is miR-34a that represses pluripotency genes such as *Sox2*, *Myc*, and *Nanog* (Choi et al., 2011). *Nanog* is a pluripotent marker that is necessary for stem cell self-renewal and expression of other pluripotent genes such as *Oct4* and *Sox2* (Silva et al., 2009; Young, 2011). Direct repression of *Nanog* is mediated by a complex of p53-mSin3a-HDAC that deacetylates and represses *Nanog* promoter in ESCs (Lin et al., 2005). Together, these studies suggest that p53-mediated repression of *Nanog* is important for ESCs and iPS differentiation. In the future, it may be possible to modulate the level of p53 during the reprogramming of somatic stem cell to generate iPS for therapeutic purposes without the concern of malignant transformation.

### 1.1.6 Regulation of p53

Multiple post-translational modifications control p53 activity including phosphorylation, acetylation, and ubiquitination. Various combinations of these p53 modifications determine the stability, activation, association with other factors, and subcellular localization of p53 (reviewed in Meek & Anderson, 2009). The cellular outcomes of p53 post-translational modifications are dependent on the nature of the stimulus and cell type.

Phosphorylation is one of the main post-translational modifications of p53. Multiple cellular stresses induce the activation of kinases that phosphorylate p53 at different sites. DNA damage promotes the activation of ATM, ATR, Chk1, Chk2 and DNA-PK kinases that phosphorylate p53 in the N-terminal transactivation domain. After DNA damage, activated kinases phosphorylate p53 at Ser15, Thr18, and Ser20. Phosphorylation at these p53 sites disrupts p53 interaction with its main negative regulator Mdm2 and increases p53 binding with co-activators including the histone acetyl transferases (HATs) CREB and p300 (Shieh et al., 1997; Lambert et al., 1998; Schon et al., 2002; Toledo & Wahl et al., 2006). *In vivo* studies of knock-in mice containing missense mutations in Ser18 or Ser23 (the murine equivalent of human Ser15 or Ser20), which make these sites unable to be phosphorylated, show the important roles of Ser18 and Ser23 in the p53-mediated response after DNA damage (Chao et al., 2003; Sluss et al., 2004; MacPherson et al., 2004). Mutation of Ser18 to Alanine (S18A) resulted in reduced expression of p53 target genes in thymocytes and fibroblasts following irradiation (IR). In these cells, the p53 C-terminus lacked acetylation suggesting that phosphorylation of Ser18 was required prior to the acetylation of p53. The level of apoptosis following IR in knock-in S18A mice was reduced relative to irradiated wild-type mice but it was higher than that observed in p53-null, in contrast, apoptosis was completely abrogated in irradiated thymocytes from double knock-in S18A/S23A mice indicating that phosphorylation at both p53 Ser18 and Ser23 is critical for p53-mediated apoptosis (Chao et al., 2006). Together, these data support the idea that multiple post-translational modifications synergistically regulate p53 function.

Consistent with the idea that phosphorylation of p53 can also promote p53 acetylation by HATs. ATM/ATR-mediated phosphorylation of p53 at Ser15 following genotoxic stress recruits the acetyltransferase p300 and CBP (CREB-binding protein). In turn, p300-CBP acetylates human p53 at the C-terminus at K370, K372, K373, K381, K382, thereby opening the p53 DNA binding domain (Gu & Roeder, 1997). Moreover, acetylation of surrounding histones at p53 target genes by p300-CBP allows chromatin to become more accessible to the activity of p53 and other factors (Goodman & Smolik, 2000). Acetylation of p53 at different sites changes the ability of p53 to bind DNA and other co-factors (Reed & Quelle, 2015). Acetylation of p53 is also reported to contribute to the activation of p53 by disrupting ubiquitin-dependent degradation mediated by Mdm2, suggesting that acetylation of p53 lysine residues can compete with ubiquitination of these same sites (Tang et al., 2008; Li et al., 2002).

In addition to phosphorylation and acetylation, p53 function and levels are regulated by ubiquitination. Ubiquitination of p53 inhibits its function and can decrease p53 cellular levels. Multiple E3 ubiquitin ligases have been determined to target p53 for proteasomal degradation including Mdm2, Pirh2, COP-1, and CHIP (Haupt et al., 1997; Honda et al., 1997; Leng et al., 2003; Dornan et al., 2004; Esser et al., 2005). However, the main gatekeeper of p53 is Mdm2. Ubiquitination of p53 by Mdm2 can exclude p53 from the nucleus and enhance its degradation by the proteasome (Geyer et al., 2000; O'Keefe et al., 2003; Boyd et al., 2000).

The regulation of p53 in both unstressed and stressed cells is important for proper cellular function. In unstressed cells, p53 basal levels are tightly controlled by its main negative regulator Mdm2 allowing cells to grow and proliferate. In contrast, during cellular stresses multiple post-translational modifications activate p53 function to regulate cell cycle arrest and apoptosis. Disruption of the multiple layers of p53 regulation contributes to an increased incidence of diseases such as cancer, thereby highlighting the importance of maintaining a proper balance in this dynamic process.

## 1.2 Mdm2: the main negative regulator of p53

The *Murine double minute 2* (*Mdm2*) gene was cloned from the mouse double minute chromosome amplified in the tumorigenic mouse cell line 3T3DM (Cahilly-Snyder et al., 1987; Fakharzadeh et al, 1991). An essential function of Mdm2 is to negatively control the activity and stability of the tumor suppressor p53 (See Figure 1.5). Mdm2 forms a complex with, and inhibits the transcriptional activity of p53 (Momand et al., 1992). The N-terminus of Mdm2 binds to the  $\alpha$ -helix within the transactivation domain of p53 (TAD1), blocking the transcriptional activity of p53 (Chen et al., 1995; Kussie et al., 1996) (See Figure 1.4). In addition, Mdm2 is an E3 ubiquitin ligase that targets p53 for degradation (Haupt et al., 1997; Honda et al., 1997). The C-terminal RING domain of Mdm2 can monoubiquitylate p53, thereby promoting the transport of the p53-Mdm2 complex from the nucleus to the cytoplasm (Honda et al., 1997). Mdm2-mediated polyubiquitination of p53 promotes the degradation of p53 by the 26S proteasome (Honda et al, 1997) (See Figure 1.4 and 1.5).

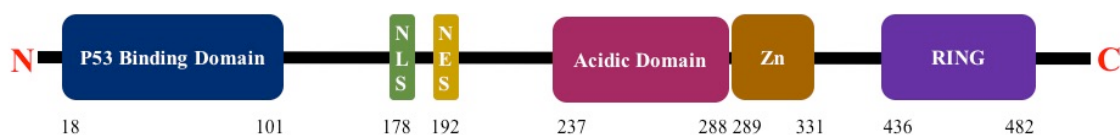


**Figure 1.4 Schematic of Mdm2 protein functional domains.** The Mdm2 N-terminus contains the p53 binding domain followed by a nuclear localization signal (NLS) and nuclear export signal (NES) domains that control Mdm2 transport to and from the nucleus. The central acidic and Zn domains of Mdm2 are important for the regulation of Mdm2 by the binding of other factors, including many ribosomal proteins. A RING domain contains the E3 ubiquitin ligase activity is localized at the C-terminus of Mdm2.

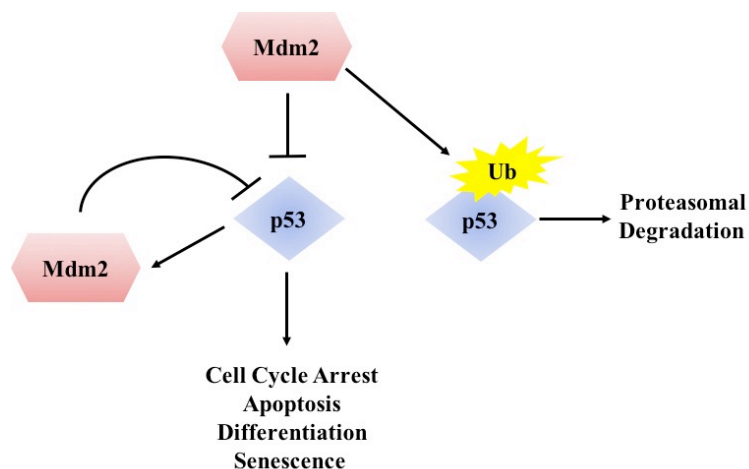


**Figure 1.5 p53 – Mdm2 negative feedback loop.** The tumor suppressor p53 is a transcription factor that regulates expression of genes involve in cell cycle arrest, apoptosis, differentiation and/or senescence when cells are under stress conditions. In addition, p53 activates the transcription of its main negative regulator *Mdm2*, creating an autoregulatory feedback loop. Mdm2 is an ubiquitin ligase that negatively regulates p53 by targeting it for proteasomal degradation or blocking its transcriptional activity.

### 1.2.1 Regulation of Mdm2

The transcriptional regulation of the *Mdm2* gene is controlled by two promoters: P1 and P2. *Mdm2* P1 is located upstream of exon 1 and controls basal expression. In contrast, *Mdm2* P2 is located in intron 1 and is inducible by p53 (Barak et al., 1993). Activated p53 induces the expression of *Mdm2* in response to multiple cellular stresses, thereby creating a negative auto-regulatory feedback loop in which p53 regulates expression of its own inhibitor (Wu et al, 1993). The Mdm2-p53 auto-regulatory loop is important to restrain p53 activity, thereby allowing cells to recover after cellular stress. Cellular stresses can also activate other proteins that control Mdm2 function. For example, Mdm2 ubiquitin ligase activity is inhibited by p14/ARF (Honda & Yasuda, 1999). ARF binds to the Mdm2 Ring domain and sequesters Mdm2 in the nucleolus away from the nucleoplasm where p53 usually is located (Tao & Levine, 1999; Weber et al., 1999). In addition, ribosomal proteins such as L11, L5 and L23 can bind to the Mdm2 C-terminus, thereby inhibiting Mdm2's E3 ubiquitin ligase activity (Lohrum et al., 2003; Dai et al., 2004; Dai & Hu, 2004).

The function of Mdm2 can be regulated by post-translational modifications. Genotoxic stresses such as irradiation and ultraviolet light activate ATM and ATR kinases, respectively. Mdm2 can be phosphorylated on Serine 395 by ATM and Serine 407 by ATR, thereby blocking Mdm2-mediated nuclear export of p53. Additionally, ATM reduces the level of the Mdm2 deubiquitinase HAUSP (Herpesvirus Associate Ubiquitin-Specific Protease), augmenting Mdm2 auto-ubiquitination and degradation during genotoxic stresses (Khoronenkova et al., 2012). However, WIP1, a serine/threonine phosphatase, reverses Mdm2 phosphorylation at Serine 395 to restore its activity towards p53 (Lu et al., 2007). Moreover, phosphorylation of Mdm2 by AKT kinase at Serine 166 and 186 can localize this protein to the nucleus to inhibit p53 activity (Zhou et al., 2001). Regulation of Mdm2 is important to maintain its basal levels since increase expression of *Mdm2* has been reported in several cancers.

### **1.2.2 Mdm2 amplification and overexpression in cancer**

The tumor suppressor p53 is mutated in approximately 50% of human cancers. In cancers in which the *TP53* gene is wild-type, the p53 protein is often functionally inactivated by other mechanisms, thus illustrating the importance of p53 function for tumor suppression. Consistent with this idea, Mdm2, the proximal negative regulator of p53, is amplified and overexpressed in many cancers in which p53 is wild-type. In a panel of soft-tissues sarcomas, 36% contained *Mdm2* amplifications (Oliner et al., 1992). Further histological analysis confirmed the amplification of *Mdm2* in sarcomas including osteosarcomas, rhabdomyosarcomas, lipomas and liposarcomas (Ladanyi et al., 1993; Cordon-Cardo et al., 1994; Nakayama et al., 1995). In addition to sarcomas, *Mdm2* is amplified in other tumors including glioblastoma multiforme, bladder urothelial carcinoma, and cholangiocarcinoma (Oliner et al., 2016). Interestingly, *Mdm2* amplification and p53 mutation events are typically mutually exclusive consistent with the idea that in absence of p53 mutations, p53 function is limited through other mechanisms (Leach et al., 1993; Cordon-Cardo et al., 1994).

In addition to *Mdm2* amplification, *Mdm2* is overexpressed in human tumors as a consequence of disrupted oncogenic signals. The expression of the *Mdm2* P2 promoter

can be induced other factors in addition to p53. MYCN is commonly overexpressed in cancers and has been reported to induce *Mdm2* expression. Binding of MYCN to the *Mdm2* promoter inducing *Mdm2* expression in MYCN-amplified neuroblastoma cells (Slack et al., 2005). Pharmacological inhibition of MYCN decreased Mdm2 levels, leading to an increase of p53 activity and apoptosis of neuroblastoma cells (Slack et al., 2005). Similar to MYCN, the nuclear factor of activated T cells 1 (NFAT-1) has a consensus binding site in the *Mdm2* P2 promoter (Zhang et al., 2012). NFAT-1 is a transcription factor commonly phosphorylated and inactivated in the cytoplasm. Influx of calcium to the cell activates calcineurin which dephosphorylates NFAT-1. NFAT-1 regulates a variety of genes involved in the immune system and cell survival, progression, migration, and angiogenesis and is found at high levels in solid and hematological malignancies (Qin et al., 2014a). In human hepatocarcinoma, high levels of NFAT-1 positively correlate with Mdm2 regardless the presence of p53 (Zhang et al., 2012). A plant compound JapA has been shown to decrease *Mdm2* expression by inhibiting the binding of NFAT-1 to Mdm2 P2 promoter and directly bind to Mdm2 and promote its degradation in breast cancer cells (Qin et al., 2014b; Qin et al., 2015). In addition to *Mdm2*, NFAT-1 has been shown to induce the expression of *c-Myc* in pancreatic cancer cells (Buchholz et al., 2006; Koenig et al., 2010). It would be interesting to know whether there is cooperation among the oncogenic proteins NFAT-1, Mdm2 and MYC to limit p53 function in human cancer.

Studies of germline single nucleotide polymorphisms (SNPs) in *Mdm2* highlight the impact of even modest changes in the level of Mdm2 expression on tumorigenesis. A SNP located at *Mdm2* nucleotide 309 can be either occupied by thymine (T) or guanine (G) resulting in differences in the level of *Mdm2* expression (Bond et al. 2004). *Mdm2* RNA levels measured in a panel of tumor cells containing either *Mdm2* SNP309T or SNP309G showed that the presence of SNP309G correlates with higher levels of *Mdm2* RNA compared to cells containing the SNP309T (Bond et al., 2004). In people affected with Li-Fraumani Syndrome, *Mdm2* SNP309G is correlated with an early onset of cancer (Bond et al., 2004). In addition, *Mdm2* SNP309G increases the risk factor for breast cancer in women (Bond et al., 2006). Mechanistically, *Mdm2* SNP309G allows for

increased binding of the transcriptional activator specific protein 1 (Sp1) resulting in increased expression of *Mdm2* (Bond et al., 2004). Sp1 is a transcription factor that regulates cell growth, and has been implicated in tumorigenesis (Vizcaino et al., 2015). The inhibition of Sp1 by either siRNA or mitramycin A reduced the increased expression of *Mdm2* due to the presence of SNP309G suggesting that the targeting of Sp1 may enhance the therapeutic response in cancer patients with *Mdm2* SNP309G (Bond et al., 2004).

### **1.2.3 Small molecules to inhibit Mdm2-p53 interaction**

Many chemotherapies that cause genotoxic damage require p53 activity to kill cancer cells. While important to kill cancer cells, many chemotherapies also damage surrounding normal healthy tissue leading to adverse side effects. Multiple therapeutic strategies are under study to selectively target the activation of wild-type p53 without causing genotoxic damage to non-tumor cells. The activation of p53 through therapeutically targeting the p53 pathway in cancer may have potentially reduce the toxicity of current chemotherapies in normal healthy tissues. Drugs that reactivate wild-type p53 in cancer are being used in combination to other drugs, including Doxorubixin which causes genotoxic stress in cancer cells. The advantage of combining genotoxic and p53 activating drugs is to decrease the doses of genotoxic chemotherapies, thereby decreasing the negative side effects in healthy tissues (Lane et al., 2010).

Disruption of Mdm2-p53 complex, in particular, is an attractive strategy by which is enhance p53 function in tumors in which p53 is wild type but functionally inactivated. Small molecules that disrupt the interaction between wild-type p53 and Mdm2 have been designed in order to functionally activate wild-type p53. Nutlins, including nutlin-3, are cis-imidazole compounds that were discovered to activate p53 by competing with the p53-binding site in the Mdm2 N-terminus (Vassilev et al., 2004). Nutlin-3 activate wild-type p53 in cultured cells and xenograft tumors, thereby inducing expression of p53-targets genes including p21, decreasing cell viability, increasing apoptosis, and decreasing tumor volume (Vassilev et al., 2004). MI-219 is a spiro-oxindole compound designed based on the crystal structure of Mdm2-p53 complex to specifically bind and

inhibit Mdm2 with higher affinity than nutlin-3 (Shangary et al., 2008). Xenografted osteosarcoma tumors treated with MI-219 showed decreased cell proliferation, increased cell apoptosis, and decreased tumor growth (Shangary et al., 2008). In addition to nutlin-3 and MI-129, using a National Cancer Institute library compound and a cell-based assay, RITA (Reactivation of p53 and Induction of Tumor Cell Apoptosis) was discovered to suppress growth of HCT116 colon carcinoma cells (Issaeva et al., 2004). Further characterization of RITA showed this compound binds directly to p53 and limits p53 binding to Mdm2 (Issaeva et al., 2004). Small molecule inhibitors that target the Mdm2 E3 ubiquitin ligase activity are also being explored as an alternative strategy to enhance wild-type p53 function (Yang et al., 2005; Roxburgh et al., 2012; Herman et al., 2011).

Reactivation of wild-type p53 could be a valuable therapeutic strategy for childhood malignancies which display infrequent mutations in p53. For instance, treatments of human medulloblastoma cell lines containing wild-type p53 with nutlin-3 decreases cell viability suggesting that treatment of this common pediatric brain tumor with Mdm2 inhibitors could be a good therapeutic strategy (Ghassemifar & Mendrysa, 2012). However, given that higher p53 levels can also kill normal cells, more information is needed about the role of p53 in developing tissues prior to using Mdm2 inhibitors to activate p53 in pediatric cancers.

#### **1.2.4 Mouse Models to study Mdm2-p53 pathway**

The deletion of *Mdm2* in mice demonstrates the important role of Mdm2 in normal, non-cancer cells. *Mdm2*-null mice die in utero before implantation of the embryo due to increased p53-mediated apoptosis demonstrating the importance of Mdm2 in p53 regulation during embryogenesis. Interestingly, co-deletion of *Mdm2* and *Trp53* rescues the embryonic lethality seen in *Mdm2*-null mice indicating that regulation of p53 by Mdm2 during embryogenesis is required for normal development (Jones et al, 1995, Montes de Oca Luna et al, 1995). Mice heterozygous for *Mdm2* are overtly normal but are more susceptible to irradiation due to low basal levels of Mdm2 and increased p53 activity compared to wild-type mice (Mendrysa & Perry, 2000). Mice containing a combination of *Mdm2* hypomorphic (*Mdm2<sup>puro</sup>*) and null (*Mdm2<sup>Δ7-12</sup>* or *Mdm2<sup>Δ7-9</sup>* alleles)

express approximately 30% of the wild-type Mdm2 level (Mendrysa et al., 2003). *Mdm2<sup>puro/Δ7-12</sup>* mice are viable indicating that the low level of basal *Mdm2* expression is sufficient to inhibit p53 activity during embryogenesis. However, *Mdm2<sup>puro/Δ7-12</sup>* mice exhibit a number of phenotypes including defects in hematopoiesis, reduced body size, and radiosensitivity (Mendrysa et al., 2003). Recently, low levels of Mdm2 in *Mdm2<sup>puro/Δ7-9</sup>* hypomorphic were demonstrated to result in defects in cerebellar development due to high levels of p53 function (Malek et al., 2011). The p53-dependent cerebellar phenotypes of *Mdm2<sup>puro/Δ7-9</sup>* mice include disorganization of cerebellar layers and increased of apoptosis in Granule Neuron Precursor (GNPs) cells. These phenotypes correlate with decreased activity of the Sonic Hedgehog pathway and increased p53-target genes expression (Malek et al., 2011). Mouse models in which the level of Mdm2 is reduced show the importance of maintaining appropriate basal levels of Mdm2 to negatively regulate p53 during embryogenesis and homeostasis.

In addition to the basal levels of Mdm2, the negative feedback loop of p53 and Mdm2 is also important during homeostasis (Table 1.1). In *Mdm2<sup>P2/P</sup>* mice, a point mutation in *Mdm2* P2 promoter leaves this gene unresponsive to p53 and has been used to study the negative feedback loop between p53 and Mdm2. *Mdm2<sup>P2/P2</sup>* mice develop normally demonstrating that the Mdm2-p53 negative feedback loop is not essential for development (Pant et al., 2013). Basal level of *Mdm2* expression from the P1 promoter is sufficient to control p53 activity in non-stressed cells. However, following irradiation, 80% of *Mdm2<sup>P2/P2</sup>* mice die due increased apoptosis of hematopoietic stem cells suggesting that the p53-Mdm2 negative auto-regulatory loop is required to limit p53 activity after cellular stress (Pant et al., 2013). Furthermore, the Mdm2 E3 ubiquitin ligase function is important to protect radiosensitive tissues during cellular stresses. *Mdm2<sup>Y487A/Y487A</sup>* mice have a point mutation in Mdm2 amino acid 487 that disrupting Mdm2 E3 ubiquitin ligase activity but is still capable of binding to and inhibiting p53 transcriptional activity. *Mdm2<sup>Y487A/Y487A</sup>* mice are viable mice illustrating that ubiquitination of p53 is not essential for restricting p53 activity during mouse development. However, 100% of irradiated *Mdm2<sup>Y487A/Y487A</sup>* mice died after 22 days compared to wild-type due to increase apoptosis and hematopoietic failure suggesting

that Mdm2 E3 ubiquitin ligase activity is required in radiosensitive tissues to inhibit p53 activity during cellular stresses (Tollini et al., 2014).

**Table 1.1 Genetic background and phenotypes of selected *Mdm2* mouse models**

Mouse Model	Genetic Background	Phenotype	Reference
<i>Mdm2</i> <sup>P2/P2</sup> (Point mutation in <i>Mdm2</i> P2 promoter where p53 binds)	>90% C57Bl/6 background	Viable, p53 cannot activate <i>Mdm2</i> for its negative feedback loop, Hematopoietic system is sensitive to irradiation	Pant et al 2013
<i>Mdm2</i> <sup>Y487A/Y487A</sup> (Point mutation in aa 487 to abrogate E3 ligase)	Backcrossed to C57Bl/6 for five generations; 97% C57Bl/6 background	Viable mice, sensitive to irradiation	Tollini et al 2014
<i>Mdm2</i> <sup>puro/Δ7-9</sup> (Combination of null and hypomorphic allele to reduce basal levels of Mdm2)	Maintained on a mixed 129/Sv 3 C57Bl/6 background	Small, radiosensitive, disrupted development of lymphocytes and cerebellum	Mendrysa et al 2003 Malek et al., 2011

### 1.3 The Rationale of this Study

Mdm2 is thought to play an important role in MB tumorigenesis. Low levels of Mdm2 in a Shh-driven MB mouse model reduced the development of preneoplastic lesions in the cerebellum (Malek et al., 2011). In addition, nutlin-3, an Mdm2 inhibitor, decreased the viability of cultured human MB cells with wild-type p53 and promoted p53-dependent apoptosis of tumor cells in mice bearing xenografted MB tumors (Ghassemifar & Mendrysa, 2012; Kunkele et al., 2012). These studies highlight the potential use of Mdm2 inhibition to treat MB. However, as low levels of Mdm2 disrupt cerebellar development in mice (Malek et al., 2011), the effect of Mdm2 inhibitors on healthy tissue should be carefully examined prior to the use of Mdm2 inhibitors in MB pediatric patients whose cerebellum is under development.

To evaluate the effects of Mdm2 inhibition, and hence p53 activation, in normal non-stressed cells of the cerebellum, I utilized a mouse model to genetically knockdown Mdm2 specifically in GNPs during postnatal cerebellar development. As discussed in

Chapter 3, the spatiotemporal deletion of *Mdm2* in GNPs provided a genetic approach to mimic pharmacological inhibition of Mdm2. Results from my analyses of postnatal cerebellar development following deletion of Mdm2 in GNPs provide new insight into the potential side effects of Mdm2 inhibitors or other strategies to enhance p53 function in MB tumors. During the course of my studies on Mdm2 in the cerebellum, it was serendipitously discovered that the mouse genetic background significantly altered the penetrance of p53-dependent phenotypes. In Chapter 4, I present my phenotypic analyses of birth defects arising in *Mdm2*<sup>*puro/Δ7-9*</sup> mice on an inbred C57BL/6 genetic background. These studies highlight the need for p53 function to be tightly regulated as even modest decreases or increases in p53 function can promote cancer or disrupt normal development, respectively.

## CHAPTER 2: MATERIALS AND METHODS

### 2.1 Animal husbandry

All mouse protocols performed during this study were approved in advance by the Purdue University Animal Care and Use Committee (PACUC). Mice were maintained in the Life Science Animal (LSA) building at Purdue University and provided with food and water ad libitum. Euthanasia of mice was performed by carbon dioxide asphyxiation followed by cervical dislocation.

### 2.2 Mouse strains

*Mdm2<sup>lox/lox</sup>* (Mendrysa et al., 2003) and *Math1-CreER<sup>TM</sup>* (Machold & Fishell, 2005) mice were bred to generate *Mdm2<sup>lox/lox</sup>; Cre (+)* and *Mdm2<sup>lox/lox</sup>; Cre (-)* mice on a mixed genetic background for postnatal cerebellar development studies. *Mdm2<sup>puro/+</sup>* and *Mdm2<sup>+/ $\Delta$ 7-9</sup>* mice maintained on an inbred C57BL/6 background were crossed to generate C57BL/6 *Mdm2<sup>+/+</sup>* (wild-type) and *Mdm2<sup>puro/ $\Delta$ 7-9</sup>* embryos. Additionally, F1 hybrid *Mdm2<sup>+/+</sup>* and *Mdm2<sup>puro/ $\Delta$ 7-9</sup>* embryos (Mendrysa et al., 2003) were generated from matings between *Mdm2<sup>puro/+</sup>* and *Mdm2<sup>+/ $\Delta$ 7-9</sup>* that were maintained on a 129/Sv and C57BL/6 background, respectively.

### 2.3 Mouse genotyping

Experimental mice were genotyped using DNA isolated from toe tissue obtained prior to postnatal day ten. DNA was isolated using a modified protocol from Genra System Isolation kit. Briefly, tissues were lysed overnight in a water bath at 55° C in 600  $\mu$ l of genomic lysis solution (20 mM Tris-Cl pH 8.0, 150 mM NaCl, 100 mM EDTA, 1% SDS, and 0.5 mg/ml Proteinase K) and cooled to room temperature (RT). After addition of 200  $\mu$ l of Protein Precipitation solution (Genra Systems Cat #D-5003), samples were centrifuged at 16,000 g for 5 minutes. Supernatants were transferred to a clean Eppendorf tube and DNA pellets precipitated with 600  $\mu$ l of isopropanol by centrifugation at 16,000 g for 10 minutes. DNA pellets were air-dried for 20 minutes and resuspended in 300  $\mu$ l of

sterile water. Genotype was determined by PCR using the GoTag Flexi DNA Polymerase kit from Promega according to manufacturer instructions. *Tp53*, *Mdm2* and *Cre* alleles were genotyped as described previously (Jacks et al., 1994; Mendrysa et al., 2003).

**Table 2.1 Primers used to genotype mice**

Gene	Forward Primer	Reverse Primer	Size (bp)
<i>Mdm2</i> <sup>+</sup>	5' CTGTGTGAGCTGAGGGAGATGTG 3'	5' CCTGGATTTAATCTGCAGCACTC 3'	310
<i>Mdm2</i> <sup>fluro</sup>	5' CTGTGTGAGCTGAGGGAGATGTG 3'	5' CCTGGATTTAATCTGCAGCACTC 3'	397
<i>Mdm2</i> <sup>Δ7-9</sup>	5' GTATTGGGCATGTG TTAGACTGG 3'	5' CCTGGATTTAATCTGCAGCACTC 3'	240
<i>ZYF</i>	5' AAGATAAGCTTACATAATCACATGGA 3'	5' CCCTATGAAATCCTTTGCTGCACATGT 3'	~600
<i>Tp53</i>	5' TATACTCAGAGCCGGCCT 3'	5' ACAGCGTGGTGGTACCTTAT 3'	~400
<i>Cre</i>	5' CATACTGGAAAATGCTTCTGTCC 3'	5' CATCGCTCGACCAGTTTAGTTACC 3'	320

## 2.4 Tamoxifen preparation, delivery and cerebellum dissection

Tamoxifen (Sigma-Aldrich Lot #WXBC0652V) dissolved in corn oil (Sigma-Aldrich) at a concentration of 10 mg/ml and maintained at 4° C up to 1 week in a light protected tube. For inducible deletion of the floxed *Mdm2* allele, newborn mice were injected intraperitoneally with 10 µl of Tamoxifen per 1 gram for two consecutive days (P0/P1 or P1/P2). At P6 or P21, cerebella were collected for examining histology, for assessing organ-specific *Mdm2* knockout efficiency by PCR-based genotype analysis, and for analyzing apoptosis by TUNEL staining.

## 2.5 Timed Matings

Male mice were introduced into females cages in the late afternoon and taken out the next morning between 7:00 and 10:00 AM. Female mice were checked for the presence of a vaginal plug. Upon removal of males, females with a vaginal plug were measured to establish a baseline body weight and again 7 days after removal of the male. Pregnant females were identified by gain of weight after 1 week of the timed mating.

## 2.6 Embryo collection, processing and cryosectioning

Embryos were dissected at embryonic day (E) 10.5, 15.5, and 17.5. Embryos at E10.5 were snap frozen in liquid nitrogen and stored at -80° C for isolation of RNA and

protein. Embryos at E15.5 and E17.5 were fixed in 10 % neural buffered formalin (Thermo Scientific) for histological analyses. For cryosectioning, embryos were placed in 30 % sucrose solution until they settled to the bottom of the tube and were subsequently embedded in optimal cutting temperature compound (OCT). Serial coronal cryosections of E15.5 and E17.5 embryos were taken at 12  $\mu\text{m}$  starting from the eyes, and continuing to the anterior part of the head. Transverse cryosections of E17.5 embryos torsos were taken at 14  $\mu\text{m}$ . Slides were stored at  $-80^{\circ}\text{C}$  until use. In addition, E17.5 embryos were dissected out for Alcian and Alizarin staining (described in section 2.10).

## **2.7 Phenotype scoring**

A phenotype scoring system was developed to quantify the penetrance of craniofacial malformations in C57BL/6 mice differing in *Mdm2* genotype. Phenotypes scored included head shape, eye shape, tongue protrusion and exencephaly. Phenotypes of E15.5 embryos were scored using a rubric from 0 - 3 for the shape of the face, eye and tongue protrusion, with a score of 0-1 being equivalent or similar to wild-type and 2-3 representing the presence and degree of abnormal phenotype.

## **2.8 Haematoxylin and Eosin staining**

Cryosections were warmed to RT and stained in Harris Haematoxylin solution (Sigma-Aldrich Lot SLBQ6493V). Differentiation and bluing of sections were performed using Scott's tap water and acid alcohol (0.5 % HCl in 70 % Ethanol). After Shandon Eosin Y Alcoholic staining (Thermo Scientific Lot 370223), sections were dehydrated in a gradual increase of ethanol and cleared with xylene.

## **2.9 TUNEL staining**

Apoptosis was detected in cryosections using ApopTag Peroxidase InSitu Apoptosis Detection Kit (S7100, EMD Millipore) according to manufacturer instructions. Cryosections were post-fixed in pre-cooled ethanol:acetic acid (2:1) for 5 minutes at  $-20^{\circ}\text{C}$  in a coplin jar. Slides were washed in two changes of 1X Phosphate Buffered Saline (PBS) for 5 minutes each. Endogenous peroxidase activity in tissues was quenched by

incubating slides in 3 % hydrogen peroxide in PBS for 5 minutes at RT followed by washing the same slides for 5 minutes in 1X PBS. Equilibration buffer was applied to the slides and incubated for at least 10 seconds at RT. Working strength TdT enzyme was immediately applied onto the sections and slides were incubated in a humidified chamber at 37° C for 1 hour. Slides were incubated for 10 minutes in a couplin jar with the working strength stop/wash buffer and washed in three changes of 1X PBS for 1 minute. Excess liquid was carefully aspirated from the sections and the anti-digoxigenin peroxidase conjugate was applied to the sections and slides incubated in humidified chamber for 30 minutes at RT. Slides were washed in four changes of 1X PBS for 2 minutes. To develop color, the peroxidase substrate DAB (Vector Laboratories Inc.; Burlingame, CA) was applied to completely cover the slides and slides placed in a humidified chamber for 10 minutes at RT. Color development was monitored by examining slides under a microscope. Slides were washed in three changes of water for 1 minute each and incubated in water for 5 minutes. Slides were incubated in a coplin jar containing methyl green 0.5 % for 10 minutes at RT and washed three times with water, dipping the slides in the water 10 times during the first and second wash, and 30 second without agitation during the third wash. Slides were washed in three changes of 100 % N-butanol in a coplin jar, by dipping slides in the water 10 times during the first and second washes, and 30 seconds without agitation during the third wash. Dehydration of tissue sections was performed using 100 % xylene for 2 minutes. Slides were mounted under a glass coverslip using Permount mounting medium.

## **2.10 Alcian and Alizarin staining in whole-mount mouse skeletons**

Bone and cartilage formation in embryos, was detected by Alcian (Acros Organics Lot A0354144) and Alizarin (Acros Organics Lot A0353916) staining that was performed as previously described with slight modification (Ovchinnikov, 2009) Following overnight incubation in 90 % ethanol at RT, dissected E17.5 embryos were warmed up in hot water, carefully skinned and eviscerated, and incubated overnight in 95 % ethanol at RT. Embryos were transferred into 15 ml falcon tubes containing acetone and incubated overnight to clear fatty tissue and permeabilize cells. Next, embryos were placed in 6-well plates and submerged in 0.05 % Alcian Blue overnight at RT. After

Alcian Blue staining, embryos were de-stained for 6 hours with several changes of 70 % ethanol at RT. Following de-staining, embryos were incubated overnight in 1 % KOH to clear the tissues. This solution was replaced with 0.005 % Alizarin Red staining and incubated overnight on a rocking platform at RT. Stained embryos were stored at RT in ultrapure glycerol (Invitrogen Lot 0365C504).

### **2.11 RNA Isolation, cDNA preparation and real-time PCR**

Total RNA isolated from E10.5 embryos was analyzed by reverse transcription and real-time PCR. E10.5 embryos were homogenized in 300  $\mu$ l of Trizol (Ambion/RNA by Life technologies) according to manufacturer instructions. Briefly, 60  $\mu$ l of chloroform was added and samples incubated for 15 minutes at RT followed by centrifugation at 14,000 g for 15 minutes at 4° C. The aqueous phase was transferred to a clean eppendorf tube. RNA was precipitated by the addition of 150  $\mu$ l of isopropanol and incubated for 15 minutes at RT followed by centrifugation at 12,000 g for 30 minutes at 4° C. RNA pellets were washed with 75 % ethanol and centrifuged at 8,000 g for 5 minutes at 4° C. Ethanol was removed and RNA pellets air-dried for 5 minutes. RNA pellets were resuspended in 20  $\mu$ l of DEPC-treated nuclease-free water (Ambion Cat# 9906 Lot# 026P062233A).

Total RNA was used to generate cDNA using Transcription First Strand cDNA Synthesis Kit from Roche according to manufacturer instructions. cDNA preparation was performed by combining 2  $\mu$ g of RNA with 2  $\mu$ l of random hexamer primers and bringing the final volume to 13  $\mu$ l with PCR-grade water. Samples were incubated 10 min at 65 ° C followed by the addition of 7  $\mu$ l of mastermix (4  $\mu$ l of RT reaction buffer, 0.5  $\mu$ l of RNase inhibitor, 2.0  $\mu$ l of 10 mM deoxynucleotides, and 0.5  $\mu$ l of RTase). Samples were incubated as follows: 25° C for 10 minutes, 55° C for 30 minutes, 85° C for 5 minutes, followed by cooling to 4° C. Prepared cDNA was stored at -20° C.

Real-time PCR reactions were set up using SYBR Green Master Mix from Applied Biosystems and run on an Applied Biosystems ViiA 7. Data were analyzed using

Microsoft Excel software. Relative gene expression levels were calculated using the formula  $2^{-\Delta\Delta CT}$  with *Tubb5* as a loading control and wild-type expression values as the calibrator. Analyses were performed in triplicate for six mice per genotype. One-way analysis of variance (ANOVA) test was done using Microsoft Excel with p-value <0.05 considered significant.

**Table 2.2 Primers used for real-time PCR**

Gene	Forward Primer	Reverse Primer
<i>Tubb5</i>	5' TGGGACTATGGACTCCGTTC 3'	5' AAAGCCTTGCAGGCAATCA 3'
<i>p21</i>	5' TTGTCGCTGTCTTGCACTCT 3'	5' GAGGGCTAAGGCCGAAGAT 3'
<i>Bax</i>	5' GGCGAATTGGAGATGAACCTGG 3'	5' GCTAGCAAAGTAGAAGAGGGC 3'
<i>CyclinG1</i>	5' GCATGGCAGCACATCCCTTTA 3'	5' TGTAGACCAGCCTGGCTTTGAAT 3'
<i>Noxa</i>	5' CGTCGGAACGCGCCAGTGAACCC 3'	5' TCCTTCCTGGGAGGTCCCTTCTGC 3'
<i>Perp</i>	5' TTTGGTGGAGGTGTTTCGAC 3'	5' GAAGCAGATGCACAGGATGA 3'
<i>Gli1</i>	5' GTGTACCACATGACTCTACTCGGG 3'	5' TCATACACAGACTCAGGCTCAGG 3'

## 2.12 Protein Isolation

Whole E10.5 embryos were lysed in 100  $\mu$ l of filtered RIPA buffer (50 mM Tris-HCl pH 7.5, 1 % Igepal, 0.5 % SDS, 0.5 % sodium deoxycholate, 150 mM NaCl, 5 mM EDTA) supplemented with protease and phosphatase inhibitors (Thermo Scientific Pierce Protease and Phosphatase Inhibitor mini tablets, EDTA-Free Prod# 88669 Lot# QE20110720) by incubation for 30 minutes on ice. Samples were centrifuged at maximum speed for 30 minutes at 4° C and supernatants containing the protein lysate transferred to new eppendorf tubes and stored at -80° C until use. Protein concentrations were determined using the DC Protein Assay (Bio-Rad) according to manufacturer's instructions. Bovine Serum Albumin (BSA) standards (0.25  $\mu$ g/ $\mu$ l, 0.50  $\mu$ g/ $\mu$ l, 1.0  $\mu$ g/ $\mu$ l, 1.5  $\mu$ g/ $\mu$ l, and 2.0  $\mu$ g/ $\mu$ l) were prepared in RIPA buffer. In a 96 well plate, 5  $\mu$ l of standards and 5  $\mu$ l of diluted whole cell lysate were plated in duplicate and mixed with 25  $\mu$ l of A' reagent (20  $\mu$ l of reagent S in 1 ml of reagent A) and 200  $\mu$ l of Reagent B. Following incubation at RT for 15 minutes, absorbance at 750 nm was read in Spectramax plate reader.

### 2.13 Western Blot

For analysis of protein expression, 40  $\mu$ g of whole cell lysate was resolved by SDS-PAGE using a 10 % gel and blotted onto a 0.45  $\mu$ m nitrocellulose membrane (Amersham Protran Premium). Membranes were blocked in 5 % non-fat milk made in 1X Western Blot (WB) buffer (150 mM NaCl, 20 mM Tris Base, and 0.5 % Ipegal; pH 8.0) and incubated with primary antibodies at 4° C overnight on a rocking platform (See Table 2.3). Membranes were washed three times for 5 minutes each with 1X WB buffer and incubated with secondary antibodies for 2 hours at room temperature on a rocking platform. After washing three times for 5 minutes each with 1X WB buffer, signals were detected by enhanced chemiluminescence (SuperSignal West Femto Maximum Sensitivity Substrate, ThermoScientific) and visualized using a Syngene G:Box system.

**Table 2.3 Antibodies used for Western Blot**

Primary	Host Specie	Purpose	Dilution	Catalog #	Manufacturer
p53 (CM5)	Rabbit	1°	1:1000	NCL-p53 CM5p	Vector
MDM2 (210)	Mouse	1°	1:1000	Ab16895	Abcam
$\beta$ -Actin	Mouse	1°	1:10000	A5441	Sigma
Anti-rabbit IgG-HRP	Donkey	2°	1:10000	NA934	Amersham
Anti-mouse IgG-HRP	Sheep	2°	1:10000	NXA931	Amersham

### 2.14 Statistical methods

Statistical significance was calculated using Microsoft Excel software. Several statistical methods were utilized to established significance based on the results analyzed: two-tailed student's t test, chi square for goodness of fit, and ANOVA with Tukey test. Tests were considered significant with a p-value < 0.05. All error bars represent standard error of the mean.

## **CHAPTER 3:THE ROLE OF MDM2 IN GRANULE NEURON PRECURSOR CELLS DURING POSTNATAL CEREBELLAR DEVELOPMENT**

### **3.1 Cerebellum: function and development**

The cerebellum is located in the posterior part of the brain and plays an important role in motor coordination, language, and cognition (Roussel & Hatten, 2011). The development of this highly organized structure begins during early embryogenesis when progenitor cells proliferate and migrate from both the ventricular zone and the rostral rhombic lip to the nascent cerebellum. Cells from the ventricular zone give rise to Purkinje cells, Bergmann glia, astrocytes, interneurons and neuron of the deep nuclei. In contrast, progenitor cells from the 4<sup>th</sup> rhombic lip give rise to Granule Neuron Precursor cells (GNPs) that will establish the External Granule Layer (EGL) in the postnatal cerebellum (Goldowitz & Hamre, 1998).

In mice, GNPs start populating the cerebellum around embryonic (E) day 13.5. Proliferation of GNPs begins at E17.5, reaches its peak at postnatal (P) days 5 to 8, and declines at day P15. Postnatal proliferation of GNPs in the EGL is a major determinant of the terminal shape and function of the cerebellum. Postnatal proliferation of GNPs is dependent on Sonic hedgehog (Shh) mitogen released from Purkinje cells. After birth, Purkinje cells release Shh to stimulate the proliferation of GNPs resulting in the expansion of the EGL and determining the foliation pattern of the mature cerebellum (Wallace, 1999; Corrales et al., 2006). In mice lacking Purkinje cells, the number of GNPs is decreased and cerebellar foliation pattern is disrupted (Caddy & Biscoe, 1979).

Following expansion of the EGL, GNPs migrate inwards in the cerebellum through Purkinje cell's dendrites in the molecular layer to form the Granule Layer (GL) where they will terminally differentiate into granule neurons 3 weeks after birth in mice and during the first year in humans (Figure 3.1). Disruption of the molecular pathways that tightly regulate the proliferation, migration, and differentiation of GNPs in development contribute to the formation of medulloblastoma (MB), a cerebellar cancer.

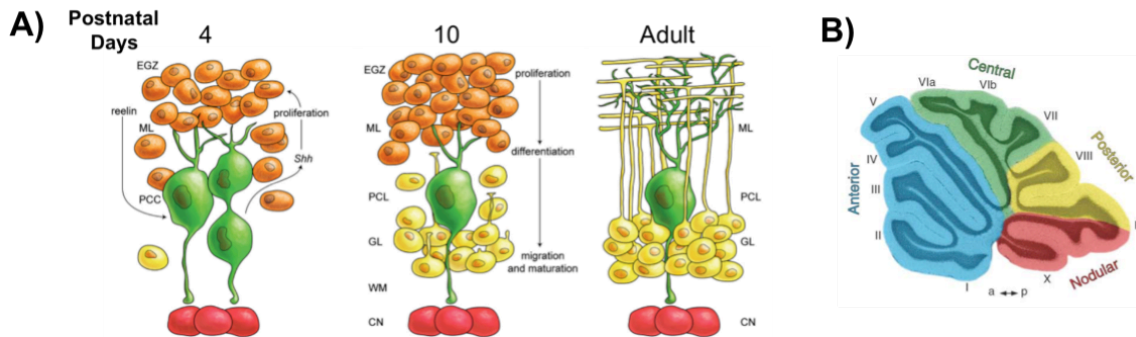


**Figure 3.1 Schematic representation of postnatal cerebellar development in mice. A)**

Shh mitogen released from Purkinje cells induces GNPs proliferation in the External Granule Layer (EGL). Following expansion of the EGL, GNPs differentiate and migrate through the Purkinje Cell Layer (PCL) to make the Granule Layer (GL). The mature cerebellum consists of three layers: Molecular Layer (ML), PCL and GL. Picture taken and modified from Marzban et al., *Frontiers in Cellular Neuroscience*, 2015. **B)** The gross anatomy of the cerebellum consists of 4 lobes: anterior, central, posterior and nodular; each containing folds called lobules (I to X). The lobularization or foliation pattern is tightly controlled during cerebellar development by Shh signaling and GNP expansion in the EGL. Figure taken from White & Sillitoe, *Developmental Biology*, 2013.

### 3.2 Medulloblastoma

MB, a malignant tumor that arises in the cerebellum, is the most common brain cancer that affects children, but also occurs in adolescents and adults. Current treatments for MB consist of craniotomy surgery to resect most of the tumor if possible followed by chemotherapy and radiotherapy. Treatment regimens are customized to a degree based on MB subtype, tumor size and location, and the patient's age. Across all MB subtypes, survival rate is approximately 65 – 70 % (Schwalbe et al., 2017). Despite this high survival rate, however, MB survivors often suffer from detrimental side effects including cognitive disorder, ototoxicity and impaired movements that negatively impact patients' quality of life. Deleterious side-effects arise largely due to the nonspecific killing of healthy tissues following MB treatments that lack specificity for MB tumor cells (Roussel & Hatten, 2011). New treatments for MB are urgently needed to selectively target MB cells while decreasing nonspecific cytotoxic effects.

Medulloblastoma is primarily classified using the World Health Organization (WHO) classification method that includes patient age, metastatic stage, level of tumor

resection, and cellular morphology. In the past few years, MB tumors have been subdivided based on their clinical features, genetics, and molecular expression into four main subtypes: Wnt, Shh, Group 3, and Group 4 (Taylor et al., 2012; Table 3.1). These subgroups show differences in their affected demographic population, clinical outcome, morphological histology, and DNA aberrations. Classification of MB subtypes continues to be refined. For example, the MB Shh subtype has recently been further subdivided into MB Shh infant and MB Shh child, and subtypes Group 3 and Group 4 have both been subdivided into high risk and low risk (Schwalbe et al., 2017). The molecular differences among these MB subgroups may help to predict their biological behavior and how they will respond to targeted treatments. The better understanding of the MB molecular subtypes and their biology has the potential to guide the development of improved targeted therapies and personalized cancer treatments.

### 3.2.1 Wnt subtype

The Wingless (Wnt) canonical pathway plays an important role during central nervous system development by promoting the proliferation, self-renewal, and differentiation of neural stem cells (reviewed in Mulligan & Cheyette, 2012). The Wnt canonical pathway is characterized by the binding of Wnt ligand to the Frizzled and low-density-lipoprotein-related protein 5/6 (LRP5/6) receptors leading to phosphorylation of Disheveled, thereby abrogating degradation of  $\beta$ -catenin by the APC/Axin/GSK3 $\beta$  destruction complex (Komiya & Habas, 2008).  $\beta$ -catenin subsequently translocates to the nucleus where it promotes the transcription of Wnt-target genes (Komiya & Habas, 2008). In humans, deregulation of  $\beta$ -catenin stemming from germline mutations in the *APC* gene result in Turcot syndrome which is characterized by increased risk of colorectal cancer as well as MB (Hamilton et al., 1995). In addition, somatic mutations in the *CTNNB1* gene encoding  $\beta$ -catenin have been detected in people suffering from sporadic MB (Zurawel et al., 1998). MB Wnt tumors typically present in the lower rhombic lip of the cerebellum with a classic large cell/anaplastic histology. MB Wnt tumors occur equally in males and females at all ages but rarely infants. In MB clinical stratification studies, MB patients with nuclear staining of  $\beta$ -catenin were shown to have

a 92 % rate of 5-year survival compared to 65 % that were negative for nuclear  $\beta$ -catenin (Ellison et al., 2005). The good prognosis of patients with MB Wnt compared to other MB subtypes supports the de-escalation of cancer treatments for patients with MB Wnt subtype (Gajjar et al., 2006; Ramaswamy et al., 2011; Taylor et al., 2012).

### 3.2.2 Shh subtype

The Sonic Hedgehog (Shh) pathway is involved in mitogenic signaling that promotes the proliferation of GNPs during postnatal cerebellar development. In the absence of Shh ligand, the patched (Ptch) receptor inhibits smoothened (Smo), causing the repression of the Shh pathway (Carballo et al., 2018). The binding of Shh ligand to Ptch releases Smo from repression leading to the activation of the Gli1 and Gli2 transcription factors which positively regulate expression of Shh gene targets (Carballo et al., 2018). In people, deregulation of Shh signaling due to germline mutations in the receptor *PTCH1* or the Shh inhibitor, Suppressor of fused homolog (*SUFU*), result in Gorlin syndrome which is characterized by increased risk of MB (Slade et al., 2011). Approximately 40 % of MB Shh tumors have loss of chromosome 9q in which the *PTCH1* gene is located (Kool et al., 2008; Northcott et al., 2011b; Cho et al., 2011). In addition, 10 – 15 % of MB Shh have somatic mutations in Shh pathway components such as *PTCH1*, *SUFU*, and *SMO* (Northcott et al., 2011b).

MB Shh tumors present most commonly in infants and adults, affecting females and males equally (Northcott et al. 2011b). Prognosis for MB Shh tumors is intermediate between the MB Wnt and Group 3 subtypes. Current strategies to specifically treat MB Shh tumors with small molecules that target the Shh pathway have shown promise for limiting Shh MB tumor progression. For example, a SMO inhibitor, GDC-0449, was effective in temporarily reducing MB metastatic tumors growth as seen by positron-emission tomography (PET) scan after two months of treatment (Rudin et al., 2009). However, after 3 months of treatment, the patient died due to relapse of tumor growth indicating that MB Shh developed resistance to GDC-0449. New therapeutic strategies against this MB subtype are needed and remain under investigation. (Rudin et al., 2009).

### 3.2.3 Group 3 subtype

Tumors of the MB group 3 have amplification or overexpression of the oncogene *OTX2* and gain of chromosome 1q suggesting that oncogenes identified in this chromosome could be driving tumorigenesis of this subtype (de Hass et al., 2006; Northcott et al., 2011a; Puri & Saba, 2014). MB group 3 tumors metastasize to the spinal cord and present with the worse prognosis of all MB subtypes despite aggressive treatments (Cho et al., 2011; Kool et al., 2008; Northcott et al., 2011a). In addition, the presence of *MYC* amplification in primary tumors worsens the prognosis of MB group 3 survivors (Cho et al., 2011). MB Group 3 tumors preferentially affect male infants and children but rarely occur in adolescents or adults.

### 3.2.4 Group 4 subtype

Tumors of the MB Group 4 have over 80 % of isochromosome 17q (i17q). As with MB Group 3 tumors, amplification of *OTX2* is also seen in MB Group 4 (Boon et al., 2005; Northcott et al., 2011b). In addition, expression of follistatin-related protein 5 (*FSTL5*) in MB Group 4 tumors correlates with poor prognosis (Remke et al., 2011). MB Group 4 tumors typically present with a classic histology and predominantly affects males (3:1 males:females). Interestingly, females affected with MB Group 4 frequently exhibit loss of chromosome X suggesting a role of the sex in the tumorigenesis of this MB subtype (Kool et al., 2008; Cho et al., 2011; Northcott et al., 2011a; Northcott et al., 2011b). The prognosis of patients with MB Group 4 tumors is similar to MB Shh subtype (Taylor et al., 2012). MB Group 4 subtype can affect people from all age groups. However, worse prognosis is identified in almost 25 % of adults affected with MB Group 4 compared to infants, children or adolescents with same subtype (Remke et al., 2011).

**Table 3.1 The four main Medulloblastoma subtypes**

MB Subtype	Demographic Males:Females	Genetic Feature	Prognosis	References
Wnt	1:1	Germline mutation in <i>APC</i> Somatic mutations in <i>CTNNβ1</i>	Good prognosis	Boon et al., 2005 de Hass et al., 2006 Kool et al., 2008 Cho et al., 2011 Remke et al., 2011 Northcott et al., 2011a Northcott et al., 2011b Taylor et al., 2012
Shh	1:1	Germline or somatic mutations in <i>PTCH</i> and <i>SUFU</i> Amplification of <i>Gli1</i> , <i>Gli2</i> , or <i>MYCN</i>	Intermediate prognosis between Wnt and Group 3	
Group 3	3:1	<i>OTX2</i> amplification or overexpression Gain of chromosome 1q <i>MYC</i> amplification	Poor prognosis	
Group 4	3:1	Isochromosome 17q (i17q); Females loss one X chromosome; Amplification of <i>OTX2</i> and <i>FSTL5</i>	Similar to MB Shh subtype	

### 3.3 p53-Mdm2 pathway in Medulloblastoma

Inactivating mutations in *TP53* are not frequently reported in MB (Saylor III et al., 1991; Pfaff et al., 2010). However, MB Wnt and Shh subtypes present *TP53* mutations at low rates (Pfaff et al., 2010; Zhukova et al., 2013). Moreover, people affected with Li-Fraumani syndrome who inherit germline mutation in *TP53* are predisposed to MB (Barel et al., 1998). The role of p53 inactivation in MB tumorigenesis has been studied in mouse models. Although p53-null mice do not develop MB, MB is frequently observed when p53 is inactivated in combination with other proteins including Rb, Parp, and DNA repair proteins (e.g. Brca2) (Donehower et al., 1992; Jacks et al., 1994; Marino et al., 2000; Eberhart, 2003; Frappart et al., 2009). In addition, deletion of *Tp53* increases the incidence of MB tumors in Shh-driven MB *Ptch1<sup>+/-</sup>* and *Sufu<sup>+/-</sup>* mouse models (Heby-Henricson et al., 2012). Together these studies suggest that loss of p53 function can contribute to MB tumorigenesis.

Recent analyses of MB Shh subtypes have revealed mutations in *TP53* are more commonly present in MB Shh tumors of children as compared to infants suggesting that

there might be different mechanism to inactivate p53 between these two populations (Schwalbe et al., 2017). In the absence of *TP53* mutations, other mechanisms could be limiting p53 function.

Consistent with the idea that p53 function is limited in MB by mechanisms other than mutation, the levels of Mdm2, the main negative regulator of p53 are increased in MB (Adesina et al., 1994; Batra et al., 1995; Kunkele et al., 2012). Recently, our lab has shown that reduction of Mdm2 levels in *Ptch1*<sup>+/-</sup> mice, a mouse model of Shh-driven MB, reduces the number of preneoplastic lesions in the cerebellum demonstrating the requirement of Mdm2 for the initiation of MB tumorigenesis (Malek et al., 2011). In addition, pharmacological disruption of the MDM2-p53 interaction with nutlin-3 decreased cell viability of human MB cell lines with wild-type p53 thereby supporting the therapeutic value of Mdm2 inhibition for the treatment of MB, particularly of the Shh subtype (Ghassemifar & Mendrysa, 2012).

As many patients with MB Shh subgroup are infant patients in which the cerebellum is still under development, the utility of Mdm2 inhibition as a therapeutic approach for MB Shh tumors is dependent, in part, on the impact of loss of Mdm2 function on postnatal cerebellar development. Prior research from our lab has revealed that *Mdm2*<sup>*puro*/Δ7-9</sup> mice that express systemic low levels of Mdm2 throughout embryogenesis have abnormal cerebellar foliation patterns at birth (P0), thus demonstrating a critical role for Mdm2 in prenatal cerebellar development. Although cerebellar defects of *Mdm2*<sup>*puro*/Δ7-9</sup> mice persisted into adulthood, it is unclear whether these defect stem from a paucity of GNPs at birth or whether Mdm2 is also required in GNPs postnatally (Malek et al., 2011). A better understanding of the role of Mdm2 in the postnatal cerebellum is needed in order to understand the potential side effects of pharmacological inhibition of Mdm2 in infants with MB tumors.

The broad objective of my research project is to evaluate the effects of Mdm2 inhibition, and hence p53 activation, on the developing postnatal cerebellum. The low level of Mdm2 throughout embryogenesis in *Mdm2*<sup>*puro*/Δ7-9</sup> mice limits the use of this model for providing insight into the specific role of Mdm2 in postnatal cerebellar

development. To circumvent the limitations of *Mdm2*<sup>puro/ $\Delta$ 7-9</sup> mice, I will employ a mouse model in which *Mdm2* can be acutely deleted specifically in GNPs during postnatal cerebellar development in newborn mice. The results from this research are predicted to provide new insight into the use of Mdm2 inhibition as a new therapeutic strategy that may selectively target MB tumor cells without affecting healthy cerebellar cells, thereby limiting detrimental side effects.

### 3.4 Mouse model to study the effect of Mdm2 inhibition on GNPs of the cerebellum

My overarching goal is to utilize pharmacological inhibition of Mdm2 to enhance p53 activity and promote cell death in MB tumor cells. Toward that goal, the specific goal of my research is to determine the effect of loss of Mdm2 in normal cerebellar GNPs during postnatal cerebellum development in order to gain insight into potential side effects associated with this novel therapeutic approach. I hypothesized that deletion of *Mdm2* in GNPs during postnatal cerebellar development would reduce the number of GNPs due to increased p53-mediated apoptosis.

The pharmacological effects of Mdm2 inhibition in GNPs was mimicked genetically using a mouse model in which *Mdm2* could be selectively deleted in GNPs during postnatal cerebellar development. *Mdm2*<sup>fl $\alpha$ /fl $\alpha$</sup>  mice utilized for these experiments have *loxP* sites flanking *Mdm2* exons 7 and 9 which are recognized by the Cre recombinase leading to conversion of the *Mdm2*<sup>fl $\alpha$</sup>  allele to the null *Mdm2* <sup>$\Delta$ 7-9</sup> allele (Mendrysa et al., 2003; Figure 3.2). *Mdm2*<sup>fl $\alpha$ /fl $\alpha$</sup>  mice were crossed with *Math1-CreER*<sup>TM</sup> mice that express a tamoxifen-inducible CreER fusion protein under control of the *Math-1* promoter (Machold & Fishell, 2005). The *Math1* promoter is expressed in proliferating GNPs and inner ear hair cells, restricting the expression of Cre recombinase to these types of cells (Ben-Arie et al., 1997; Chow et al., 2006). Postnatally, expression of *Math1-CreER*<sup>TM</sup> is restricted predominantly to GNPs of the EGL in the cerebellum. While the *CreER*<sup>TM</sup> expression is spatially restricted to GNPs, the activation of this enzyme is controlled temporally by the addition of tamoxifen which binds the mutated hormone-binding domain of estrogen receptor (Feil et al., 2009). The binding of tamoxifen to CreER<sup>TM</sup> recombinase in *Mdm2*<sup>fl $\alpha$ /fl $\alpha$</sup> ; *Cre* (+) mice causes CreER<sup>TM</sup> to

translocate from the cytoplasm to the nucleus where it mediates the recombination of the  $Mdm2^{lox}$  allele to a  $Mdm2^{\Delta7-9}$  null allele. This mouse model allows me to assess the spatiotemporal consequences of Mdm2 loss of function during early postnatal cerebellar development and thus gain potential insights into consequences of pharmacological inhibition of Mdm2 inhibition in GNPs.

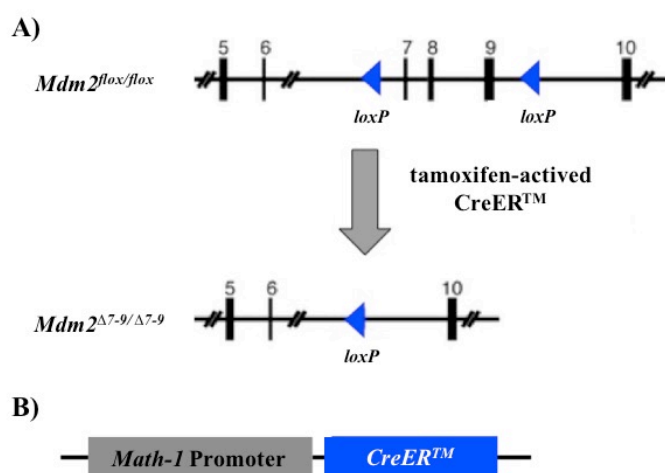


**Figure 3.2  $Mdm2^{lox/lox}$  and Math1-CreER<sup>TM</sup> mouse models used to spatiotemporally knockdown Mdm2 in postnatal GNPs.** **A)** Schematic representation of the  $Mdm2^{lox}$  allele.  $Mdm2$  loxP sites flanking exons 7 and 9 are recombined by tamoxifen-activated CreER<sup>TM</sup> recombinase to generate a  $Mdm2^{\Delta7-9}$  null allele. **B)** The expression of CreER<sup>TM</sup> is controlled by the Math1 promoter, which is activated in postnatal proliferating GNPs.

### 3.5 $Mdm2$ recombination is detected in $Mdm2^{lox/lox}; Cre (+)$ mice injected with tamoxifen at P0/P1 or P1/P2

To determine whether  $Mdm2$  inactivation in GNPs impairs postnatal cerebellar development, I established  $Mdm2^{lox/lox};$  in which the  $Math1-CreER$  transgene was present [ $Mdm2^{lox/lox}; Cre (+)$ ] or absent [ $Mdm2^{lox/lox}; Cre (-)$ ]. All  $Mdm2^{lox/lox}$  mice, with (+) or without (-) Cre, were intraperitoneally injected with tamoxifen at P0/P1 or P1/P2 and euthanized at P6 when GNPs start to reach peak proliferation. Conversion of  $Mdm2$  floxed alleles to  $Mdm2$  null alleles by CreER recombinase was confirmed by non-quantitative PCR analyses of  $Mdm2^{lox}$ ,  $Mdm2^{\Delta7-9}$ , and  $CreER$  DNA. Robust deletion of  $Mdm2$  was detected specifically in DNA isolated from cerebella of  $Mdm2^{lox/lox}; Cre (+)$  mice injected with tamoxifen. In contrast, the null  $Mdm2^{\Delta7-9}$  allele was not detected in

the cerebella of  $Mdm2^{flox/flox}; Cre (-)$  that were injected with tamoxifen but lacked the CreER transgene (Figure 3.3 Lanes 3 and 4 versus 1 and 2). Although the null  $Mdm2^{\Delta7-9}$  allele was generated in in the cerebellum following tamoxifen treatment of  $Mdm2^{flox/flox}; Cre (+)$  mice, the  $Mdm2^{flox/flox}$  allele was still amplified by PCR in these samples (Figure 3.3 Lanes 3 and 4). The presence of the  $Mdm2^{flox/flox}$  allele in  $Mdm2^{flox/flox}; Cre (+)$  mice following tamoxifen is likely due to DNA from non-GNP cell populations within the cerebellum in which the Math-1 promoter is not expressed and hence Cre not activated. Together, these results demonstrate that Mdm2 can be selectively inactivated in the postnatal cerebellum.

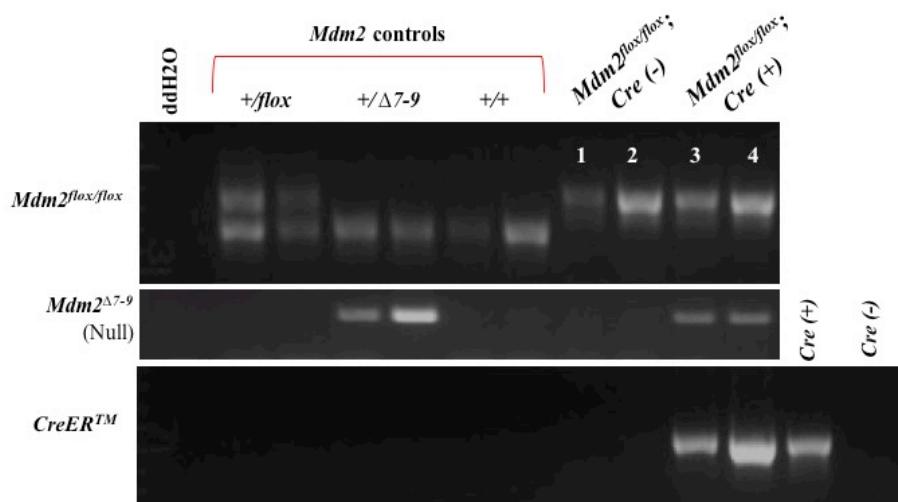


**Figure 3.3 Mdm2 recombination in  $Mdm2^{flox/flox}; Cre (+)$  mice injected with tamoxifen.** Mice from lanes #1 through #4 were injected with tamoxifen (lanes #1 and #3 at P0/P1; lanes #2 and #4 at P1/P2). All these mice were euthanized at P6 and cerebellar DNA isolated for PCR.  $Mdm2^{flox/flox}; Cre (+)$  (lanes #3 and #4) have bands for  $Mdm2^{flox/flox}$ ,  $Mdm2^{\Delta7-9}$  alleles, and  $CreER^{TM}$  alleles. In contrast,  $Mdm2^{flox/flox}; Cre (-)$  (lanes #1 and #2) only have bands for  $Mdm2^{flox/flox}$  alleles.

### 3.6 Deletion of *Mdm2* in GNPs decreased cerebellar size and disrupted lobules morphology

Next, to determine whether acute deletion of *Mdm2* in the postnatal GNPs affected cerebellar morphology, cerebellum size and EGL thickness were analyzed by H&E staining. *Mdm2* deletion at P0/P1 in the cerebella of *Mdm2<sup>fllox/fllox</sup>; Cre (+)* mice resulted in smaller cerebella compared to control *Mdm2<sup>fllox/fllox</sup>; Cre (-)* (Figure 3.4 A). Quantification of cerebellar area shows that *Mdm2<sup>fllox/fllox</sup>; Cre (+)* injected with tamoxifen at P0/P1 have statistically significant smaller cerebella compared to control *Mdm2<sup>fllox/fllox</sup>; Cre (-)* (Figure 3.6 A). In contrast, cerebellar area at P6 was not significantly from controls when different when *Mdm2<sup>fllox/fllox</sup>; Cre (+)* mice were injected at P1/P2 (Figure 3.6 B). In addition to cerebellar area, *Mdm2<sup>fllox/fllox</sup>; Cre (+)* mice have disrupted morphology of anterior cerebellar lobules II and III compared to control *Mdm2<sup>fllox/fllox</sup>; Cre (-)* (Figures 3.4 B and 3.5 B). Despite the disrupted morphology of anterior cerebellar lobules II and III of *Mdm2<sup>fllox/fllox</sup>; Cre (+)* mice, quantitation of EGL thickness in cerebellar lobule II revealed no significant reduction in thickness due to acute *Mdm2* deletion in mice injected (Figure 3.7). Together, these results suggest that deletion of *Mdm2* in GNPs negatively affects the cerebellum size and disrupts the morphology of cerebellar lobules in particular the anterior lobules II and III but does not affect the thickness of EGL.

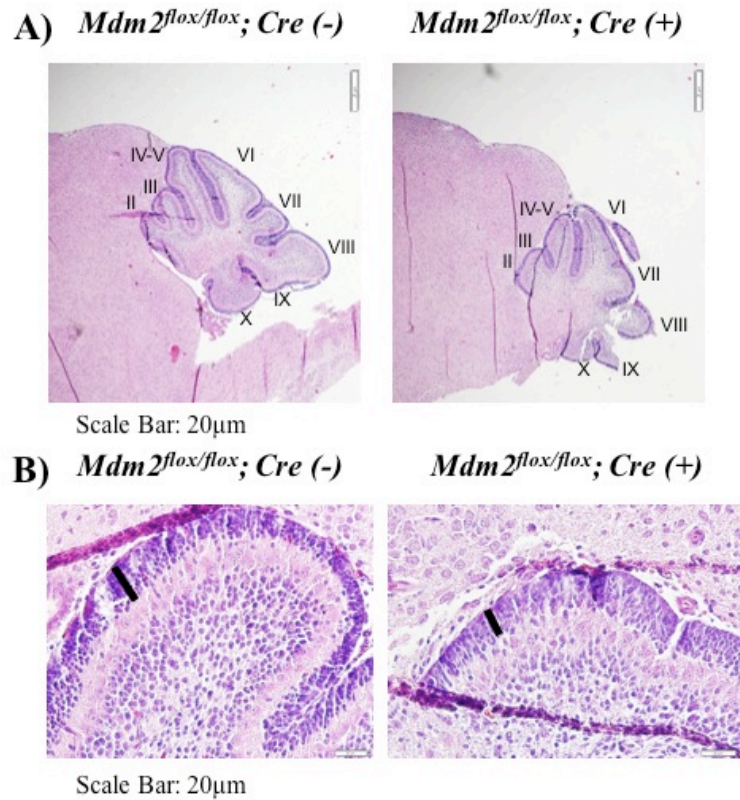


**Figure 3.4 Decreased cerebellar size and disrupted morphology of anterior cerebellar lobules in *Mdm2<sup>flox/flox</sup>; Cre (+)* cerebellum due to tamoxifen activated Cre recombination of *Mdm2* at P0/P1. A) H&E stained sections taken at 4X show that *Mdm2* deletion results in small cerebellum and disrupted morphology of anterior lobules II and III. B) H&E stained sections of lobule II EGL at 40X showing thinner EGL due to *Mdm2* deletion.**

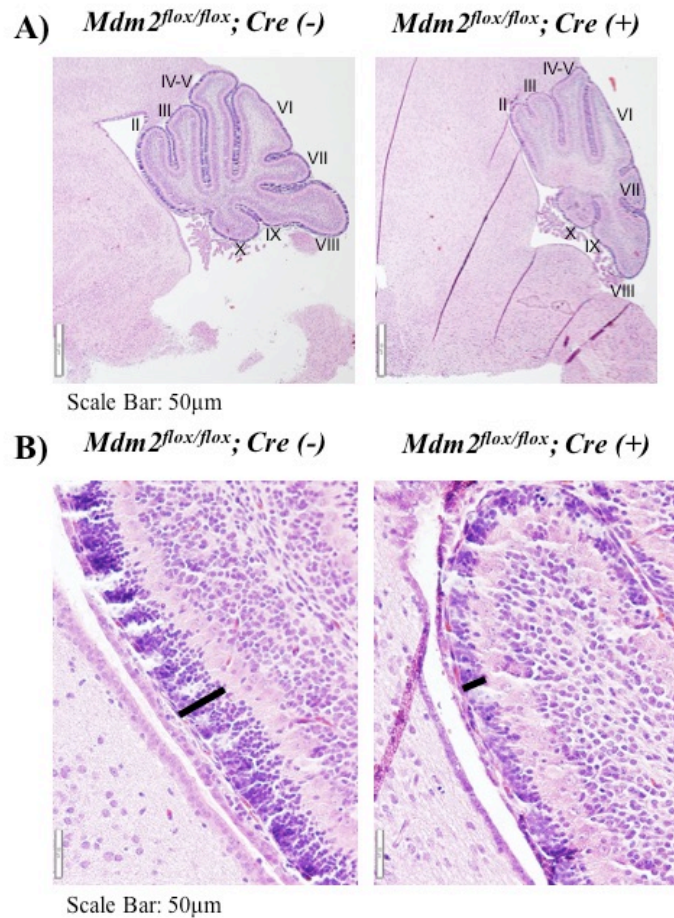


**Figure 3.5 *Mdm2<sup>flox/flox</sup>; Cre (+)* mice injected at P1/P2 have smaller cerebella and disrupted morphology of anterior lobules II and III. A) H&E stained sections at 4X show small cerebellum and abnormal morphology of anterior lobules II and III in *Mdm2<sup>flox/flox</sup>; Cre (+)*. B) H&E stained sections of lobule II at 40X shows thinner EGL in *Mdm2<sup>flox/flox</sup>; Cre (+)*.**

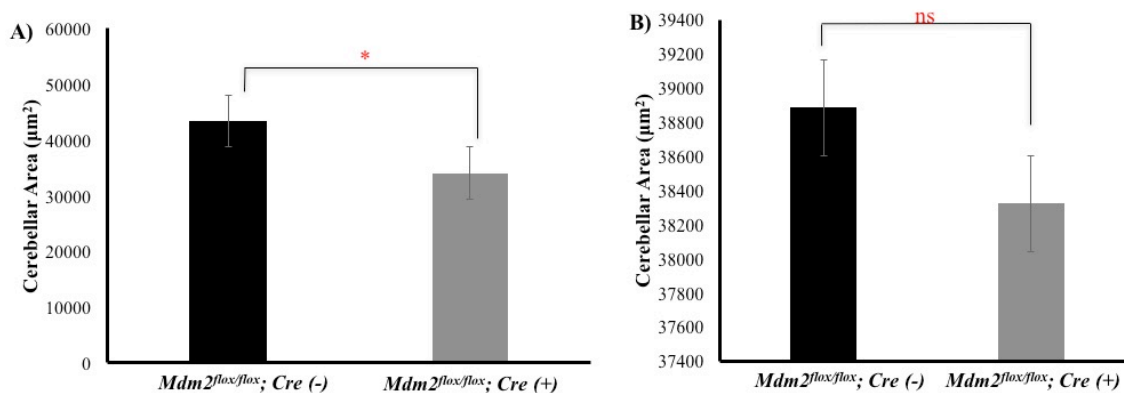


**Figure 3.6 Cerebellar area is significant smaller in  $Mdm2^{flox/flox}; Cre (+)$  mice injected with tamoxifen at P0/P1. A) Average cerebellar area of P0/P1  $Mdm2^{flox/flox}; Cre (-)$  (n=7) and  $Mdm2^{flox/flox}; Cre (+)$  (n=9) tamoxifen-injected mice. \*  $p < 0.05$  B) Average cerebellar area of P1/P2  $Mdm2^{flox/flox}; Cre (-)$  (n=4) and  $Mdm2^{flox/flox}; Cre (+)$  (n=4) tamoxifen-injected mice. ns = not significant,  $p = 0.92$ .**

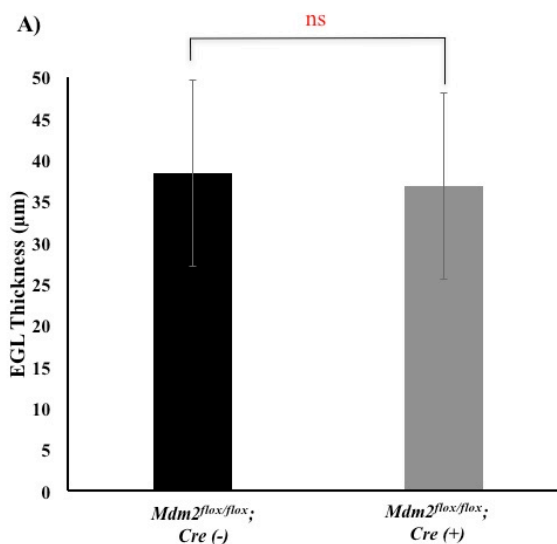


**Figure 3.7 EGL thickness is not significantly reduced in mice after acute deletion of  $Mdm2$ .** The thickness of first lobule was measured in mice with and without  $Mdm2$  deletion in GNPs. The results show there is no significant reduction in the thickness of EGL in  $Mdm2^{flox/flox}; Cre (+)$  compared to  $Mdm2^{flox/flox}; Cre (-)$  ns = not significant,  $p = 0.73$ .

To evaluate the long-term effects of *Mdm2* deletion in GNPs, the cerebella of mice injected with tamoxifen at P0/P1 or P1/P2 was analyzed at P21 when the development of the cerebellum is largely complete. At P21, H&E analyses revealed that the anterior cerebellar lobules of *Mdm2<sup>flox/flox</sup>; Cre (+)* have smaller anterior lobules than control, consistent with the smaller cerebella at P6 mice. These studies suggest that deletion of *Mdm2* during early stages of cerebellar development elicits a reduction of GNPs in the anterior lobules which persists until adulthood and negatively affects the foliation of mature cerebellum.

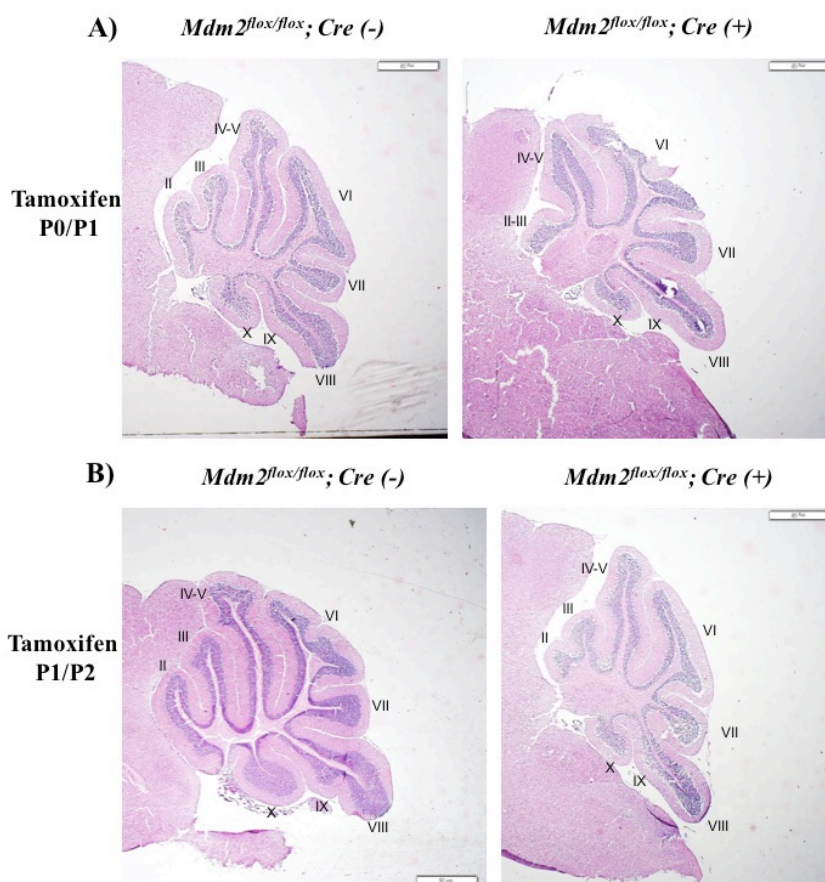


**Figure 3.8 Deletion of *Mdm2* in GNPs disrupts the morphology of anterior cerebellar lobules of three-week-old *Mdm2<sup>flox/flox</sup>; Cre (+)* mice. A) Smaller anterior lobules II and III of three-week-old *Mdm2<sup>flox/flox</sup>; Cre (+)* mice that had been injected with tamoxifen at P0/P1 B) *Mdm2<sup>flox/flox</sup>; Cre (+)* mice injected with tamoxifen at P1/P2 have smaller anterior cerebellar lobules.**

### 3.7 Deletion of *Mdm2* did not significantly increase apoptosis of GNPs in the External Granule Layer of mice

As *Mdm2* limits the apoptotic function of p53, we next determined whether disrupted cerebellar size and morphology of anterior lobules could be attributed to decreased GNP survival. To identify apoptotic cells, I performed TUNEL staining in situ on P6 cerebella. Although the number of TUNEL positive nuclei present in P6 cerebella of *Mdm2<sup>flox/flox</sup>; Cre (+)* appeared qualitatively to be increase, quantitative analyses show there is no significant different between *Mdm2<sup>flox/flox</sup>; Cre (+)* and control *Mdm2<sup>flox/flox</sup>; Cre (-)* mice (Figure 3.8 A and B). These results are consistent with the insignificant difference of EGL thickness measured between *Mdm2<sup>flox/flox</sup>; Cre (+)* and control *Mdm2<sup>flox/flox</sup>; Cre (-)* mice (Figure 3.7). Thus, acute deletion of *Mdm2* does not enhance tapoptosis in GNPs during postnatal cerebellar development.

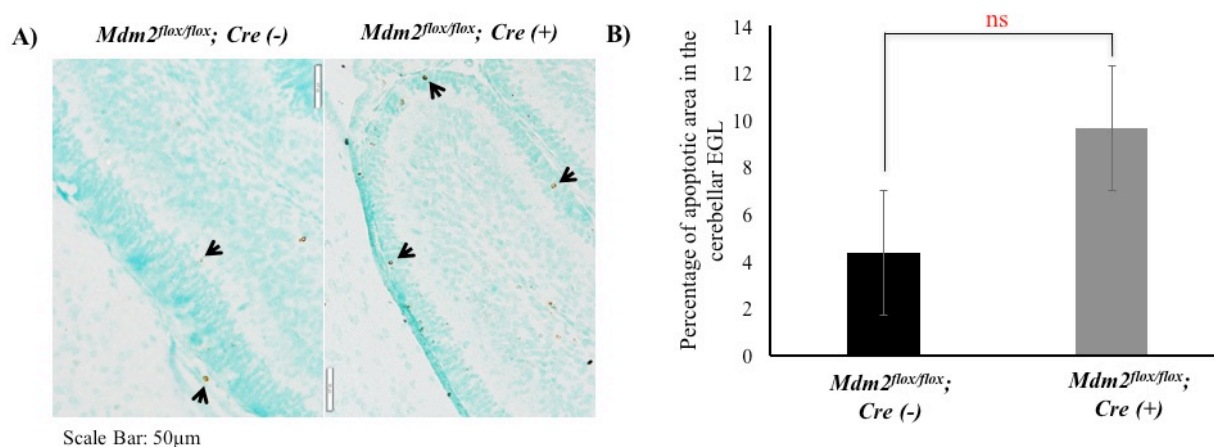


**Figure 3.9 Deletion of *Mdm2* in GNPs does not increase GNPs apoptosis in the EGL.**  
**A)** TUNEL stained sections of lobule II at 40X of mice injected with tamoxifen at P0/P1. TUNEL positive or apoptotic cells (brown nuclei) are indicated with black arrows. **B)** Percentage of apoptotic area in the cerebellar EGL of *Mdm2<sup>flox/flox</sup>; Cre (-)* (n=3) and *Mdm2<sup>flox/flox</sup>; Cre (+)* (n=3) mice. **ns**, p = 0.49

### 3.8 Loss of function of *Mdm2* in GNPs does not affect mice behavior

The cerebellum plays a key role in the control of coordination and motor movements. In order to determine whether *Mdm2* deletion in GNPs negatively affects motor coordination, mice injected with tamoxifen at P0/P1 or P1/P2 were monitored at

P21 for imbalance and hindlimb claspings, neurological signs of loss of coordination characteristic of ataxia (Guyenet et al., 2010). Although loss of Mdm2 negatively impacted cerebellar size and lobule morphology (Figure 3.6) spatiotemporal deletion of *Mdm2* in postnatal GNPs had no effect on the balance and coordination. These observations are consistent with previous analyses of *Mdm2<sup>puro/Δ7-9</sup>* mice in which systemic low levels of Mdm2 resulted in disorganization of cerebellar layers with an increase of GNPs apoptosis in the EGL, reduced cerebellar size and defects in foliation, but failed to impair coordination and motor movements (Malek et al., 2011).

### 3.9 Discussion

Several studies suggest that Mdm2 may be good therapeutic target for treatment of MB Shh subtype. A low level of Mdm2 in *Ptch1<sup>+/-</sup>* mice, a mouse model of Shh-driven MB, suppresses tumor initiation (Malek et al., 2011). In addition, p53 activation by nutlin-3, a small molecule that disrupts the Mdm2 and p53 interaction, causes cell death of human MB cell lines with wild-type p53 (Ghassemifar & Mendrysa, 2012). In mice nutlin-3 decrease the growth of medulloblastoma tumors in a subcutaneous xenograft model concomitant with activation of p53-target gene expression, decreased cell proliferation, and increased tumor cell death (Kunkele et al., 2012). Although these studies highlight the potential of Mdm2 inhibition for treating MB, the role of Mdm2 in postnatal GNPs in the normal developing cerebellum is still not well understood.

Previous studies have shown abnormal development of the cerebellum in *Mdm2<sup>puro/Δ7-9</sup>* mice expressing low levels of Mdm2 throughout embryogenesis (Malek et al., 2011). The cerebella from *Mdm2<sup>puro/Δ7-9</sup>* mice are small in size and have disruption of the foliation pattern, disorganization of cerebellar layers, and increased GNPs apoptosis in the EGL. However, the low levels of Mdm2 in all cells throughout embryogenesis of *Mdm2<sup>puro/Δ7-9</sup>* mice make it challenging to pinpoint the exact time where Mdm2 exert its function in cerebellar development. Although studies with *Mdm2<sup>puro/Δ7-9</sup>* mice demonstrate a role for Mdm2 in prenatal cerebellum development, it is unclear from this model whether Mdm2 continues to occupy a role for GNPs during postnatal cerebellum development. To circumvent these limitations of *Mdm2<sup>puro/Δ7-9</sup>* mice, I have used

*Mdm2<sup>lox/lox</sup>; Math1-CreEr<sup>TM</sup>* mice which allow for spatiotemporal control of *Mdm2* deletion in GNPs specifically during postnatal cerebellar development.

The acute deletion of *Mdm2* in GNPs during postnatal cerebellar development results in smaller cerebella and anterior cerebellar lobules. *Mdm2* loss in GNPs during postnatal cerebellar development could be activating p53-mediated apoptosis causing disrupted anterior lobules morphology. Histology analyses showed that there was a qualitatively increase of TUNEL positive nuclei in the EGL of tamoxifen-injected *Mdm2<sup>lox/lox</sup>; Cre (+)* cerebella suggesting that deletion of *Mdm2* due to Cre recombination activate p53. However, quantification of TUNEL positive nuclei in the EGL revealed no significant difference between *Mdm2<sup>lox/lox</sup>; Cre (-)* and *Mdm2<sup>lox/lox</sup>; Cre (+)* indicating that the acute deletion of *Mdm2* during postnatal cerebellar development does not cause apoptosis of GNPs. At present, we cannot exclude the possibility that non-apoptotic functions of p53 such as cell cycle arrest or early differentiation of GNP contribute to the small size of cerebella with postnatal loss of *Mdm2* in GNPs. The smaller anterior cerebellar lobules in mice with acute deletion of *Mdm2* are consistent with the known pattern of Shh signaling during cerebellar development. *Gli1*, a Shh target gene, is expressed primarily in the anterior and the most posterior cerebellar lobules (Corrales et al., 2006). Deletion of *Mdm2* in proliferating postnatal GNPs could be disturbing *Gli1* expression in the anterior lobules necessary for proper proliferation of GNPs and cerebellar foliation. Indeed, expression of Shh target genes is decreased in the cerebellum of *Mdm2<sup>puro/A7-9</sup>* mice (Malek et al., 2011), indicating that loss of *Mdm2* negatively impacts Shh signaling. In the future, it would be interesting to evaluate whether Shh signaling is altered in the anterior lobules following postnatal deletion of *Mdm2* in GNPs.

Although there is postnatal deletion of *Mdm2* in GNPs negatively affects cerebellar morphology, motor coordination of mice is not negatively impacted in these mice. This lack of motor coordination defects suggests that pharmacological inhibition of *Mdm2* in normal GNPs may not grossly impair cerebellar function. However, in our current model we cannot eliminate the possibility that there is a subset of GNPs in which

the *Mdm2* floxed allele failed to recombine following tamoxifen injection. Cre recombinase efficiency may not optimally induce deletion of *Mdm2* in all GNPs in the cerebellum, resulting in a mosaic of GNPs with and without *Mdm2* deletion. GNPs in which *Mdm2* was not deleted could potentially proliferate and compensate for the loss of cells in which *Mdm2* was deleted. In the future, the efficiency of Cre recombination in GNPs could be evaluated by crossing *Mdm2<sup>flox/flox</sup>; Math1-CreEr<sup>TM</sup>* with Rosa26 reporter (R26R) mice. Mice expressing the R26R have the *LacZ* gene encoding  $\beta$ -galactosidase ( $\beta$ -gal) expressed after Cre-mediated recombination of *loxP* sites (Soriano, 1999). The presence of  $\beta$ -galactosidase activity in GNPs can allow the identification of cells that undergo recombination of the *Mdm2* alleles after activation of Cre recombinase with tamoxifen.

An alternative explanation to see some mice smaller cerebella and anterior lobules after *Mdm2* deletion in GNPs could be their genetic background. Recently, we have observed the phenotype of *Mdm2<sup>puro/ $\Delta$ 7-9</sup>* mice is largely influenced by the genetic background. *Mdm2<sup>puro/ $\Delta$ 7-9</sup>* mice on a 129/Sv x C57BL/6 F1 genetic background are viable and phenotypes including small size and disrupted cerebellar development described before (Mendrysa et al., 2003; Malek et al., 2011). In contrast, *Mdm2<sup>puro/ $\Delta$ 7-9</sup>* mice on an inbred C57BL/6 genetic background die late in gestation or at birth. C57BL/6 *Mdm2<sup>puro/ $\Delta$ 7-9</sup>* embryos display an array of craniofacial deformities (described in Chapter 4). Interestingly, these phenotypes were rescued when p53 was deleted demonstrating that Developmental malformations and perinatal lethality of C57BL/6 *Mdm2<sup>puro/ $\Delta$ 7-9</sup>* mice are p53-dependent. Phenotypic differences between F1 hybrid and inbred C57BL/6 *Mdm2<sup>puro/ $\Delta$ 7-9</sup>* mice suggest that the genetic background may contribute to the modulation p53 activity. In the current study of *Mdm2* in postnatal GNPs, the genetic background of *Mdm2<sup>flox/flox</sup>; Math1-CreEr<sup>TM</sup>* is mixed with a large percentage of 129/Sv. We hypothesize that the genetic background is affecting the cerebellar phenotype in *Mdm2<sup>flox/flox</sup>; Math1-CreEr<sup>TM</sup>* mice when *Mdm2* is deleted in GNPs by the tamoxifen activated Cre recombinase. In conclusion, the new data highlights the importance of the genetic background in p53 activity suggesting the possibility that genetic background of MB patients may influence future treatments of MB that rely on activation of p53.

## **CHAPTER 4: THE ROLE OF MDM2 IN CRANIOFACIAL DEVELOPMENT**

### **4.1 Craniofacial development**

The vertebrate head is a complex structure that protects the brain and provides a scaffold to sustain vital activities such as feeding, breathing and hearing. The development of craniofacial structures is similar between mice and humans beginning during embryonic day (E) 9.5 in mice and 4-5 weeks in humans (Figure 4.1; Suzuki et al., 2015). The structures of the head arise from the growth and fusion of seven processes: frontonasal and paired lateral/medial nasal, maxillary and mandibular. The thickening of the frontonasal process forms the nasal placodes that will give rise to the lateral and medial nasal processes. The maxillary processes emerge from the first branchial arch and grow medially towards the lateral and medial nasal process. Merging of the lateral and medial nasal processes form the primary palate. Palatal shelves of the maxillary processes grow medially and fuse in the midline, giving rise to the secondary palate.

Abnormal development of the head and face is presented in about one third of human birth defects (Trainor, 2010). Frequently, craniofacial abnormalities are observed in people suffering from different congenital syndromes. Individuals presenting craniofacial malformations undergo multiple surgical interventions along their life representing a significant socio-psychological and economic burden for them and their families (Bemmels et al., 2013). An improved understanding of the molecular genes and pathways involved in normal and disrupted craniofacial development could provide potentially valuable information to guide the development of early detection methods and prenatal treatments to prevent head and face defects in newborns. Towards this goal, major attention has been given to the development and maturation of neural crest cells (NCCs) since disruption of this cell population has been implicated in several congenital syndromes with craniofacial abnormalities (Trainor, 2010).

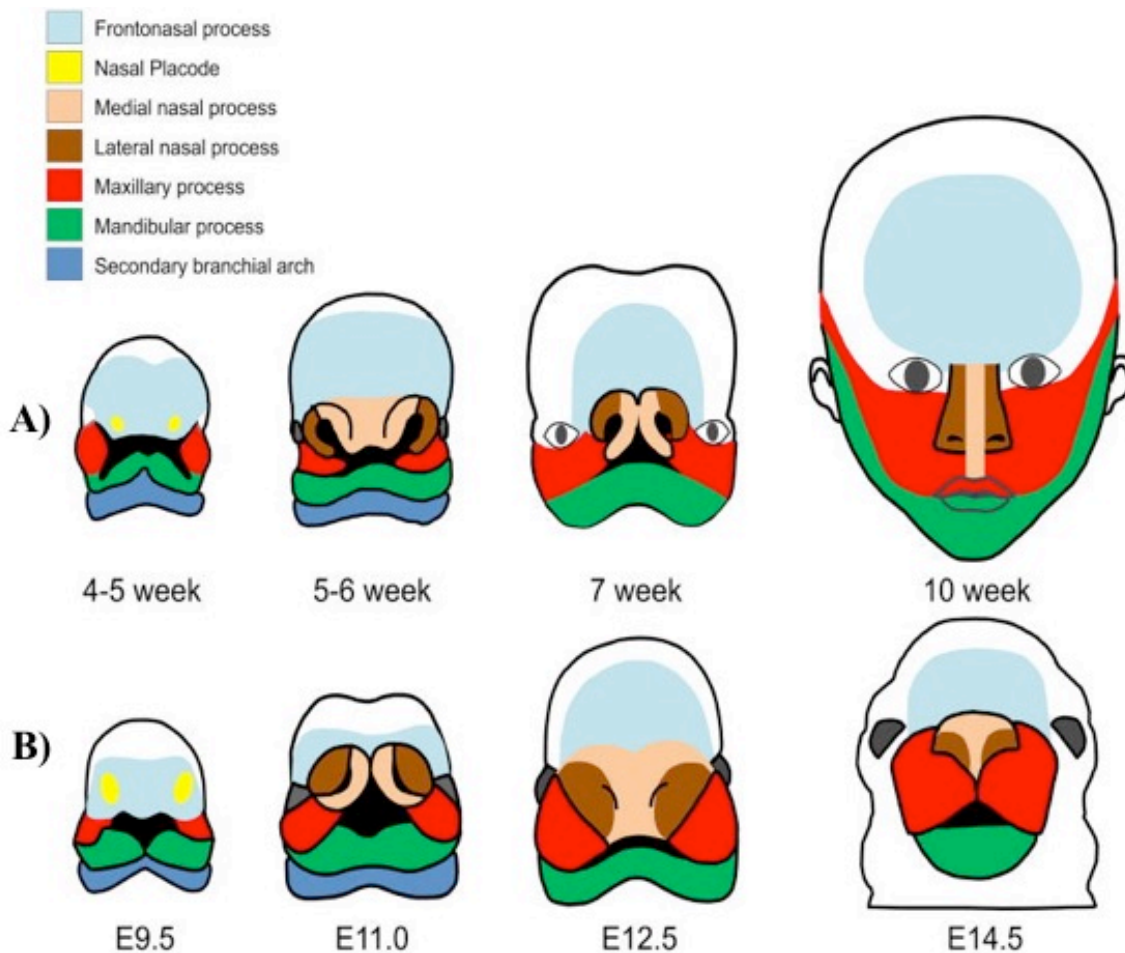


**Figure 4.1 Similarities between murine and human craniofacial development. A)** Human craniofacial development from 4 to 10 weeks. **B)** Murine craniofacial development from embryonic days 9.5 to 14.5. (Figure taken and modified from Suzuki *et al.*, 2015.)

#### 4.1.1 The contribution of neural crest cells (NCCs) in embryo development

During development, NCCs in conjunction with embryonic tissue regulate the morphogenesis of craniofacial structures and other organs. NCCs are pluripotent cells born in the interface between neuroectoderm and surface ectoderm referred as the neural plate border (Selleck & Bronner-Fraser, 1995). During neurulation, the neural plate border undergoes morphological changes to form the neural tube in which NCCs will be induced along its axis. The formation of NCCs in avians, fish and amphibians is controlled by signaling pathways including WNT, BMP and FGF. Less well understood are the pathways involved in mammalian NCC induction (Crane and Trainor, 2006).

NCC delamination from the neural tube is controlled by Snail genes, promoting an epithelial to mesenchymal transition (Bhatt et al., 2013). NCCs migrate by following region-specific pathways to populate the frontonasal area and the 1<sup>st</sup>, 2<sup>nd</sup>, 3<sup>rd</sup> and 4<sup>th</sup> branchial arches (Cordero et al., 2011). NCC-derivative tissues arise from cells that delaminate from the neural tube cranial to posterior axis and migrate to their final cranial, cardiac, trunk and sacral destinations (Vega-Lopez et al., 2018). During head formation, cranial neural crest cells (CNCs) populate different regions of developing craniofacial structures and differentiate into bone, cartilage and connective tissue (Helms et al., 2005). Previous studies have shown that CNC interactions with muscle progenitor cells (derived from mesoderm) are important to establish the musculoskeletal architecture of the head (Rinon et al., 2007; Tzahor et al., 2003). Impairment of NCC proliferation, migration and differentiation is implicated in a diverse class of developmental defects collectively referred to as neurocristopathies (NCP) (Vega-Lopez et al., 2018).

#### **4.2 The role of p53 in craniofacial malformations**

As discussed in Chapter 1, p53 is an important tumor suppressor which limits cancer initiation and progression through its anti-proliferative and pro-apoptotic cellular functions. The primary function of p53 is to induce cell cycle arrest when cells are under moderate stress that negatively affects DNA integrity (El-Deiry et al., 1994; Ho et al., 2005; Hermeking et al., 1997; Xiao et al., 2000). When DNA damage is irreparable, p53 activate genes involve in programmed cell death or apoptosis (Haupt et al., 2003). Additionally, p53 has been determined to play a role in a variety of essential cellular functions such as metabolism, DNA repair, and ribosome biogenesis (Kung & Murphy, 2016; Williams & Schumacher, 2016; Golomba et al., 2014). Though important for tumor suppression, p53 activation during embryogenesis has been implicated in the pathophysiology of congenital syndromes characterized by craniofacial malformations (Table 4.1). Disruptions in developmental pathways and mutations in essential genes that result in birth defects also frequently activate p53 (Danilova et al., 2008). For example, mouse models of congenital syndromes Treacher Collins, CHARGE, Di-George and Diamond-Blackfan Anemia all exhibit heightened p53 activity despite arising from

mutations in diverse genes (Table 4.1; Jones et al., 2008; Watkins-Chow et al., 2013; Van Nostrand et al., 2014; Caprio & Baldini, 2014).

#### 4.2.1 Congenital syndromes that exhibit heightened activation of p53

Treacher Collins Syndrome (TCS) is an autosomal dominant congenital syndrome that affects facial development. Common physical features of TCS patients include ear malformations resulting in hearing loss, downward slanting eyes that can be accompanied with colobomas of lower eyelids, underdeveloped lower jaw and zygomatic bones, and cleft palate (Jones et al., 2008). People affected with TCS typically have mutations in the *TCOF1* gene which encodes the nucleolar phosphoprotein Treacle (Valdez et al., 2004). Treacle occupies an important role in ribosome biogenesis by interacting with key components of pre-ribosomal machinery for ribosomal DNA transcription (Valdez et al., 2004). In addition, Treacle interacts with the NOP56 protein, part of the pre-ribosomal methylation complex, to methylate 18S pre-RNA (Gonzales et al., 2005). Mice heterozygous for *Tcofl*, a model of human TCS, have disrupted ribosomal biogenesis and exhibit craniofacial defects. In these mice, the disruption of ribosomal biogenesis induces p53-dependent apoptosis of neuroepithelial cells that impairs development of NCCs (Jones et al., 2008). Notably, craniofacial defects in *Tcofl*<sup>+/-</sup> mice are mitigated by genetic deletion of p53 as well as prenatal pharmacological inhibition of p53 (Jones et al., 2008). Together, these results underline the importance of p53 and proper ribosome biogenesis during NCC development in order to prevent TCS pathologies.

Enhanced p53 activation is also thought to underlie, in part, the pathophysiology of Diamond-Blackfan Anemia (DBA), a NCP arising from mutations in ribosomal proteins (RPs). People affected with DBA have red cell aplasia during their first year of life and can also present with craniofacial, skeletal, urogenital and heart abnormalities (Vlachos et al., 2008). The phenotype of DBA affected individuals is dependent on which RP is mutated. For instance, mutation in *RPL5* is associated with cleft palate while mutation in *RPL35A* affects genitourinary development. Common amongst cells from patients with DBA arising from mutation of different RPs is the robust activation of p53. Accumulation of p53 protein has been observed in DBA patient-derived CD34+

hematopoietic progenitor cells with mutation in RPS19 leading to p53-dependent cell cycle arrest. Similarly, p53 promoted apoptosis in CD34<sup>+</sup> hematopoietic cells in persons with DBA that arises from mutation in RPL11 (Moniz et al., 2012). In mice, haploinsufficiency for *Rsp7* results in multiple DBA-related phenotypes including vertebral fusion, gross embryonic developmental delay, erythroid maturation delay, and central nervous system (CNS) apoptosis, which can be rescued by *Tp53* haploinsufficiency, demonstrating that p53 contributes to DBA phenotypes seen in these mice (Watkins-Chow et al., 2013). Moreover, *in vitro* studies have shown that overexpression of *RPL5* in H1299 and U2OS cells abrogates Mdm2-mediated inhibition of p53, leading to activation of p53 and cell cycle arrest (Dai & Lu, 2004). Together, studies of DBA have shown that disruption of multiple ribosomal proteins results in p53 activation which, in turn, contributes to the pathogenesis of DBA phenotypes.

Another congenital disorder that exhibits heightened p53 activation is CHARGE syndrome. CHARGE is an acronym for the most common features seen in patients affected with this syndrome which are ocular coloboma, hear defects, choanal atrisia, retarded growth and development, genitourinary hypoplasia, and ear abnormalities. Approximately 70 % of CHARGE patients exhibit mutations in *CHD7*, a gene encoding an ATP-dependent chromatin remodeler (Van Nostrand & Attardi, 2014). Recently, CHARGE syndrome phenotypes including coloboma, cleft palate, and skeletal/ear/heart defects were seen in *Tp53*<sup>25,26,53,54/+</sup> mice that express a transactivation-dead *Tp53* (*Tp53*<sup>25,26,53,54</sup>) which stabilized and heightened wild-type p53 activity (Van Nostrand et al., 2014). *Chd7* binds to the *Tp53* promoter and inhibits its expression in murine NCCs (Van Nostrand et al., 2014). NCCs lacking *Chd7* exhibit increased basal levels of p53 and expression of p53 target genes. Similarly, fibroblasts isolated from CHARGE patients that harbor *CHD7* mutations exhibit increased p53 protein levels and p53 target gene expression (Van Nostrand et al., 2014). These results show the importance of p53 in regulating the pathology of CHARGE syndrome.

DiGeorge syndrome (DGS) is characterized by a microdeletion in chromosome region 22q11.2, and is the most common cause of congenital heart disease (CHD). People

affected with this syndrome present CHD as a consequence of a malformations in the aortic arch and/or cardiac outflow tract (OFT) (Scuccimarri & Rodd, 1998). Other common features of DGS are defects in the thymus and parathyroid gland affecting T cell development and calcium levels, respectively (Scuccimarri & Rodd, 1998). *Tbx1* encodes a transcription factor that regulates the differentiation of the second heart field (SHF) cells in OFT of the developing heart (Watanabe et al., 2012). In *Tbx1*<sup>+/-</sup> mice, haploinsufficiency of the T-box transcription factor 1 recapitulates many of the phenotypes seen in human DGS patients, particularly CHD defects. The cardiac phenotype *Tbx1*<sup>+/-</sup> mice is partially rescued by deletion of  *Tp53* (Caprio & Baldini, 2014). TBX1 and p53 were discovered to share a common target, *Gbx2* (Caprio & Baldini, 2014), which is required for proper NCC migration and patterning in the pharyngeal arches and cardiovascular development (Byrd & Meyers, 2004). *Tbx1* haploinsufficiency led to an increase on p53 levels and a down-regulation of *Gbx2*. In *Tbx1*<sup>+/-</sup> mice lacking  *Tp53*, *Gbx2* levels were reestablished, thereby promoting NCC migration into the pharyngeal arches and heart (Caprio & Baldini, 2014).

Together, these congenital syndromes illustrate the importance of maintain strict controls on p53 function during embryonic development. Interestingly, many of the pathologies associated with these syndromes in mice can be partially rescued by deletion of  *Tp53*, demonstrating the therapeutic potential of inhibiting p53 prenatally.

**Table 4.1 Activation of p53 is involved in the pathology of a variety of congenital syndromes**

<b>Congenital Syndrome</b>	<b>Mouse Model</b>	<b>Defects</b>	<b>Reference</b>
Treacher Collins	<i>TCOF1</i> <sup>+/-</sup>	Increase apoptosis of neural crest cells causes severe frontonasal hypoplasia, doming of skull and severe microphthalmia.	Jones et al, 2008, Nature Medicine
CHARGE	<i>Tp53</i> <sup>25,26,53,54/+</sup>	Coloboma, heart defects, growth retardation, ear defects, cleft palate, mandibular hypoplasia, kidney defects, bone/cartilage defects, thymus aplasia, exencephaly	Van Nostrand et al, 2014, Cell Cycle
Diamond-Blackfan Anemia	<i>Rsp7</i> <sup>Zma/+</sup>	Vertebral fusion, disorganization within neural arches, asymmetric attachment of ribs to sternum, short sternum, delayed development of ossification centers in lumbar and sacral vertebrae, minor delay of optic fissure closure to severe microphthalmia and internalization of entire eye structure, reduction of melanoblast (white belly spot), neuronal apoptosis, reduction in cortical and hippocampal size, enlarged ventricles, deficit in working memory	Watkins-Chow et al, 2013, PLOS Genetics
Di-George	<i>Tbx1</i> <sup>+/-</sup> and <i>Tbx1</i> <sup>-/neo2</sup>	Hypoplasia or aplasia of fourth pharyngeal arch arteries, Defect in the heart outflow tract * <i>p53</i> reduce dosage modified phenotype on <i>Tbx1</i> hypomorphic not null mice.	Caprio & Baldini, 2014, PNAS

#### 4.3 Mouse model to study activation of wild-type p53 during development

Mice containing a combination of hypomorphic (*Mdm2*<sup>puro</sup>) and null (*Mdm2*<sup>Δ7-9</sup>) alleles for *Mdm2* on a F1 129/C57BL/6 genetic background have shown decreased expression of about 30 % of wild-type Mdm2 but their viability has only been reported to be negatively affected when exposed to irradiation (Figure 4.2; Mendrysa et al., 2003).

However, *Mdm2* hypomorphic mice on a F1 129/C57BL/6 genetic background are radiosensitive due to heightened p53 levels (Mendrysa et al., 2003). In contrast, only a few *Mdm2* hypomorphic mice in an inbred C57BL/6 *Mdm2*<sup>puro/Δ7-9</sup> genetic background were born despite repeated crossings of *Mdm2*<sup>+//Δ7-9</sup> and *Mdm2*<sup>puro/+</sup> mice, suggesting that the low level of Mdm2 on this genetic background results in a lethal condition. We have observed a high percentage of p53-dependent craniofacial deformities on inbred C57BL/6 *Mdm2*<sup>puro/Δ7-9</sup> embryos. Most importantly, these developmental defects are dependent on the mouse genetic background since *Mdm2*<sup>puro/Δ7-9</sup> on a F1 129/C57BL/6 genetic background had no craniofacial deformities.

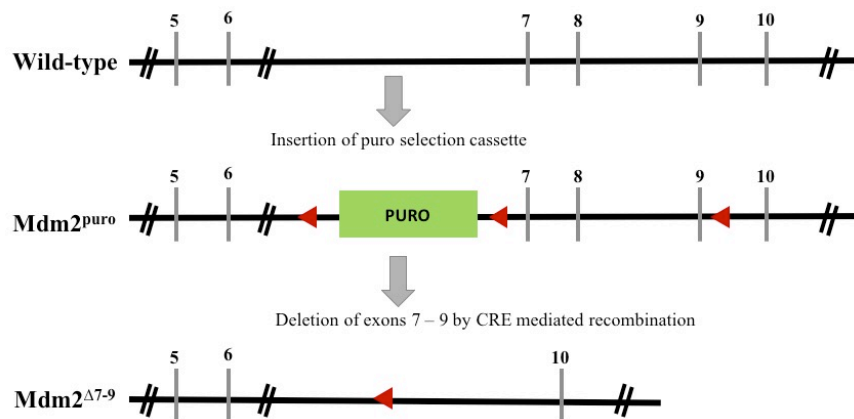


**Figure 4.2 Schematic of *Mdm2* hypomorphic and null alleles.** (A) The *Mdm2*<sup>puro</sup> hypomorphic allele was created by insertion of a puromycin resistance cassette (PURO) after exon 6. *LoxP* sites are present flanking the puromycin resistance cassette and after exon 9. Cre-mediated recombination deleted the puromycin resistance cassette resulting in the generation of the *Mdm2*<sup>Δ7-9</sup> null allele (Mendrysa et al., 2003).

#### 4.4 Perinatal lethality of C57BL/6 *Mdm2* hypomorphic embryos

To delineate the timing of C57BL/6 *Mdm2*<sup>puro/Δ7-9</sup> lethality, *Mdm2*<sup>+//Δ7-9</sup> and *Mdm2*<sup>puro/+</sup> mice were crossed and embryos collected at several stages of development. A chi-square ( $X^2$ ) test of goodness-of-fit was performed to determine whether the four genotypes *Mdm2*<sup>+/+</sup>, *Mdm2*<sup>puro/+</sup>, *Mdm2*<sup>+//Δ7-9</sup>, and *Mdm2*<sup>puro/Δ7-9</sup> were equally present at the expected Mendelian frequency of 25 % each. Genotypic analyses revealed that C57BL/6 *Mdm2*<sup>puro/Δ7-9</sup> embryos were present at the expected Mendelian frequency at E10.5 (n=284,  $X^2=5.324$ ,  $p>0.05$ ), E15.5 (n=210,  $X^2=2.229$ ,  $p>0.05$ ) and E17.5 (n=210,

$X^2=2.266$ ,  $p>0.05$ ) (Table 4.2). Together these results suggest that C57BL/6  $Mdm2^{puro/\Delta7-9}$  embryos die perinatally, between E17.5 and P0.

**Table 4.2 Expected and observed genotype of offspring from C57BL/6  $Mdm2^{puro/+}$  and  $Mdm2^{+/\Delta7-9}$  intercrosses at different embryonic days**

Genotype	E10.5	E15.5	E17.5
	Observed (Expected)	Observed (Expected)	Observed (Expected)
<i>Mdm2</i> <sup>+/+</sup>	86 (71)	45 (53)	25 (20)
<i>Mdm2</i> <sup>puro/+</sup>	68 (71)	59 (53)	18 (20)
<i>Mdm2</i> <sup>+/<math>\Delta</math>7-9</sup>	59 (71)	50 (53)	20 (20)
<i>Mdm2</i> <sup>puro/<math>\Delta</math>7-9</sup>	71 (71)	56 (53)	16 (20)
Total	284	210	79
	$X^2=5.324$ $p=0.149$	$X^2=2.229$ $p=0.526$	$X^2=2.266$ $p=0.519$

#### 4.5 Loss of Mdm2 results in craniofacial malformations in C57BL/6 mice

To begin to characterize the perinatal lethality of inbred C57BL/6  $Mdm2^{puro/\Delta7-9}$  embryos, E15.5 embryos expressing different levels of Mdm2 were collected and examined.  $Mdm2^{puro/\Delta7-9}$  embryos dissected at E15.5 embryos exhibit coloboma (rupture in the structures that compose the eye), tongue protrusion and squared faces compared to their wild-type counterparts. In addition, a subset of  $Mdm2^{puro/\Delta7-9}$  embryos exhibited exencephaly (Table 4.3; Figure 4.3).

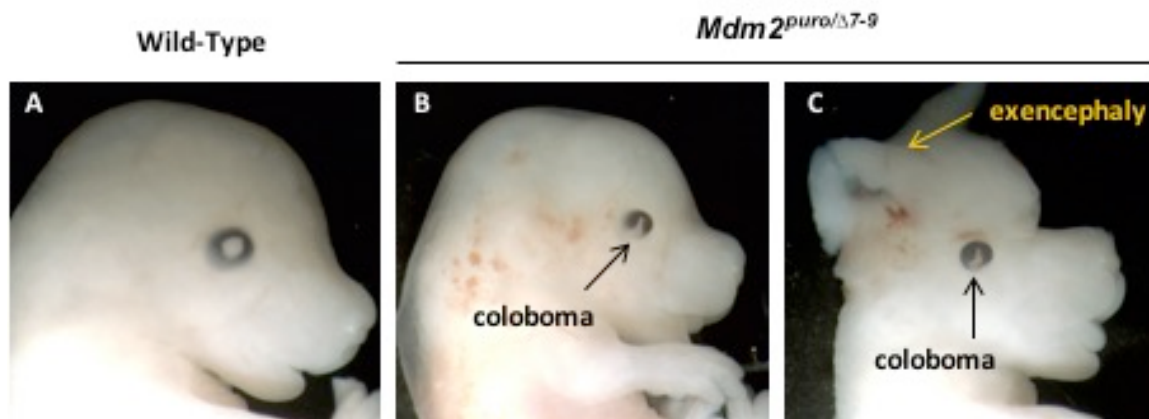


**Figure 4.3 C57BL/6 inbred mice hypomorphic for *Mdm2* exhibit craniofacial malformations.** In contrast to wild-type controls (A), E15.5 *Mdm2<sup>puro/Δ7-9</sup>* embryos (B, C) show an array of craniofacial deformations including squared faces, tongue protrusion, coloboma (black arrows), and exencephaly (yellow arrow).

**Table 4.3 Incidence of phenotypes observed in embryos dissected at E15.5**

Genotype	Number of Embryos	Exencephaly	Coloboma	Squared Faces	Tongue Protrusion
<i>Mdm2<sup>+/+</sup></i>	39	0	4	5	3
<i>Mdm2<sup>puro/+</sup></i>	43	0	4	6	5
<i>Mdm2<sup>+/Δ7-9</sup></i>	48	0	6	16	8
<i>Mdm2<sup>puro/Δ7-9</sup></i>	47	7	21	26	25
Chi-square ( $X^2$ ) test of goodness-of-fit					
Genotype	Number of Embryos	Exencephaly	Coloboma	Squared Faces	Tongue Protrusion
<i>Mdm2<sup>+/+</sup></i>	39	0	4	5	3
<i>Mdm2<sup>puro/Δ7-9</sup></i>	47	7*	21*	26*	25*
Results		$X^2=5.809$ $p=0.016$	$X^2=8.689$ $p=0.003$	$X^2=10.679$ $p=0.001$	$X^2=13.552$ $p=0.0002$

#### 4.6 Bone ossification is decreased in *Mdm2* hypomorphic embryos

In addition to overt craniofacial abnormalities, C57BL/6 *Mdm2<sup>puro/Δ7-9</sup>* embryos are small in size ( $11.928 \pm 1.352$  mm) compared to their wild-type counterparts ( $13.342 \pm 0.816$  mm) suggesting growth retardation (Figure 4.4). Bone development is divided into endochondral and intramembranous ossification. The endochondral ossification is characterized by a cartilage intermediate that is formed by mesenchymal cells and is

found predominantly in the long bones of the appendicular skeleton. In contrast, intramembranous ossification occurs primarily in the bones of the skull directly by mesenchymal cells differentiation into osteoblasts without forming a cartilage intermediate. To determine the effect of Mdm2 loss on cartilage and bone formation, Alcian (blue stain for cartilages) and Alizarin (red stain for bones) staining was performed on E17.5 wild-type and *Mdm2<sup>puro/Δ7-9</sup>* embryos. Bone ossification in skeletons of *Mdm2<sup>puro/Δ7-9</sup>* embryos was reduced as seen by a decrease in of Alizarin (red) staining compared to wild-type skeleton (Figure 4.5 A and D). The parietal and frontal bones of the skull have decreased ossification and appear transparent due to the development as intramembranous bones (Figure 4.5 E). In addition to skull, C57BL/6 *Mdm2<sup>puro/Δ7-9</sup>* embryos also exhibited a considerably decreased mineralization of vertebrae (Figure 4.5 F). The percentage of ossification quantified of the long bones of E17.5 embryos show that *Mdm2* hypomorphic embryos have significant decreased ossification compared to wild-type embryos (Table 4.4; Figure 4.6). Together, these results reveal that a low level of Mdm2 disrupts ossification of the cranial and long bones contributing to the craniofacial and developmental defects observed in the *Mdm2* hypomorphic embryos.

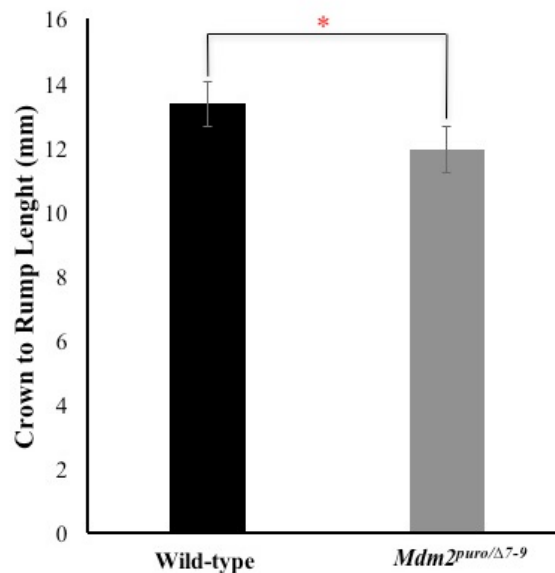


**Figure 4.4 Small size of embryos expressing a low level of Mdm2.** The crown to rump length measurement of E15.5 embryos were taken with an electronic caliper after embryo dissection and before processing tissues for histology. The results show a significant reduction in length of *Mdm2<sup>puro/Δ7-9</sup>* (n=5) as compared wild-type (n=11) embryos (\*p<0.05).

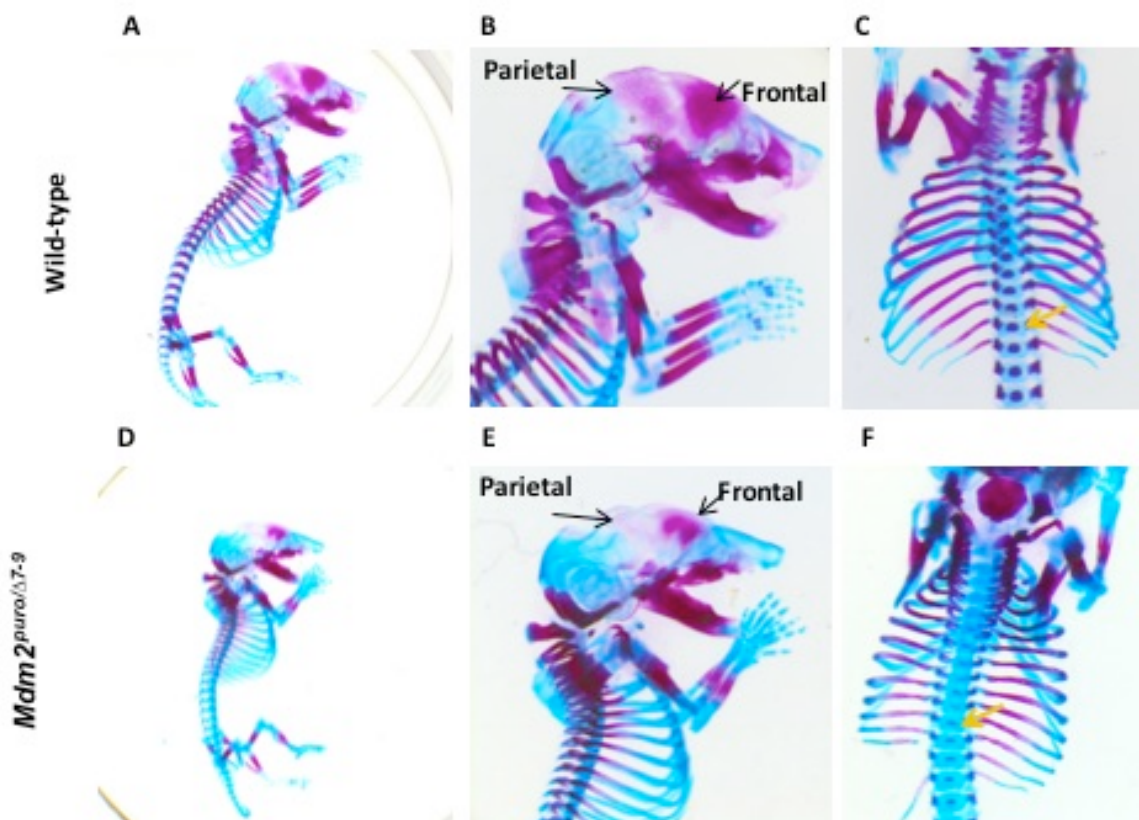


**Figure 4.5 Loss of Mdm2 impairs bone ossification.** Alcian and Alizarin staining was performed on wild-type (A-C) and  $Mdm2^{puro/\Delta 7-9}$  (D-F) embryos at E17.5 to detect bone and cartilage formation. Examination of the whole skeleton shows decreases in bone ossification in  $Mdm2^{puro/\Delta 7-9}$  embryo (D) compared with their wild-type counterpart (A).

Higher magnification of  $Mdm2^{puro/\Delta 7-9}$  embryo in (A) show delayed ossification of parietal and frontal bone (B versus E) and vertebrae (C versus F) as shown as lack of alizarin staining. Black arrows in (B) and (E) pointed to parietal and frontal bones. Yellow arrows in (C) and (F) pointed to ossification centers in the vertebrae. Embryos were stained by Stasa Tumpa and photographed by JCC and Stasa Tumpa.

**Table 4.4 Summary of percentage of the long bone ossification**

Bone	Wild-Type (%)	$Mdm2^{puro/\Delta 7-9}$ (%)	t-test two tailed
Femur	48.002 ± 4.265	36.652 ± 4.769	p=0.004
Tibia	50.855 ± 3.978	42.887 ± 3.806	p=0.012
Humerus	54.889 ± 4.225	48.310 ± 4.252	p=0.039
Ulna	56.589 ± 6.154	43.571 ± 8.563	p=0.024
Radius	56.068 ± 8.693	44.670 ± 6.613	p=0.047

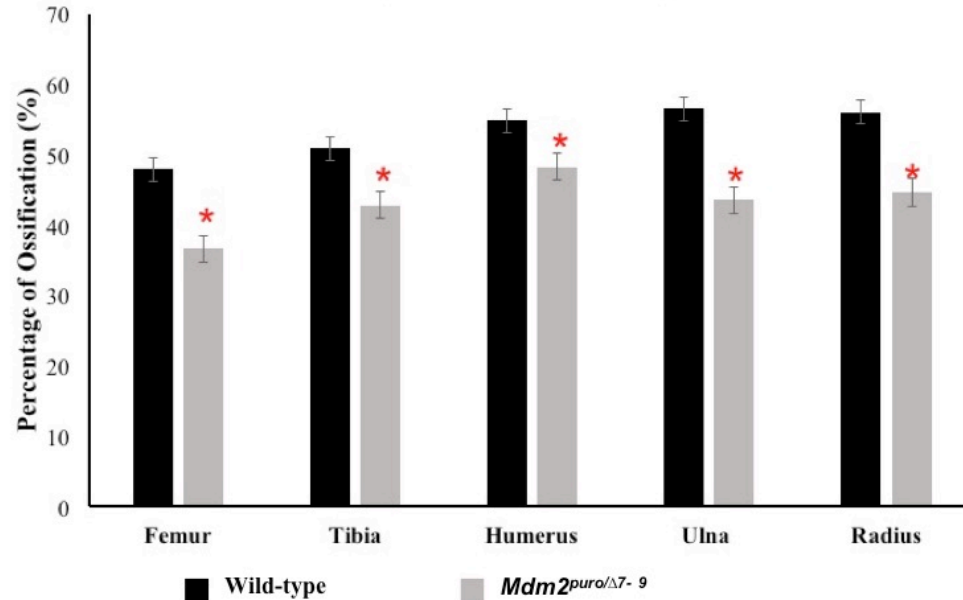


**Figure 4.6 Decreased ossification in *Mdm2<sup>puro/Δ7-9</sup>* embryos.** Graphed is the percentage of bone ossification in long bones of wild-type (n=5) and *Mdm2<sup>puro/Δ7-9</sup>* (n=5) embryos at E17. Quantification was performed using ImageJ software. Ossification in *Mdm2<sup>puro/Δ7-9</sup>* embryos is significantly decreased as compared with wild-type controls (\*p<0.05).

#### 4.7 Palate development is delayed due to low levels of Mdm2

*Mdm2* hypomorphic embryos exhibit squared faces and tongue protrusion, similar to phenotypes identified in the *Tp53<sup>25,26,53,54/+</sup>* mouse model of human CHARGE syndrome in which wild-type p53 function is aberrantly activated (Van Nostrand et al., 2014). As *Tp53<sup>25,26,53,54/+</sup>* mice also exhibit cleft palate we investigated whether activation of p53 in *Mdm2<sup>puro/Δ7-9</sup>* embryos similarly resulted in cleft palate. H&E staining of the developing palate at E15.5 revealed that the Medial Epithelial Seam (MES) located in the developing palate is resolved in all nine wild-type controls (Figure 4.7 A-C), indicating complete fusion of the palatal shelves. In contrast, the MES structure is observed in 50 % (4 out of 8) of *Mdm2<sup>puro/Δ7-9</sup>* embryos, consistent with a delay in the fusion of the palatal shelves (Figure 4.7 F-H). In 25 % (2 out of 8) *Mdm2<sup>puro/Δ7-9</sup>* embryos cleft palate was identified (Figure 4.7 I). Since the disappearance of the MES is controlled by apoptosis (Cecconi et al., 1998; Cuervo and Covarrubias, 2004; Martinez-Alvarez et al., 2004; Vaziri et al., 2005), TUNEL staining was performed to examine apoptotic nuclei along the MES structure in the palate. Apoptotic nuclei were detected in 75 % of *Mdm2<sup>puro/Δ7-9</sup>* (Figure 4.7 J) and 100 % of wild-type (Figure 4.7 K) showing no qualitatively differences

between these genotypes. These results show that  $Mdm2^{puro/\Delta7-9}$  embryos present delayed development of the palate.

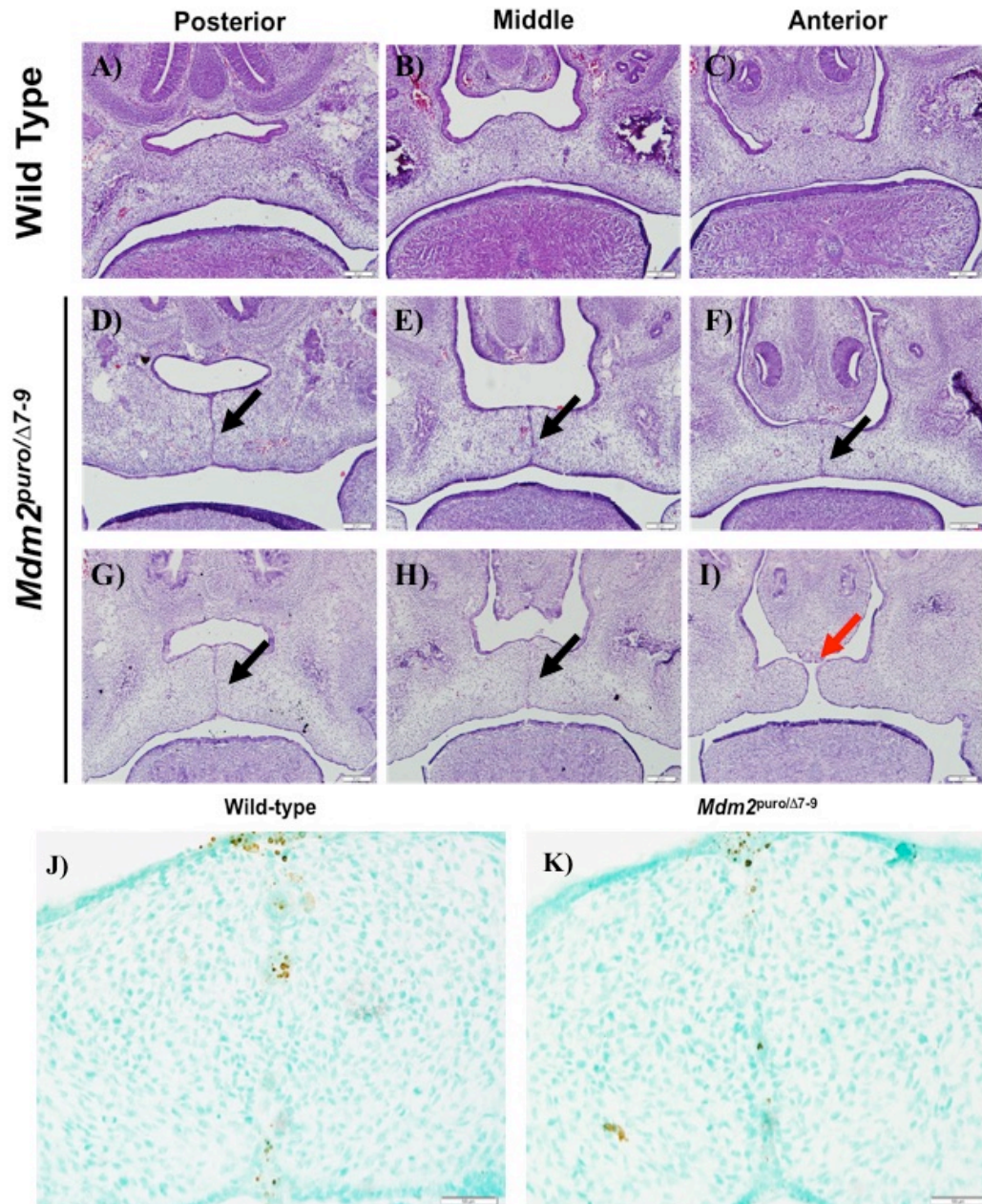


**Figure 4.7 Delayed palatal fusion due to low levels of Mdm2.** A-I) H&E staining on coronal palate of E15.5 wild-type embryos (A-C, n=9) and  $Mdm2^{puro/\Delta7-9}$  (D-I, n=8) and. Black arrows point to MEE structure in pictures D through H. Red arrow points to cleft palate in picture I. Pictures were taken at 10X. Scale bar 20  $\mu$ m. J-K) TUNEL staining slides on coronal palate of E15.5 wild-type (J, n=4) and  $Mdm2^{puro/\Delta7-9}$  (K, n=5) palates. Pictures were taken at 40X. Scale bar 50  $\mu$ m.

#### 4.8 Abnormal eye development due to low levels of Mdm2

In humans, ocular coloboma is frequently associated with craniofacial malformations. Consistent with that observation, gross inspection of E17.5 embryos revealed that 45 % of C57BL/6 *Mdm2<sup>puro/Δ7-9</sup>* embryos exhibited coloboma. The increase in coloboma in *Mdm2<sup>puro/Δ7-9</sup>* relative to wild-type embryos was statistically significant based on chi-square test of goodness-of-fit (n=86,  $X^2= 8.689$ ,  $p < 0.05$ ; Table 4.3). In contrast, coloboma was observed in only 10 % of wild-type embryos. *Mdm2<sup>puro/+</sup>* and *Mdm2<sup>+/Δ7-9</sup>* embryos in which the levels of Mdm2 are modestly reduced exhibited 9 % and 12.5 % coloboma, respectively (Table 4.3; Figure 4.8). Histologically, rupture of the retina resembling coloboma was observed in 17% (1 out of 6) *Mdm2<sup>puro/Δ7-9</sup>* H&E stained eyes (red arrow in Figure 4.8 C). *Mdm2* hypomorphic embryos have microphthalmia (small eyes) compared to wild-type (Figure 4.8 A-C). Quantification of eye areas confirmed the observation that *Mdm2<sup>puro/Δ7-9</sup>* eyes are significantly smaller compared to their wild-type counterparts (Figure 4.8 F). Besides the differences in eye morphology, apoptotic nuclei were only observed in the retina of 4 out of 6 stained *Mdm2* hypomorphic eyes compared to 0 of 4 in their wild-type counterparts (Figure 4.8 E).

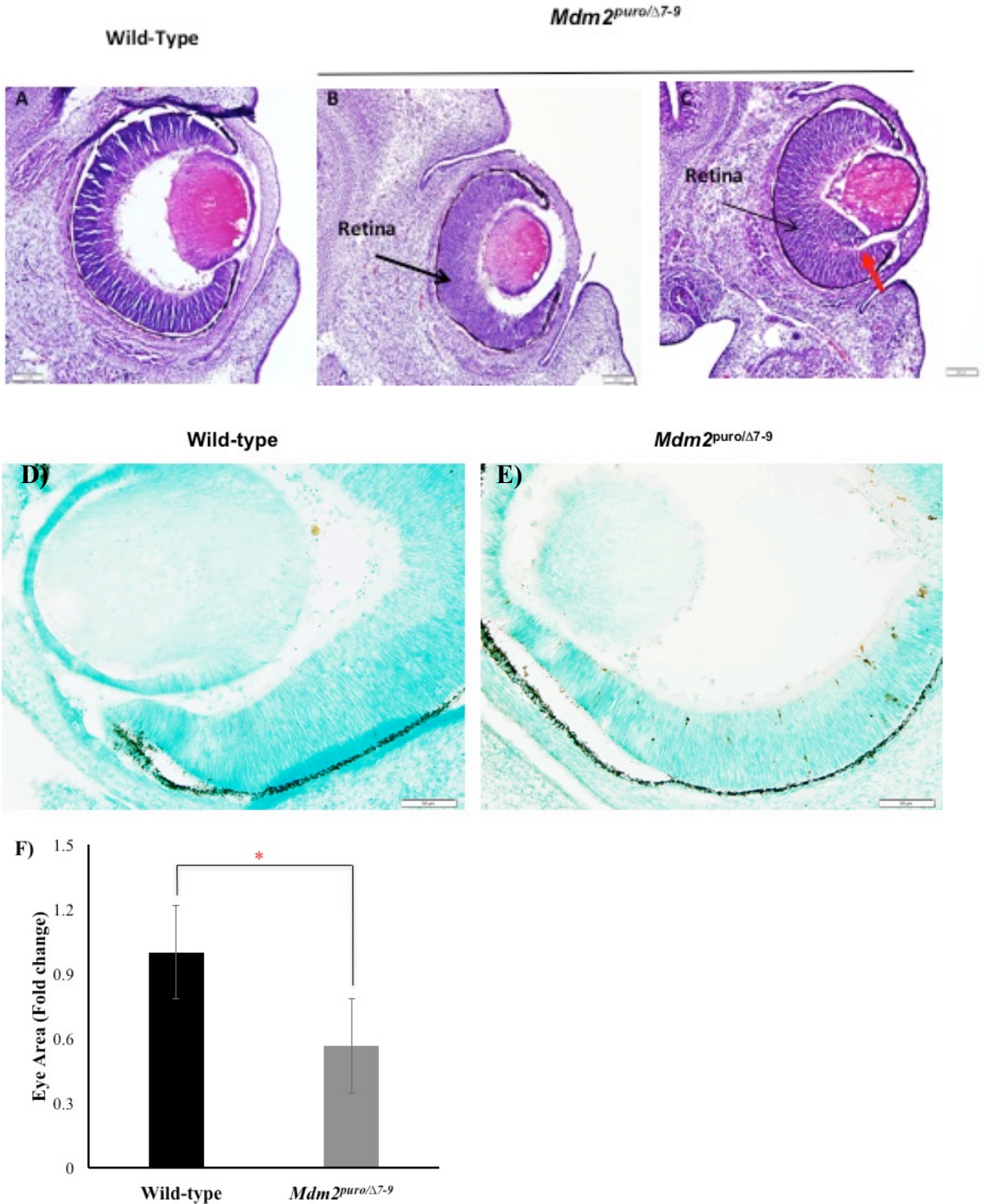


**Figure 4.8 Mice deficient for Mdm2 exhibit microphthalmia, coloboma and increased apoptosis in the retina. A-C) H&E staining in coronal eye of Wild-type (n=3) and *Mdm2* hypomorphic (n=6) embryos. Black arrows (B and C) point to the retina and red arrow (C) points to a rupture in the retina. D-E) TUNEL staining in coronal eye of Wild-type (n=4) and *Mdm2* hypomorphic (n=6) embryos. F) Quantification of eye area of 3 Wild-type and 6 *Mdm2* hypomorphic eyes. \*p<0.05.**

#### 4.9 p53 targets gene expression is increased in embryos expressing a low level of Mdm2

Previously reported phenotypes of  $Mdm2^{puro/\Delta7-9}$  mice on a 129S6/B6 F1 genetic background were p53-dependent, arising from enhanced p53 activity due to a systemically low level of Mdm2 (Mendrysa et al., 2003; Malek et al., 2011). Given the increased severity of phenotypes of  $Mdm2^{puro/\Delta7-9}$  mice on a C57BL/6 genetic background, I hypothesized that p53 activity was higher in  $Mdm2^{puro/\Delta7-9}$  mice on the inbred C57BL/6 compared to F1 129S6/B6 genetic background. To test this hypothesis, p53 protein levels in C57BL/6 and 129S6/B6 F1  $Mdm2$  hypomorphic E10.5 embryos were compared. The results show an increase of p53 levels in  $Mdm2^{puro/\Delta7-9}$  on both genetic backgrounds, compared to their respective wild-type controls (Figure 4.9 A). Surprisingly, the level of p53 level was higher in the  $Mdm2^{puro/\Delta7-9}$  embryos on the 129S6/B6 F1 compared to C57BL/6 background. To corroborate this data, densitometry analysis was performed showing no significant differences of p53 levels between  $Mdm2^{puro/\Delta7-9}$  and WT on both genetic backgrounds (B6,  $p=0.116$ ; F1,  $p=0.263$ ) (Figure 4.9 B). In the future, it would be worth investigating the phosphorylation and activation status of p53 in these genetic backgrounds.

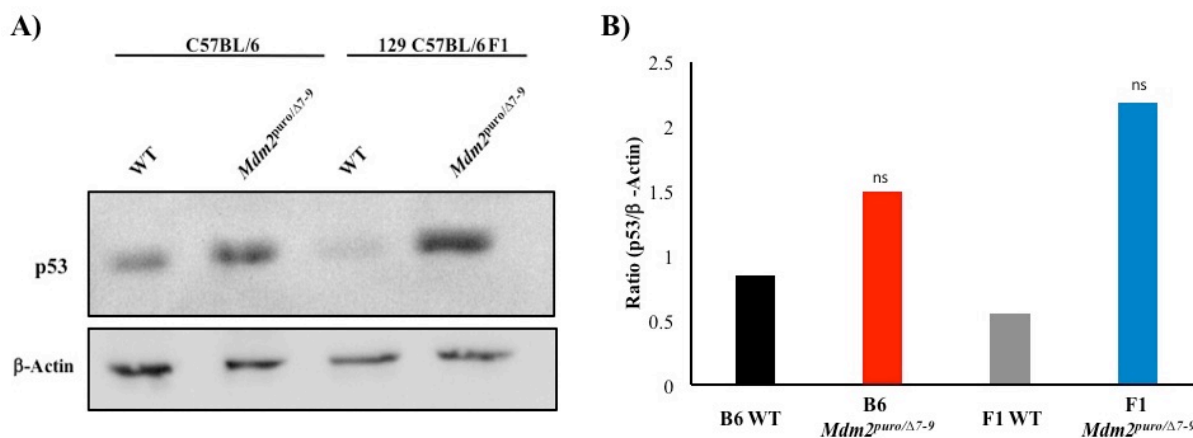


**Figure 4.9 Increased levels of Mdm2 in  $Mdm2^{puro/\Delta7-9}$  embryos.** **A)** WB analysis of p53 levels in E10.5 embryos of indicated genotype and genetic background.  $\beta$ -Actin was used as a loading control. **B)** Densitometry analysis of two independent WB using  $\beta$ -Actin as a loading control. ns=not significance.

In addition to analyzing p53 protein levels, real-time PCR was performed to determine the level of expression of p53 target genes including cell cycle arrest genes *p21* and *CyclinG1* as well as the pro-apoptotic genes *Bax*, *Noxa* and *Perp* in order to compare the activity of p53 expressed in C57BL/6 and 129S6/B6 F1 *Mdm2<sup>puro/Δ7-9</sup>* embryos. For both the 129S6/B6 F1 and C57BL/6 genetic backgrounds, expression of *p21*, *Bax*, *CyclinG1*, *Noxa* and *Perp* was significantly increased in *Mdm2<sup>puro/Δ7-9</sup>* embryos compared to WT (\* $p < 0.01$ ) (Figure 4.10). The increase expression of p53 target genes in *Mdm2<sup>puro/Δ7-9</sup>* embryos confirms in both genetic backgrounds that p53 was activated in the absence of a wild-type levels of Mdm2. To determine whether there is statistically significance difference of the gene expression between B6 and F1 genetic backgrounds, an ANOVA with Tukey test was performed. Based on the results, *CyclinG1* was the only gene significantly different between B6 and F1 *Mdm2<sup>puro/Δ7-9</sup>* embryos (\*\* $p < 0.01$ ).

Previous studies have shown that disruption in Shh signaling pathway leads to decrease NCC proliferation and craniofacial malformations (Brugmann et al., 2010). In addition, studies in our lab have shown that low levels of Mdm2 affected Shh target genes (Malek et al., 2011). Besides p53 target genes, Shh target gene *Gli1* expression was evaluated. The result shows no change in *Gli1* expression among all the four genotypes in E10.5 embryos (Figure 4.10). These results show that p53 activation due to low levels of Mdm2 is increasing the expression of genes that promote cell cycle arrest and apoptosis, which could negatively affect mouse embryogenesis but is not affecting Shh pathway.

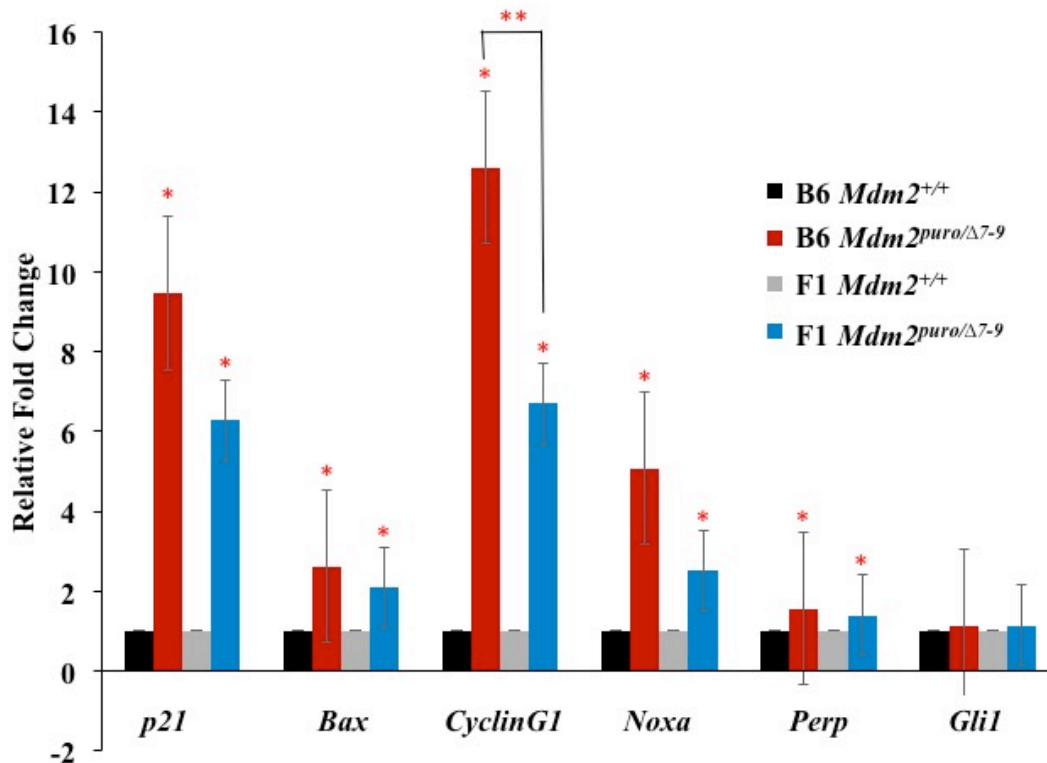


**Figure 4.10 p53 signaling is increased in B6 and F1 embryos expressing low levels of Mdm2.** Expression of p53 target genes *p21*, *Bax*, *CyclinG1*, *Noxa*, and *Perp* and Shh target gene *Gli1* in whole E10.5 embryos was determined by real-time PCR and normalized to *Tubb5*. Graphed is the average fold change in gene expression of p53- and Shh-target genes on the indicated mouse genetic background (B6 = C57BL/6; F1 = 129S6/C57BL/6 F1) and *Mdm2*<sup>puro/Δ7-9</sup> relative to *Mdm2*<sup>+/+</sup> controls (n = 6, \*p<0.05, ANOVA, \*\* p<0.05, ANOVA with Tukey Test).

**Table 4.5 Phenotypes shared among CHARGE syndrome patients and mouse models**

Phenotypes	CHARGE Syndrome (humans)	<i>Tp53</i> <sup>25,26,53,54/+</sup> mice	<i>Mdm2</i> <sup>puro/<math>\Delta</math>7-9</sup> mice
Coloboma	Major	+	+
Exencephaly	Not reported	+	+
Growth Retardation	Minor	+	+
Bone/Cartilage Defects	Minor	+	+
Cleft Palate	Minor	+	+
Ear defects	Major	+	nd
Heart defects	Major	+	*
<b>Mechanism of p53 activation</b>	Loss of CHD7 (Van Nostrand et al., 2014)	Mutant p53 ( <i>Tp53</i> <sup>25,26,53,54</sup> ) (Van Nostrand et al., 2014)	Wild-type p53

+ = determined; nd = not determined; \* = work in progress

#### 4.10 Discussion

In this research project, I characterized the craniofacial phenotype exhibited in inbred C57BL/6 *Mdm2*<sup>puro/ $\Delta$ 7-9</sup> mice that express a systemically low level of Mdm2, the negative regulator of p53. The majority of C57BL/6 *Mdm2*<sup>puro/ $\Delta$ 7-9</sup> embryos exhibited coloboma, tongue protrusion and squared faces compared to their wild-type counterparts. Exencephaly was also detected only in a subset of C57BL/6 *Mdm2*<sup>puro/ $\Delta$ 7-9</sup> embryos. These developmental abnormalities are consistent with those observed in *Tp53*<sup>25,26,53,54/+</sup> mice, model of human CHARGE syndrome, in which wild-type p53 is aberrantly stabilized by a mutant p53 (Table 4.5; Van Nostrand et al., 2014). In contrast, p53 protein is wild-type and its stability and activation under normal cellular controls in *Mdm2*<sup>puro/ $\Delta$ 7-9</sup> mice, this making a *Mdm2*<sup>puro/ $\Delta$ 7-9</sup> mice a robust system for evaluating the consequences of enhanced p53 function in developing and homeostatic tissues.

Inbred C57BL/6 *Mdm2*<sup>puro/ $\Delta$ 7-9</sup> mice die perinatally and exhibit multiple phenotypes including small body size and decreased bone ossification. In a prior study, conditional deletion of *Mdm2* in osteoblast progenitor cells activated p53 causing skeletal defects such as fused lumbar vertebrae, porous cranial bones and reduced bone length and mineralization (Lengner et al, 2006), thereby illustrating the importance of p53 regulation by Mdm2 in osteoblast differentiation. The significant decrease in bone ossification in the long bones of *Mdm2* hypomorphic embryos is consistent with the deletion of *Mdm2* in osteoblast progenitor cells which impair bone formation by decreasing Runx2, a transcription factor expressed in differentiated osteoblast (Lengner et al. 2006). In the future, will be interesting to determine whether *Runx2* expression is decreased in C57BL/6 *Mdm2*<sup>puro/ $\Delta$ 7-9</sup> which would suggest that a threshold of level of Mdm2-p53 is required for proper osteoblast differentiation. We have also shown that a low level of Mdm2 impairs bone ossification, especially in the parietal and frontal bones. Interestingly, embryos lacking p53 show decrease bone density in frontal and parietal bones (Rinon, et al 2011). These results demonstrate that an appropriate level of p53 is required for normal bone skull development and Mdm2 may play an essential role in maintaining the appropriate level of p53.

In addition to decreased bone ossification, delayed palatal shelves fusion with low frequency of cleft palate was detected in a subset of C57BL/6 *Mdm2*<sup>puro/ $\Delta$ 7-9</sup> embryos. Cleft palate represents one the most common birth defect in humans. Multiple environmental and genetic factors have been involved in the etiology of cleft palate (Bush & Jiang, 2012). A better understanding in the molecular pathways that regulate palate development (palatogenesis) would help to design ways for early detection and/or prevention of cleft palate. During mouse development at E10, palatal shelves protruding from the maxillary processes grow vertically along the tongue. At E12-E15 these palatal shelves grow horizontally above the tongue and their Medial Edge Epithelial (MEE) cells fuse to form the Medial Epithelial Seam (MES) (Suzuki et al., 2015). The complete fusion of the palate occurs when MES disappears. Dysregulation of pathways controlling palatal shelves proliferation, fusion or MES disappearance can lead to cleft palate (Iwata et al. 2013). It will be interesting to examine the palate of younger embryos to identify

what is causing the delay in palatal fusion in C57BL/6 *Mdm2<sup>puro/Δ7-9</sup>* mice. In addition, we can examine the palate of older embryos to determine whether MES persist through palate development or it disappear. Studies on the fate of MES during palatogenesis have shown that these cells undergo apoptosis (Xu et al., 2006). One pathway involved in the degeneration of MES is TGFβ which positively regulates *Irf6* and *p21* to coordinate the disappearance of MEE (Iwata et al., 2013). Disruption in TGFβ-mediated *Irf6* lead to submucosal cleft palate, which is characterized by a mucous membrane lining the cleft. The results from the examination of palates in *Mdm2<sup>puro/Δ7-9</sup>* embryos will allow us to determine whether p53 activation disrupt TGFβ during palatogenesis and MEE disappearance.

Craniofacial malformations often arise as a result of congenital syndromes. Recently, p53 have been involved in the pathogenesis of Treacher Collins and CHARGE syndromes, which are characterized by craniofacial defects. Inhibition of p53 in Treacher Collins mouse model prevents the abnormal development of head and face. This result suggests that prenatal inhibition of p53 could be an option to treat craniofacial malformations improving the quality of life of affected individuals. However, phenotypic variations are seen in affected individuals with mutations in the same genes, demonstrating that clinical outcome varies based on genetic background. Interestingly, the only gene that was significantly expressed between C57BL/6 and 129S6/B6 F1 hybrid genetic backgrounds was *CyclinG1* (Figure 4.10). Similarly, upregulation of *CyclinG1* was detected in E8.5 *Tcof<sup>+/-</sup>* embryos, mouse model of Treacher Collins (Jones et al., 2008). In this research project, I had identified that phenotypic penetrance of craniofacial deformities due to deficiency in Mdm2 is dependent on the inbred C57BL/6 mouse genetic background as *Mdm2<sup>puro/Δ7-9</sup>* on a 129S6/B6 F1 hybrid genetic background lacked overt craniofacial phenotypes and survived to adulthood. This observation suggests the existence of p53 modifiers that regulate the activity of this protein. *Mdm2<sup>puro/Δ7-9</sup>* C57BL/6 and 129S6/B6 F1 mice will allow to study the impact of genetic background on the activity of p53 during craniofacial development. *Mdm2<sup>puro/Δ7-9</sup>* mice provide the opportunity of identifying genetic modifiers that are responsible for increasing or attenuating the activity of p53 during embryogenesis.

Future steps in this research project is to determine how activation of p53 is causing these craniofacial defects. I hypothesize that p53 is disrupting NCC development, migration or differentiation based on the structures that were abnormally developed in the inbred C57BL/6 *Mdm2<sup>puro/Δ7-9</sup>* mice. Due to the role of p53 in cell cycle arrest and apoptosis, TUNEL staining of E10.5 C57BL/6 *Mdm2<sup>puro/Δ7-9</sup>* embryos can give us an idea if these cells are undergoing apoptosis during their migration process. In addition, whole mount in situ hybridization using Sox10 marker can be performed to determine whether p53 is disrupting NCC migration. The results from these experiments will reveal whether the craniofacial malformations seen in C57BL/6 *Mdm2<sup>puro/Δ7-9</sup>* mice are a cause of disruption in NCC development. Moreover, RNA sequencing can be performed to gain an insight into the pathways that are deregulated in C57BL/6 *Mdm2<sup>puro/Δ7-9</sup>* compared to C57BL/6 and 129S6/B6 *Mdm2<sup>puro/Δ7-9</sup>* F1 hybrids. This particular experiment will allow the identification of differentially expressed genes in *Mdm2<sup>puro/Δ7-9</sup>* from both genetic backgrounds.

## REFERENCES

- Adesina, A.M., Nalbantoglu, J., and Cavenee, W.K. (1994). p53 gene mutation and mdm2 gene amplification are uncommon in medulloblastoma. *Cancer Res.* 54, 5649–5651.
- Attardi, L. D., Reczek, E. E., Cosmas, C., Demicco, E. G., McCurrach, M. E., Lowe, S. W., and Jacks, T. (2000). PERP, an apoptosis-associated target of p53, is a novel member of the PMP-22/gas3 family. *Genes Dev.* 14; 704–718.
- Baker, S.J., Fearon, E.R., Nigro, J.M., Hamilton, S.R., Preisinger, A.C., Jessup, J.M., vanTuinen, P., Ledbetter, D.H., Barker, D.F., Nakamura, Y., et al. (1989). Chromosome 17 deletions and p53 gene mutations in colorectal carcinomas. *Science* 244; 217–221.
- Barak, Y., Juven, T., Haffner, R., and Oren, M. (1993). *Mdm2* expression is induced by wild type p53 activity. *Embo J.* 12; 461–468.
- Barel, D., Avigad, S., Mor, C., Fogel, M., Cohen, I.J., and Zaizov, R. (1998). A Novel Germ-Line Mutation in the Noncoding Region of the p53 Gene in a Li-Fraumeni Family. *Cancer Genet. Cytogenet.* 103, 1–6.
- Batra, S.K., McLendon, R.E., Koo, J.S., Castelino-Prabhu, S., Fuchs, H.E., Krischer, J.P., Friedman, H.S., Bigner, D.D., and Bigner, S.H. (1995). Prognostic implications of chromosome 17p deletions in human medulloblastomas. *J. Neurooncol.* 24, 39–45.
- Bemmels, H., Biesecker, B., Schmidt, J.L., Krokosky, A., Guidotti, R., and Sutton, E.J. (2013). Psychological and Social Factors in Undergoing Reconstructive Surgery Among Individuals With Craniofacial Conditions: An Exploratory Study. *Cleft Palate Craniofacial Journal*, 50(2); 158–167.
- Ben-Arie, N., Belen, H. J., Armstrong, D. L., McCall, A. E., Gordadze, P. R., Guo, Q., et al. (1997). *Math1* is essential for genesis of cerebellar granule neurons. *Nature* 390; 169–172.
- Bennett, M., Macdonald, K., Chan, S., Luzio, J.P., Simari, R., and Weissberg, P. (1998). Cell Surface Trafficking of Fas: A Rapid Mechanism of p53-Mediated Apoptosis. *Science* vol. 282 issue 5387; 290–293.
- Bhatt, S., Diaz, R., and Trainor, P.A. (2013). Signals and Switches in Mammalian Neural Crest Cell Differentiation. *Cold Spring Harb Perspect Biol* 5; a008326.

Bond, G.L., Hu, W., Bond, E.E., Robins, H., Lutzker, S.G., Arva, N.C., Bargonetti, J., Bartel, F., Taubert, H., Wuerl, P., Onel, K., Yip, L, Hwang, S.J., Strong, L.C., Lozano, G., and Levine, A.J. (2004). A single nucleotide polymorphism in the MDM2 promoter attenuates the p53 tumor suppressor pathway and accelerates tumor formation in humans. *Cell* vol. 119; 591–602.

Bond, G.L., Hirshfield, K.M., Kirchhoff, T., Alexe, G., Bond, E.E., Robins, H., Bartel, F., Taubert, F., Wuerl, P., Hait, W., Toppmeyer, D., Offit, K., and Levine, A.J. (2006). MDM2 SNP309 accelerates tumor formation in a gender specific and hormone-dependent manner. *Cancer Research* vol. 66; 5104–5110.

Boon, K., Eberhart, C.G., and Riggins, G.J. (2005). Genomic Amplification of Orthodenticle Homologue 2 in Medulloblastomas. *Cancer Research* 65: (3); 703–707.

Bouvard, V., Zaitchouk, T., Vacher, M., Duthu, A., Canivet, M., Choisy-Rossi, C., Nieruchalski, M., and May, E. (2000). Tissue and cell-specific expression of the p53-target genes: *bax*, *fas*, *mdm2* and *waf1/p21*, before and following ionizing irradiation in mice. *Oncogene* 19; 649–660.

Boyd SD, Tsai KY, Jacks T (2000) An intact HDM2 RING-finger domain is required for nuclear exclusion of p53. *Nat Cell Biol* 2; 563–568.

Brugmann, S.A., Cordero, D.R., and Helms, J.A. (2010). Craniofacial Ciliopathies: A New Classification for Craniofacial Disorders. *American Journal of Medical Genetics Part A* 152; 2995–3006.

Brynczka, C., Labhart, P., and Merrick, B.A. (2007). NGF-mediated transcriptional targets of p53 in PC12 neuronal differentiation. *Bmc Genomics* 8; 139.

Buchholz M, Schatz, A., Wagner, M., Michl, P., Linhart, T., Adler, G., Gress, T.M., and Ellenrieder, V. (2006). Overexpression of c-myc in pancreatic cancer caused by ectopic activation of NFATc1 and the Ca<sup>2+</sup>/calcineurin signaling pathway. *The EMBO Journal* 25; 3714–3724.

Burns, T. F., Bernhard, E. J., and El-Deiry, W. S. (2001). Tissue specific expression of p53 target genes suggests a key role for KILLER/DR5 in p53- dependent apoptosis in vivo. *Oncogene* 20; 4601–4612.

Bush, J.O. and Jiang, R. (2012) Palatogenesis: morphogenetic and molecular mechanisms of secondary palate development. *Development* 139; 231–243.

Byrd, N.A., and Meyers, E.N. (2005). Loss of Gbx2 results in neural crest cell patterning and pharyngeal arch artery defects in the mouse embryo. *Developmental Biology* 284(1); 233–245.

- Caddy, K. W. and Biscoe, T. J. (1979). Structural and quantitative studies on the normal C3H and Lurcher mutant mouse. *Philos. Trans. R. Soc. Lond. B Biol. Sci.* 287; 167–201.
- Cahilly-Snyder, L., Yang-Feng, T., Francke, U., and George, D.L. (1987). Molecular Analysis and Chromosomal Mapping of Amplified Genes Isolated from a Transformed Mouse 3T3 Cell Line. *Somatic Cell and Molecular Genetics* vol. 13 no. 3; 235 – 244.
- Caprio, C. and Baldini, A. (2014). p53 suppression partially rescues the mutant phenotype in mouse models of DiGeorge syndrome. *PNAS* vol. 111 no. 37; 13385–13390.
- Carballo, G.B., Honorato, J.R., de Lopes, G.P.F., and Spohr, T.C.L.S.E. (2018). A highlight on Sonic hedgehog pathway. *Cell Communication and Signaling* vol. 16 no. 11; 1–15.
- Cecconi, F., Alvarez-Bolado, G., Meyer, B. I., Roth, K. A., and Gruss, P. (1998). Apaf1 (CED-4 homolog) regulates programmed cell death in mammalian development. *Cell* 94; 727–737.
- Chao, C., Hergenahn, M., Kaeser, M.D., Wu, Z., Saito, S., Iggo, R., Hollstein, M., Appella, E., and Xu, Y. (2003). Cell Type- and Promoter-specific Roles of Ser18 Phosphorylation in Regulating p53 Responses. *Journal of Biological Chemistry* 278; 41028–41033.
- Chao, C., Herr, D., Chun, J., and Xu, Y. (2006). Ser18 and 23 phosphorylation is required for p53-dependent apoptosis and tumor suppression. *EMBO J.* 25; 2615–2622.
- Chari, N.S., Pinaire, N.L., Thorpe, L., Medeiros, L.J., Routbort, M.J., and McDonnell, T.J. (2009). The p53 tumor suppressor network in cancer and the therapeutic modulation of cell death. *Apoptosis* 14; 336–347.
- Chen, J., Lin, J., & Levine, A. J. (1995). Regulations of transcription functions of the p53 tumor suppressor by the mdm-2. *Molecular Medicine*, 1 (2); 142–152.
- Cho, Y., Gorina, S., Jeffrey, P.D., and Pavletic, N.P. (1994). Crystal structure of a p53 tumor suppressor-DNA complex: understanding tumorigenic mutations. *Science* vol. 265; 346–355.
- Cho, Y.-J., Tsherniak, A., Tamayo, P., Santagata, S., Ligon, A., Greulich, H., Berhoukim, R., Amani, V., Goumnerova, L., Eberhart, C.G., et al. (2011). Integrative genomic analysis of medulloblastoma identifies a molecular subgroup that drives poor clinical outcome. *J. Clin. Oncol.* 29; 1424–1430.

- Choi, Y. J., Lin, C. P., Ho, J. J., He, X., Okada, N., Bu, P., Zhong, Y., Kim, S. Y., Bennett, M. J., Chen, C., Ozturk, A., Hicks, G.G., Hannon, G.J., and He, L. (2011). miR-34 miRNAs provide a barrier for somatic cell reprogramming. *Nature Cell Biology* 13; 1353–1360.
- Chow, L., Tian, Y., Weber, T., Corbett, M., Zuo, J., Baker, S.J., (2006). Inducible Cre Recombinase Activity in Mouse Cerebellar Granule Cell Precursors and Inner Ear Hair Cells. *Developmental Dynamics* 235; 2991–2998.
- Cordon-Cardo, C., Latres, E., Drobnyak, M., Oliva, M.R., Pollack, D., Woodruff, J.M., Marechal, V., Chen, J., Brennan, M.F., Levine, A.J. (1994). Molecular abnormalities of *mdm2* and *p53* genes in adult soft tissue sarcomas. *Cancer Res* 54; 794–799.
- Cordero, D.R., Brugmann, S., Chu, Y., Bajpai, R., Jame, M., Helms, J.A. (2011). Cranial neural crest cells on the move: Their roles in craniofacial development. *Am J Med Genet Part A* 155; 270–279.
- Corrales, J.D., Blaess, S., Mahoney, E.M., and Joyner, A.J. (2006). The level of sonic hedgehog signaling regulates the complexity of cerebellar foliation. *Development* 133; 1811–1821.
- Crane, J.F. and Trainor, P.A. (2006). Neural Crest Stem and Progenitor Cells. *Annual Review of Cell and Developmental Biology* 22:1; 267–286.
- Cuervo, R., and Covarrubias, L. (2004). Death is the major fate of medial edge epithelial cells and the cause of basal lamina degradation during palatogenesis. *Development* 131; 15–24.
- Dai, M.S., Zeng, S.X., Jin, Y., Sun, X.X., David, L., and Lu, H. (2004). Ribosomal Protein L23 Activates p53 by Inhibiting MDM2 Function in Response to Ribosomal Perturbation but Not to Translation Inhibition. *Molecular and Cellular Biology*, vol. 24 no. 17; 7654–7668.
- Dai, M.S. and Lu, H. (2004). Inhibition of MDM2-mediated p53 Ubiquitination and Degradation by Ribosomal Protein L5\*. *The Journal of Biological Chemistry* vol. 279 no. 43; 44475–44482.
- Danilova, N., Sakamoto, K.M., and Lin, S. (2008) Role of p53 Family in Birth Defects: Lessons from Zebrafish. *Birth Defects Research (Part C)* 84; 215–227.
- de Haas, T., Oussoren, E., Grajkowska, W., Perek-Polnik, M., Popovic, M., Zadavec-Zalatel, L., Perera, M., Corte, G., Wirths, O., van Sluis, P., Pietsch, T., Troost, D., Baas, F., Versteeg, R., Kool, M. (2006). OTX1 and OTX2 expression correlates with the clinicopathologic classification of medulloblastomas. *J Neuropathol Exp Neurol* 65; 1–11.

Deng, C., Zhang, P., Harper, J.W., Elledge, S.J., and Leder, P. (1995) Mice Lacking p21<sup>CIP1/WAF1</sup> Undergo Normal Development, but Are Defective in G1 Checkpoint Control. *Cell* vol. 82; 875–884.

Donehower, L.A., Harvey, M., Slagle, B.L., McArthur, M.J., Montgomery, C.A., Jr, Butel, J.S., and Bradley, A. (1992). Mice deficient for p53 are developmentally normal but susceptible to spontaneous tumours. *Nature* 356; 215–221.

Donehower L. A. (1996). The p53-deficient mouse: a model for basic and applied cancer studies. *Seminars in Cancer Biology* vol.7(5); 269–278.

Dornan, D., Wertz, I., Shimizu, H., Arnott, D., Frantz, G.D., Dowd, P., O'Rourke, K., Koeppen, H., Dixit, V.M. (2004) *Nature* 429; 86–92.

Dulic, V., Kaufmann, W.K., Wilson, S.J., Tlsty, T.D., Lees, E., Harper, J.W., Elledge, S.J., and Reed, S.I. (1994). p53-dependent inhibition of cyclin- dependent kinase activities in human fibroblasts during radiation-induced G1 arrest. *Cell* 76; 1013–1023.

Eberhart, C.G. (2003). Medulloblastoma in mice lacking p53 and PARP: all roads lead to Gli. *Am. J. Pathol.* 162, 7–10.

Eizenberg, O., Faber-Elman, A., Gottlieb, E., Oren, M., Rotter, V., and Schwartz, M. (1996). p53 plays a regulatory role in differentiation and apoptosis of central nervous system-associated cells. *Mol. Cell. Biol.* 16; 5178–5185.

Eliyahu, D., Raz, A., Gruss, P., Givol, D., and Oren, M. (1984). Participation of p53 cellular tumour antigen in transformation of normal embryonic cells. *Nature.* 312; 646–649.

El-Deiry, W.S., Harper, J.W., O'Connor, P.M., Velculescu, V.E., Canman, C.E., Jackman, J., Pietenpol, J.A., Burrell, M., Hill, D.E., and Wang, Y. (1994). WAF1/CIP1 is induced in p53-mediated G1 arrest and apoptosis. *Cancer Res.* 54; 1169–1174.

Ellison, D.W., Onilude, O.E., Lindsey, J.C., Lusher, M.E., Weston, C.L., Taylor, R.E., Pearson, A.D., and Clifford, S.C. (2005).  $\beta$ -Catenin status predicts a favorable outcome in childhood medulloblastoma: The United Kingdom Children's Cancer Study Group Brain Tumour Committee. *Journal of Clinical Oncology* vol. 23 no. 31; 7951–7957.

Esser, C., Scheffner, M., Hohfeld, J. (2005). The chaperone-associated ubiquitin ligase CHIP is able to target p53 for proteasomal degradation. *Journal of Biological Chemistry* vol. 280 no. 29; 27443–27448.

Fakharzadeh, S.S., Trusko, S.P., and George, D.L. (1991). Tumorigenic potential associated with enhanced expression of a gene that is amplified in a mouse tumor cell line. *Embo J.* 10; 1565–1569.

- Feil, S., Valtcheva, N., and Feil, R. (2009). Inducible Cre Mice. (R. Kuhn, & W. Wurst, Eds.) *Gene Knockout Protocols: Second Edition* 530; 343–363.
- Frappart, P.-O., Lee, Y., Russell, H.R., Chalhoub, N., Wang, Y.-D., Orii, K.E., Zhao, J., Kondo, N., Baker, S.J., and McKinnon, P.J. (2009). Recurrent genomic alterations characterize medulloblastoma arising from DNA double-strand break repair deficiency. *Proc. Natl. Acad. Sci. U. S. A.* 106, 1880–1885.
- Gajjar, A., Chintagumpala, M., Ashley, D., Kellie, S., Kun, L.E., Merchant, T.E., Woo, S., Wheeler, G., Ahern, V., Krasin, M.J., Fouladi, M., Broniscer, A., Krance, R., Hale, G.A., Stewart, C.F., Dauser, R., Sanford, R.A., Fuller, C., Lau, C., Boyett, J.M., Wallace, D., and Gilbertson, R.J. (2006). Risk-adapted craniospinal radiotherapy followed by high-dose chemotherapy and stem-cell rescue in children with newly diagnosed medulloblastoma (St Jude Medulloblastoma-96): long-term results from a prospective, multicentre trial. *Lancet Oncology* vol. 7 no. 10; 813–820.
- Geyer, R.K., Yu, Z.K., and Maki, C.G. (2000). The MDM2 RING-finger domain is required to promote p53 nuclear export. *Nat. Cell Biol.* 2; 569–573.
- Ghassemifar, S., and Mendrysa, S.M. (2012) MDM2 antagonism by nutlin-3 induces death in human medulloblastoma cells. *Neuroscience Letters* 513; 106–110.
- Golomba, L., Volarevic, S., Oren, M. (2014) p53 and ribosome biogenesis stress: the essentials. *Federation of European Biochemical Societies Letters*; 2571–2579.
- Goldowitz, D. and Hamre, K. (1998). The cells and molecules that make a cerebellum. *Trends in Neurosciences*, 21 (9); 375–382.
- Gonzales, B., Henning, D., So, R.B., Dixon, J., Dixon, M.J., Valdez, B.C. (2005). The Treacher Collins syndrome (TCOF1) gene product is involved in pre-rRNA methylation. *Hum Mol Genet* 14; 2035–2043.
- Goodman, R.H. and Smolik, S. (2000). CBP/p300 in cell growth, transformation, and development. *Genes & Development* 14;1553–1577.
- Gu, W. and Roeder, R.G. (1997). Activation of p53 Sequence-Specific DNA Binding by Acetylation of the p53 C-Terminal Domain. *Cell* vol. 90; 595–606.
- Guyenet, S.J., Furrer, S.A., Damian, V.M., Baughan, T.D., La Spada, A.R., and Garden, G.A. (2010). A Simple Composite Phenotype Scoring System for Evaluating Mouse Models of Cerebellar Ataxia. *JoVE*. 39.
- Hamilton, S.R., Liu, B., Parsons, R.E., Papadopoulos, N., Jen, J., Powell, S.M., Krush, A.J., Berk, T., Cohen, Z., and Tetu, B. (1995). The molecular basis of Turcot's syndrome. *N. Engl. J. Med.* 332; 839–847.

- Harper, J.W., Adami, G.R., Wei, N., Keyomarsi, K. and Elledge, S.J. (1993) The p21 Cdk-Interacting Protein Cipl Is a Potent Inhibitor of G1 Cyclin-Dependent Kinases. *Cell* vol. 75; 805–816.
- Haupt, Y., Maya, R., Kazaz, A., and Oren, M. (1997). Mdm2 promotes the rapid degradation of p53. *Nature* vol. 387 issue 6630; 296–299.
- Haupt, S., Berger, M., Goldberg, Z., and Haupt, Y. (2003). Apoptosis – the p53 network. *Journal of Cell Science* 116; 4077–4085.
- Heby-Henricson, K., Bergström, A., Rozell, B., Toftgard, R., and Teglund, S. (2012). Loss of Trp53 promotes medulloblastoma development but not skin tumorigenesis in Sufu heterozygous mutant mice. *Mol. Carcinog.* 51, 754–760.
- Helms, J.A., Cordero, D., and Tapadia, M.D. (2005). New insights into craniofacial morphogenesis. *Development* 132; 851–861.
- Herman, A.G., Hayano, M., Poyurovsky, M.V., Shimada, K., Skouta, R., Prives, C., and Stockwell, B.R. (2011). Discovery of Mdm2-MdmX E3 Ligase Inhibitors Using a CellBased Ubiquitination Assay. *Cancer Discovery* 1(4); 312–325.
- Hermeking, H., Lengauer, C., Polyak, K., He, T.C., Zhang, L., Thiagalingam, S., Kinzler, K.W., and Vogelstein, B. (1997). 14-3-3sigma is a p53-regulated inhibitor of G2/M progression. *Molecular Cell* vol.1; 3–11.
- Ho, J.S.L., Ma, W., Mao, D.Y.L., and Benchimol, S. (2005). p53-Dependent transcriptional repression of c-myc is required for G1 cell cycle arrest. *Mol. Cell. Biol.* 25; 7423–7431.
- Hollstein M., Sidransky D., Vogelstein B. and Harris C. C. (1991). p53 mutations in human cancers. *Science* 253; 49–53.
- Honda, R., Tanaka, H., & Yasuda, H. (1997). Oncoprotein MDM2 is a ubiquitin ligase E3 for tumor suppressor p53. *Federation of European Biochemical Societies*; 25–27.
- Honda, R. and Yasuda, H. (1999). Association of p19ARF with Mdm2 inhibits ubiquitin ligase activity of Mdm2 for tumor suppressor p53. *The EMBO Journal* vol.18 no.1; 22–27.
- Hong, H., Takahashi, K., Ichisaka, T., Aoi, T., Kanagawa, O., Nakagawa, M., Okita, K., and Yamanaka, S. (2009). Suppression of induced pluripotent stem cell generation by the p53-p21 pathway. *Nature* 460; 1132–1135.
- Issaeva, N., Bozko, P., Enge, M., Protopopova, M., Verhoef, L.G., Masucci, M., Pramanik, A., and Selivanova, G. (2004). Small molecule RITA binds to p53, blocks p53-HDM-2 interaction and activates p53 function in tumors. *Nat Med.* 10:132; 1–8.

Iwata, J.I., Suzuki, A., Pelikan, R.C., Ho, T.V., Sanchez-Lara, P.A., Urata, M., Dixon, M.J., Chai, Y. (2013) Smad4-Irf6 genetic interaction and TGF $\beta$ -mediated IRF6 signaling cascade are crucial for palatal fusion in mice. *Development* 140; 1220–1230.

Jacks, T., Remington, L., Williams, B.O., Schmitt, E.M., Halachmi, S., Bronson, R.T., Weinberg, R.A. (1994). Tumor spectrum analysis in p53-mutant mice. *Curr Biol* 4(1); 1–7.

Jain, A.K. and Barton, M.C. (2018). p53: emerging roles in stem cells, development and beyond. *Development* 145; 1–10.

Jenkins JR, Rudge K, Currie GA (1984) Cellular immortalization by a cDNA clone encoding the transformation-associated phosphoprotein p53. *Nature* 312; 651–654.

Jin, S., Antinore, M.J., Lung, F.D., Dong, X., Zhao, H., Fan, F., Colchagie, A.B., Blanck, P., Roller, P.P., Fornace, Jr. A.J., and Zhan, Q. (2000). The GADD45 Inhibition of Cdc2 Kinase Correlates with GADD45-mediated Growth Suppression. *The Journal of Biological Chemistry* vol. 275 no. 22; 16602–16608.

Jones, N. C., Lynn, M., Gaudenz, K., Sakai, D., Aoto, K., Rey, J. P., Glynn E. F., Ellington, L., Du, C., Dixon, J., Dixon, M. J., Trainor, P. (2008). Prevention of the neurocristopathy Treacher Collins syndrome through inhibition of p53 function. *Nature Medicine* 125; 133.

Jones, S. N., Roe, A. E., Donehower, L. A., and Bradley, A. (1995) Rescue of embryonic lethality in Mdm2-deficient mice by absence of p53. *Nature* 378; 207.

Kawamura, T., Suzuki, J., Wang, Y. V., Menendez, S., Morera, L. B., Raya, A., Wahl, G. M. and Belmonte, J. C. I. (2009). Linking the p53 tumour suppressor pathway to somatic cell reprogramming. *Nature* 460; 1140–1144.

Khoronenkova, S.V. and Dianov, G.L. (2012). Regulation of USP7/HAUSP in response to DNA damage Yet another role for ATM. *Cell Cycle* 11:13; 2409–2410.

Kim, E., and Deppert, W. (2004). Transcriptional Activities of Mutant p53: When Mutations Are More Than a Loss. *Journal of Cellular Biochemistry* 93; 878–886.

Ko, L.J. and Prives, C. (1996). p53: puzzle and paradigm. *Genes & Development* 10; 1054–1072.

Koenig, A., Linhart, T., Schlegemann, K., Reutlinger, K., Wegele, J., Adler, G., Singh, G., Hofmann, L., Kunsch, S., Buch, T., Schafer, E., Gress, T.M., Fernandez-Zapico, M.E., and Ellenrieder, V. (2010). NFAT-Induced Histone Acetylation Relay Switch Promotes c-Myc-Dependent Growth in Pancreatic Cancer Cells. *Gastroenterology* 138;1189–1199.

Komiya, Y. and Habas, R. (2008). Wnt signal transduction pathways. *Organogenesis* vol. 4 no. 2; 68–75.

Kool, M., Koster, J., Bunt, J., Hasselt, N.E., Lakeman, A., van Sluis, P., Troost, D., Meeteren, N.S., Caron, H.N., Cloos, J., et al. (2008). Integrated Genomics Identifies Five Medulloblastoma Subtypes with Distinct Genetic Profiles, Pathway Signatures and Clinicopathological Features. *Plos One* 3.

Korsmeyer, S.J., Wei1, M.C., Saito, M., Weiler, S., Oh, K.J., and Schlesinger, P.H. (2000). Pro-apoptotic cascade activates BID, which oligomerizes BAK or BAX into pores that result in the release of cytochrome c. *Cell Death and Differentiation* 7; 1166–1173.

Kress, M., May, E., Cassingena, R., and May, P. (1979). Simian virus 40- transformed cells express new species of proteins precipitable by anti-simian virus 40 tumor serum. *J. Virol.* 31; 472–483.

Kung, C.P. and Murphy, M.E. (2016) The role of the p53 tumor suppressor in metabolism and diabetes. *Journal of Endocrinology*.

Kunkele, A., De Preter, K., Heukamp, L., Thor, T., Pajtler, K.W., Hartmann, W., Mittelbronn, M., Grotzer, M.A., Deubzer, H.E., Speleman, F., Schramm, A., Eggert, A., and Schulte, J.H. (2012). Pharmacological activation of the p53 pathway by nutlin-3 exerts anti-tumoral effects in medulloblastomas. *Neuro-Oncology* 14(7); 859–869.

Kussie P. H., Gorina S., Marechal V., Elenbaas B., Moreau J., Levine A. J. and Pavletich N. P., (1996). Structure of the MDM2 oncoprotein bound to the p53 tumor suppressor transactivation domain. *Science* 274; 948–953.

Ladanyi, M., Cha, C., Lewis, R., Jhanwar, S.C., Huvos, A.G., Healey, J.H. (1993). MDM2 gene amplification in metastatic osteosarcoma. *Cancer Res* 53; 16–18.

Lambert, P.F., Kashanchi, F., Radonovich, M.F., Shiekhhattar, R., and Brady, J.N. (1998). Phosphorylation of p53 Serine 15 Increases Interaction with CBP. *The Journal of Biological Chemistry* vol. 273 no. 49; 33048–33053.

Lane, D.P., and Crawford, L.V. (1979). T antigen is bound to a host protein in SY40-transformed cells. *Nature* 278; 261–263.

Lane, D.P., Cheek, C.F., and Lain, S. (2010). p53-based Cancer Therapy. *Cold Spring Harb Perspect Biol*; 1–24.

Leach, F.S., Tokino, T., Meltzer, P., Burrell, M., Oliner, J.D., Smith, S., Hill, D.E., Sidransky, D., Kinzler, K.W., Vogelstein, B. (1993). p53 Mutation and MDM2 amplification in human soft tissue sarcomas. *Cancer Res* 53; 2231–2234.

- Leng, R.P., Lin, Y., Ma, W., Wu, H., Lemmers, B., Chung, S., Parant, J.M., Lozano, G., Hakem, R., and Benchimo, S. (2003). Pirh2, a p53-Induced Ubiquitin-Protein Ligase, Promotes p53 Degradation. *Cell* vol. 112; 779–791.
- Lengner, C.J., Steinman, H.A., Gagnon, J., Smith, T.W., Henderson, J.E., Kream, B.E., Stein, G.S., Lian, J.B., Jones, S.N. (2006) Osteoblast differentiation and skeletal development are regulated by Mdm2–p53 signaling. *Journal of Cell Biology* vol 172; 909–921.
- Li, M., Luo, J., Brooks, C.L., and Gu, W. (2002). Acetylation of p53 Inhibits Its Ubiquitination by Mdm2. *The Journal of Biological Chemistry*, vol 277 no. 52, issue of December 27; 50607– 50611.
- Lin, T., Chao, C., Saito, S., Mazur, S. J., Murphy, M. E., Appella, E., and Xu, Y. (2005). p53 induces differentiation of mouse embryonic stem cells by suppressing Nanog expression. *Nature Cell Biology* 7; 165–171.
- Linzer, D.I., and Levine, A.J. (1979). Characterization of a 54K dalton cellular SV40 tumor antigen present in SV40-transformed cells and uninfected embryonal carcinoma cells. *Cell* 17; 43–52.
- Liu, X., Kim, C.N., Yang, J., and Wang, X. (1996). Induction of Apoptotic Program in Cell-Free Extracts: Requirement for dATP and Cytochrome C. *Cell* vol. 86; 147–157.
- Lohrum, M.A.E., Ludwig, R.L., Kubbutat, M. H.G., Hanlon, M., and Vousden, K.H. (2003). Regulation of HDM2 activity by the ribosomal protein L11. *Cancer Cell* vol. 3; 577–587.
- Lu X., Ma O., Nguyen T. A., Jones S. N., Oren M. and Donehower L. A., (2007). The Wip1 Phosphatase acts as a gatekeeper in the p53-Mdm2 autoregulatory loop. *Cancer Cell* 12; 342–54.
- Machold, R. and Fishell, G. (2005). Math1 Is Expressed in Temporally Report Discrete Pools of Cerebellar Rhombic-Lip Neural Progenitors. *Neuron* vol. 48; 17–24.
- Malek, R., Matta, J., Taylor, N., Perry, M. E., and Mendrysa, S. M. (2011). The p53 Inhibitor MDM2 Facilitates Sonic Hedgehog-Mediated Tumorigenesis and Influences Cerebellar Foliation. *PLoS ONE*, 6 (3); 1-13.
- Marino, S., Vooijs, M., van Der Gulden, H., Jonkers, J., and Berns, A. (2000). Induction of medulloblastomas in p53-null mutant mice by somatic inactivation of Rb in the external granular layer cells of the cerebellum. *Genes and Development* 14; 994–1004.
- Marion, R. M., Strati, K., Li, H., Murga, M., Blanco, R., Ortega, S., Fernandez Capetillo, O., Serrano, M., and Blasco, M. A. (2009). A p53-mediated DNA damage response limits reprogramming to ensure iPSC cell genomic integrity. *Nature* 460; 1149–1153.

Martinez-Alvarez, C., Blanco, M. J., Perez, R., Rabadan, M. A., Aparicio, M., Resel, E., Martinez, T., and Nieto, M. A. (2004). Snail family members and cell survival in physiological and pathological cleft palates. *Developmental Biology* 265; 207–218.

Marzban, H., Del Bigio, M. R., Alizadeh, J., Ghavami, S., Zachariah, R. M., & Rastegar, M. (2015). Cellular commitment in the developing cerebellum. *Frontiers in Cellular Neuroscience* 8; 1-26.

MacPherson, D., Kim, J., Kim, T., Rhee, B.K., Van Oostrom, C.T., DiTullio, R.A., Venere, M., Halazonetis, T.D., Bronson, R., De Vries, A., et al. (2004). Defective apoptosis and B-cell lymphomas in mice with p53 point mutation at Ser 23. *EMBO J.* 23; 3689–3699.

McLure, K.G., Lee, P.W.K. (1998) How p53 binds DNA as a tetramer. *The EMBO Journal* vol.17 no.12; 3342–3350.

Meek, D.W. and Anderson, C.W. (2009). Posttranslational Modification of p53: Cooperative Integrators of Function. *Cold Spring Harb Perspect Biol*; 1–16.

Melero, J.A., Stitt, D.T., Mangel, W.F., and Carroll, R.B. (1979). Identification of new polypeptide species (48-55K) immunoprecipitable by antiserum to purified large T antigen and present in SV40-infected and -transformed cells. *Virology* 93; 466–480.

Mendrysa, S.M. and Perry, M.E. (2000). The p53 Tumor Suppressor Protein Does Not Regulate Expression of Its Own Inhibitor, MDM2, Except under Conditions of Stress. *Molecular and Cellular Biology* vol. 20 no. 6; 2023–2030.

Mendrysa, S.M., McElwee, M.K., Michalowski, J., O’Leary, K.O., Young, K.M., Perry, M.E. (2003). mdm2 Is Critical for Inhibition of p53 during Lymphopoiesis and the Response to Ionizing Irradiation. *Molecular and Cellular Biology* vol 23; 462–473.

Miyashita, T., and Reed, J.C. (1995). Tumor Suppressor p53 is a Direct Transcriptional Activator of the Human Bax Gene. *Cell* 80; 293–299.

Momand, J., Zambetti, G.P., Olson, D.C., George, D., and Levine, A.J. (1992). The mdm-2 oncogene product forms a complex with the p53 protein and inhibits p53-mediated transactivation. *Cell* 69; 1237–1245.

Montes de Oca Luna, R., Wagner, D.S., and Lozano, G. (1995). Rescue of early embryonic lethality in mdm2-deficient mice by deletion of p53. *Nature* 378; 203–206.

Moniz, H., Gastou, M., Leblanc, T., Hurtaud, C., Cretien, A., Lecluse, Y., Raslova, H., Larghero, J., Croisille, L., Faubladier, M., Bluteau, O., Lordier, L., Tchernia, G., Vainchenker, W., Mohandas, N., Da Costa, L. (2012). Primary hematopoietic cells from DBA patients with mutations in RPL11 and RPS19 genes exhibit distinct erythroid phenotype in vitro. *Cell Death and Disease*.

- Muller, M., Wilder, S., Bannasch, D., Israeli, D., Lehlbach, K., Li-Weber, M., Friedman, S. L., Galle, P. R., Stremmel, W., Oren, M., and Krammer, P.H. (1998). p53 activates the CD95 (APO-1/Fas) gene in response to DNA damage by anticancer drugs. *Journal of Experimental Medicine* 188; 2033–2045.
- Mulligan, K.A. and Cheyette, B.N.R. (2012). Wnt Signaling in Vertebrate Neural Development and Function. *J Neuroimmune Pharmacol* vol. 7 no. 4; 774–787.
- Muzio, M. (1998). Signaling by proteolysis: death receptors induce apoptosis. *Int. J. Clin. Lab. Res.* 28; 141–147.
- Nakano, K. and Vousden, K.H. (2001). PUMA, a Novel Proapoptotic Gene, Is Induced by p53. *Molecular Cell* vol. 7; 683–694.
- Nakayama, T., Toguchida, J., Wadayama, B., Kanoe, H., Kotoura, Y., Sasaki, M.S. (1995). MDM2 gene amplification in bone and soft-tissue tumors: Association with tumor progression in differentiated adipose-tissue tumors. *Int J Cancer* 64; 342–346.
- Northcott, P.A., Korshunov, A., Witt, H., Hielscher, T., Eberhart, C.G., Mack, S., Bouffet, E., Clifford, S.C., Hawkins, C.E., French, P., et al. (2011a). Medulloblastoma comprises four distinct molecular variants. *J. Clin. Oncol. Off. J. Am. Soc. Clin. Oncol.* 29; 1408–1414.
- Northcott, P.A., Hielscher, T., Dubuc, A., Mack, S., Shih, D., Remke, M., Al-Halabi, H., Albrecht, S., Jabado, N., Eberhart, C.G., et al. (2011b). Pediatric and adult sonic hedgehog medulloblastomas are clinically and molecularly distinct. *Acta Neuropathol. (Berl.)* 122; 231–240.
- O’Farrell, T.J., Ghosh, P., Dobashi, N., Sasaki, C.Y. and Longo, D.L. (2004) Comparison of the Effect of Mutant and Wild-Type p53 on Global Gene Expression. *Cancer Research* 64; 8199–8207.
- O’Keefe, K., Li, H., and Zhang, Y. (2003). Nucleocytoplasmic shuttling of p53 is essential for MDM2-mediated cytoplasmic degradation but not ubiquitination. *Mol. Cell. Biol.* 23; 6396–6405.
- Oda, E., Ohki, R., Murasawa, H., Nemoto, J., Shibue, T., Yamashita, T., Tokino, T., Taniguchi, T., Tanaka, N. (2000). Noxa, a BH3-only member of the bcl-2 family and candidate mediator of p53-induced apoptosis. *Science* vol. 288 issue 5468; 1053–1058.
- Oliner, J.D., Kinzler, K.W., Meltzer, P.S., George, D.L., Vogelstein, B. (1992). Amplification of a gene encoding a p53-associated protein in human sarcomas. *Nature* 358; 80–83.
- Oliner, J.D., Saiki, A.Y., Caenepeel, S. (2016). The Role of MDM2 Amplification and Overexpression in Tumorigenesis. *Cold Spring Harb Perspect Med*; 1–15.

Oren, M. and Rotter, V. (2010). Mutant p53 Gain-of-Function in Cancer. *Cold Spring Harb Perspect Biol*; 2; a001107.

Ovchinnikov, D. (2009) Alcian Blue/Alizarin Red Staining of Cartilage and Bone in Mouse. *Cold Spring Harbor Protocols* vol. 4 issue 3; 1-2.

Pant, V., Xiong, S., Jackson, J.G., et al. (2013). The p53-Mdm2 feedback loop protects against DNA damage by inhibiting p53 activity but is dispensable for p53 stability, development, and longevity. *Genes Dev.* 27, 1857–1867.

Parada, L.F., Land, H., Weinberg, R.A., Wolf, D., and Rotter, V. (1984). Cooperation between gene encoding p53 tumour antigen and ras in cellular transformation. *Nature* 312; 649–651.

Pfaff, E., Remke, M., Sturm, D., Benner, A., Witt, H., Milde, T., O. von Bueren, A., Wittmann, A., Schottler, A., Jorch, N., Graf, N., Kulozik, A.E., Witt, O., Scheurlen, W., von Deimling, A., Rutkowski, A., Taylor, M.D., Tabori, U., Lichter, P., Korshunov, A., and Pfister, S.M. (2010). TP53 Mutation Is Frequently Associated With CTNNB1 Mutation or MYCN Amplification and Is Compatible With Long-Term Survival in Medulloblastoma. *Journal of Clinical Oncology* 28, no. 35; 5188–5196.

Puri, L. and Saba, J. (2014). Getting a Clue from 1q: Gain of Chromosome 1q in Cancer. *Journal of Cancer Biology and Research* vol. 2 no. 3; 1–5.

Qin, J.J., Nag, S., Wang, W., Zhou, J., Zhang, W.D., Wang, H., and Zhang, R. (2014a). NFAT as cancer target: Mission possible?. *Biochimica et Biophysica Acta* 1846; 297–311.

Qin, J.J., Wang, W., Voruganti, S., Wang, H., Zhang, H.D., and Zhang, R. (2014b). Identification of a new class of natural product MDM2 inhibitor: In vitro and in vivo anti-breast cancer activities and target validation. *Oncotarget* vol. 6 no.5; 2623–2640.

Qin, J.J., Wang, W., Voruganti, S., Wang, H., Zhang, W.D., and Zhang, R. (2015). Inhibiting NFAT1 for breast cancer therapy: New insights into the mechanism of action of MDM2 inhibitor JapA. *Oncotarget* vol. 6 no. 32; 33106–33119.

Ramaswamy, V., Northcott, P.A., and Taylor, M.D. (2011). FISH and chips: the recipe for improved prognostication and outcomes for children with medulloblastoma. *Cancer Genet.* 204; 577–588.

Reed, S. and Quelle, D.E. (2015) p53 Acetylation: Regulation and Consequences. *Cancers* vol. 7; 30–69.

Remke, M., Hielscher, T., Northcott, P.A., Witt, H., Ryzhova, M., Wittmann, A., Benner, A., von Deimling, A., Scheurlen, W., Perry, A., Croul, S., Kulozik, A.E., Lichter, P., Taylor, M.D., Pfister, S.M., and Korshunov, A. (2011). Adult Medulloblastoma Comprises Three Major Molecular Variants. *Journal of Clinical Oncology* vol. 29 no. 19; 2717–2723.

Rinon, A., Lazar, A., Marshall, H., Buchmann-Moller, S., Neufeld, A., Elhanany-Tamir, H., Taketo, M.M., Sommer, L., Krumlauf, R., and Tzahor, E. (2007). Cranial neural crest cells regulate head muscle patterning and differentiation during vertebrate embryogenesis. *Development* 134; 3065–3075.

Rinon, A., Molchadsky, A., Nathan E., Yovel, G., Rotter, V., Sarig, R., Tzahor, E. (2011) p53 coordinates cranial neural crest cell growth and epithelial-mesenchymal transition/delamination processes. *Development* 138; 1827–1838

Roemer, K. (1999). Mutant p53: Gain-of-Function Oncoproteins and Wild-Type p53 Inactivators. *Biological Chemistry* vol. 380 issue 7-8; 879–887.

Roussel, M. F. and Hatten, M. E. (2011). Cerebellum: Development and Medulloblastoma. *Current Topic in Developmental Biology*, 94; 235–282.

Roxburgh, P., Hock, A.K., Dickens, M.P., Mezna, M., Fischer, P.M., Vousden, K.H. (2012). Small molecules that bind the Mdm2 RING stabilize and activate p53. *Carcinogenesis* vol. 33, Issue 4; 791–798.

Rudin, C.M., Hann, C.L., Laterra, J., Yauch, R.L., Callahan, C.A., Fu, L., Holcomb, T., Stinson, J., Gould, S.E., Coleman, B., LoRusso, P.M., Von Hoff, D.D., de Sauvage, F.J., Low, J.A. (2009). Treatment of medulloblastoma with hedgehog pathway inhibitor GDC-0449. *N Engl J Med* 361; 1173–1178.

Saylor III, R.L., Sidransky, D., Friedman, H.S., Bigner, S.H., Bigner, D.D., Vogelstein, B., Brodeur, G.M. (1991). Infrequent p53 Gene Mutations in Medulloblastomas. *Cancer Research*, 51; 4721–4723.

Schmid, P., Lorenz, A., Hameister, H., and Montenarh, M. (1991). Expression of p53 during mouse embryogenesis. *Development* 113; 857–865.

Schon, O., Friedler, A., Bycroft, M., Freund, S.M.V., and Fersht, A.L. (2002). Molecular Mechanism of the Interaction between MDM2 and p53. *Journal of Molecular Biology* 323; 491–501.

Schwalbe, E.C., Lindsey, J.C., Nakjang, S., Crosier, S., Smith, A.J., Hicks, D., Rafiee, G., Hill, R.M., Iliasova, A., Stone, T., Pizer, B., Michalski, A., Joshi, A., Wharton, S.B., Jacques, T.S., Bailey, S., Williamson, D., and Clifford, S.C. (2017). Novel molecular subgroups for clinical classification and outcome prediction in childhood medulloblastoma: a cohort study. *Lancet Oncology* vol. 18; 958–971.

- Scuccimarri, R., and Rodd, C. (1998). Thyroid abnormalities as a feature of DiGeorge syndrome: a patient report and review of the literature. *J. Pediatr. Endocrinol. Metab.* 11; 273–276.
- Selleck, M.A.J. and Bronner-Fraser, M. (1995). Origins of the avian neural crest: the role of neural plate-epidermal interactions. *Development* 121; 525–538.
- Semi, K., Matsuda, Y., Ohnishi, K., and Yamada, Y. (2013). Cellular reprogramming and cancer development. *Int. J. Cancer* 132; 1240–1248.
- Shangary, S., Qin, D., McEachern, D., Liu, M., Miller, R.S., Qiu, S., Nikolovska-Coleska, Z., Ding, K., Wang, G., Chen, J., Bernard, D., Zhang, J., Lu, Y., Gu, Q., Shah, R.B., Pienta, K.J., Ling, X., Kang, S., Guo, M., Sun, Y., Yang, D., and Wang, S. (2008). Temporal activation of p53 by a specific MDM2 inhibitor is selectively toxic to tumors and leads to complete tumor growth inhibition. *PNAS* vol. 105 no. 10; 3933–3938.
- Shaulsky, G., Goldfinger, N., Peled, A., Rotter, V. (1991). Involvement of wild-type p53 in pre-B-cell differentiation in vitro. *Proc. Natl. Acad. Sci. USA* vol. 88; 8982–8986.
- Shieh, S.Y., Ikeda, M., Taya, Y., and Prives, C. (1997). DNA Damage-Induced Phosphorylation of p53 Alleviates Inhibition by MDM2. *Cell* vol. 91; 325–334.
- Silva, J., Nichols, J., Theunissen, T. W., Guo, G., van Oosten, A. L., Barrandon, O., Wray, J., Yamanaka, S., Chambers, I., and Smith, A. (2009). Nanog is the gateway to the pluripotent ground state. *Cell* 138; 722–737.
- Singh, V.K., Kalsan, M., Kumar, N., Saini, A, and Chandra, R. (2015). Induced pluripotent stem cells: applications in regenerative medicine, disease modeling, and drug discovery. *Frontiers in Cell and Developmental Biology* vol. 3; 1–18.
- Slack, A., Chen, Z., Tonelli, R., Pule, M., Hunt, L., Pession, A., and Shohet, J.M. (2005). The p53 regulatory gene MDM2 is a direct transcriptional target of MYCN in neuroblastoma. *Proc. Natl. Acad. Sci.* 102, 731–736.
- Slade, I., Murray, A., Hanks, S., Kumar, A., Walker, L., Hargrave, D., Douglas, J., Stiller, C., Izatt, L., and Rahman, N. (2011). Heterogeneity of familial medulloblastoma and contribution of germline PTCH1 and SUFU mutations to sporadic medulloblastoma. *Fam Cancer* vol. 10; 337–342.
- Sluss, H.K., Armata, H., Gallant, J., and Jones, S.N. (2004). Phosphorylation of serine 18 regulates distinct p53 functions in mice. *Mol. Cell. Biol.* 24; 976–984.
- Smith, A.E., Smith, R., and Paucha, E. (1979). Characterization of different tumor antigens present in cells transformed by simian virus 40. *Cell* 18; 335–346.

Soriano, P. (1999). Generalized lacZ expression with the ROSA26 Cre reporter strain. *Nature Genetics* vol. 21; 70–71.

Srivastava, S., Zou, Z., Pirollo, K., Blattner, W., and Chang, E. (1990) Germ-line transmission of a mutated p53 gene in a cancer-prone family with Li–Fraumeni syndrome. *Nature* vol. 348; 747–749.

Suzuki, A., Sangani, D.R., Ansari, A., Iwata, J. (2015) Molecular Mechanisms of Midfacial Developmental Defects. *Developmental Dynamics* 245; 276–293.

Takahashi, M; Buma, Y; Hiai, H; Takahashi, M. *Oncogene* (1989) Isolation of ret proto-oncogene cDNA with an amino-terminal signal sequence. *Oncogene* vol.4(6); 805–806.

Tang Y., Zhao W., Chen Y., Zhao Y. and Gu W. (2008). Acetylation is indispensable for p53 activation. *Cell* 133, 612-26.

Tao, W. and Levine, A.J. (1999). Nucleocytoplasmic shuttling of oncoprotein Hdm2 is required for Hdm2-mediated degradation of p53. *Proc. Natl. Acad. Sci. USA* vol. 96; 3077 – 3080.

Taylor, M.D., Northcott, P.A., Korshunov, A., Remke, M., Cho, Y., Clifford, S.C., Eberhart, C.G., Parsons, D.W., Rutkowski, S., Gajjar, A., Ellison, D.W., Lichten, P., Gilbertson, R.J., Pomeroy, S.L., Kool, M., Pfister, S.M. (2012). Molecular subgroups of medulloblastoma: the current consensus. *Acta Neuropathol* 123; 465–472

Toledo, F. and Wahl, G.M. (2006). Regulating the p53 pathway: in vitro hypotheses, in vivo veritas. *Nature Reviews Cancer* vol. 6; 909–923.

Tollini, L.A., Jin, A., Park, J., et al. (2014). Regulation of p53 by Mdm2 E3 ligase function is dispensable in embryogenesis and development, but essential in response to DNA damage. *Cancer Cell* 26; 235–247.

Trainor, P.A. (2010) Craniofacial Birth Defects: The Role of Neural Crest Cells in the Etiology and Pathogenesis of Treacher Collins Syndrome and the Potential for Prevention. *American Journal of Medical Genetics Part A*; 2984-2994.

Tzahor, E., Kempf, H., Mootosamy, R. C., Poon, A. C., Abzhanov, A., Tabin, C. J., Dietrich, S. and Lassar, A. B. (2003). Antagonists of Wnt and BMP signaling promote the formation of vertebrate head muscle. *Genes Dev.* 17; 3087–3099.

Utikal, J., Polo, J. M., Stadtfeld, M., Maherali, N., Kulalert, W., Walsh, R. M., Khalil, A., Rheinwald, J. G., and Hochedlinger, K. (2009). Immortalization eliminates a roadblock during cellular reprogramming into iPS cells. *Nature* 460; 1145–1148.

Valdez, B.C., Henning, D., So, R.B., Dixon, J., Dixon, M.J., (2004). The Treacher Collins syndrome (TCOF1) gene product is involved in ribosomal DNA gene transcription by interacting with upstream binding factor. *Proc. Natl. Acad. Sci. USA* 101; 10709–10714.

Van Maerken, T., Rihani, A., Van Goethem, A., De Paepe, A., Speleman, F., and Vandesompele, J. (2014). Pharmacologic activation of wild-type p53 by nutlin therapy in childhood cancer. *Cancer Lett* 344; 157–165.

Van Nostrand, J.L., Brady, C.A., Jung, H., Fuentes, D.R., Kozak, M.M., Johnson, T.M., Lin, C.Y., Lin, C.J., Swiderski, D.L., Vogel, H., Bernstein, J.A., Attie-Bitach, T., Chang, C.P., Wysocka, J., Martin, D.M., Attardi L.A. (2014) Inappropriate p53 activation during development induces features of CHARGE syndrome. *Nature* vol 000; 1–19.

Van Nostrand, J.L and Attardi, L.D. (2014). Guilty as CHARGED: p53's expanding role in disease. *Cell Cycle*, vol. 13 no. 24; 3798–3807.

Vaseva, A.V., and Moll, U.M. (2009). The mitochondrial p53 pathway. *Biochimica et Biophysica Acta* 1787; 414–420.

Vassilev, L.T., Vu, B.T., Graves, B., Carvajal, D., Podlaski, F., Filipovic, Z, Kong, N., Kammlott, U., Lukacs, C., Klein, C., Fotouhi, N, and Liu, E.A. (2004). In Vivo Activation of the p53 Pathway by Small-Molecule Antagonists of MDM2. *Science* vol. 303 issue 5659; 844–848.

Vaziri, Sani F., Hallberg, K., Harfe, B. D., McMahon, A. P., Linde, A., and Gritli-Linde, A. (2005). Fate-mapping of the epithelial seam during palatal fusion rules out epithelial-mesenchymal transformation. *Developmental Biology* 285; 490–495.

Vega-Lopez, G.A., Cerrizuela, S., Tribulo, C., Aybar, M.J. (2018). Neurocristopathies: New insights 150 years after the neural crest discovery. *Developmental Biology*.

Vizcaino, C., Mansilla, S., and Portugal, J. (2015). Sp1 transcription factor: A long-standing target in cancer chemotherapy. *Pharmacology & Therapeutics* 152; 111–124.

Vlachos, A., Ball, S., Dahl, N., Alter, B.P., Sheth, S., Ramenghi, U., Meerpohl, J., Karlsson, S., Liu, J.M., Leblanc, T., Paley, C., Kang, E.M., Leder, E.J., Atsidaftos, E., Shimamura, A., Bessler, M., Glader, B; and Lipton, J.M. (2008). Diagnosing and treating Diamond Blackfan anaemia: results of an international clinical consensus conference. *British Journal of Haematology* 142; 859 – 876.

Waga, S., Hannon, G.J., Beach, D. and Stillman, B. (1994) The p21 inhibitor of cyclin-dependent kinases controls DNA replication by interaction with PCNA. *Nature* vol 369; 574–578

- Walker, D.R., Bond, J.P., Tarone, R.E., Harris, C.C., Makalowski, W., Boguski, M.S., and Greenblatt, M.S. (1999). Evolutionary conservation and somatic mutation hotspot maps of p53: correlation with p53 protein structural and functional features. *Oncogene* 19; 211–218.
- Wallace, V. A. (1999). Purkinje-cell-derived Sonic hedgehog regulates granule neuron precursor cell proliferation in the developing mouse cerebellum. *Current Biology*, 9:8; 445–448.
- Watanabe, Y., Zaffran, S., Kuroiwa, A., Higuchi, H., Ogura, T., Harvey, R.P., Kelly, R.G., Buckingham, M. (2012). Fibroblast growth factor 10 gene regulation in the second heart field by Tbx1, Nkx2-5, and Islet1 reveals a genetic switch for down-regulation in the myocardium. *Proc Natl Acad Sci USA* 109(45); 18273–18280.
- Watkins-Chow, D.E., Cooke, J., Pidsley, R., Edwards, A., Slotkin, R., Leeds, K.E., Mullen, R., Baxter, L.L., Campbell, T.G., Salzer, M.C., Biondini, L., Gibney, G., Phan Dinh Tuy, F., Chelly, J., Morris, H.D., Riegler, J., Lythgoe, M.F., Arkell, R.M., Loreni, F., Flint, J., Pavan, W.J., Keays, D.A. (2013). Mutation of the Diamond-Blackfan Anemia Gene Rps7 in Mouse Results in Morphological and Neuroanatomical Phenotypes. *PLOS Genetics* volume 9 issue 1; e1003094.
- Weber, J.D., Taylor, L.J., Roussel, M.F., Sherr, C.J., and Bar-Sagi, D. (1999). Nucleolar Arf sequesters Mdm2 and activates p53. *Nature Cell Biology*, Vol 1, 20 – 27
- White, J.J. and Sillitoe, R.V. (2013). Development of the cerebellum: from gene expression patterns to circuit maps. *WIREs Dev Biol* 2;149–164.
- Williams, A.B. and Schumacher, B. (2016) p53 in the DNA damage repair response process. *Cold Spring Harb Perspect Med*.
- Willis, A., Jung E.J., Wakefield, T., Chen, X. (2004) Mutant p53 exerts a dominant negative effect by preventing wild-type p53 from binding to the promoter of its target genes. *Oncogene* vol 23; 2330–2338.
- Wolff, S., Erster, S., Palacios, G., and Moll, U.M. (2008). p53's mitochondrial translocation and MOMP action is independent of Puma and Bax and severely disrupts mitochondrial membrane integrity. *Cell Research* 18; 733–744.
- Wu, X., Bayle, J.H., Olson, D., and Levine, A.J. (1993). The p53-mdm-2 autoregulatory feedback loop. *Genes Dev.* 7; 1126–1132.
- Wu, G. S., Burns, T. F., McDonald, E. R., Jiang, W., Meng, R., Krantz, I. D., Kao, G., Gan, D. D., Zhou, J. Y., Muschel, R., Hamilton, S.R., Spinner, N.B., Markowitz, S., Wu, G., and El-Deiry, W.S. (1997). KILLER/DR5 is a DNA damage-inducible p53-regulated death receptor gene. *Nature Genetics* 17; 141–143.

Xiao, G., Chicas, A., Olivier, M., Taya, Y., Tyagi, S., Kramer, F.R., and Bargonetti, J. (2000). A DNA Damage Signal Is Required for p53 to Activate gadd45. *Cancer Research* vol. 60; 1711–1719.

Xu, X., Han, J., Ito, Y., Bringas Jr. P., Urata, M.M., Chai, Y. (2006) Cell autonomous requirement for Tgfbr2 in the disappearance of medial edge epithelium during palatal fusion. *Developmental Biology* 297; 238–248.

Yang, Y., Ludwig, R.L., Jensen, J.P., Pierre, S.A., Medaglia, M.V., Davydov, I.V., Safiran, Y.J., Oberoi, P., Kenten, J.H., Phillips, A.C., Weissman, A.M., and Vousden, K.H. (2005). Small molecule inhibitors of HDM2 ubiquitin ligase activity stabilize and activate p53 in cells. *Cancer Cell* vol. 7; 547–559.

Yi, L., Lu, C., Hu, W., Sun, Y., and Levine, A. J. (2012). Multiple roles of p53-related pathways in somatic cell reprogramming and stem cell differentiation. *Cancer Research* 72; 5635–5645.

Young, R. A. (2011). Control of the embryonic stem cell state. *Cell* 144; 940–954.

Yu, J., Zhang, L., Hwang, P.M., Kinzler, K.W., and Vogelstein, B. (2001). PUMA Induces the Rapid Apoptosis of Colorectal Cancer Cells. *Molecular Cell* vol. 7; 673–682.

Yu, J., Wang, Z., Kinzler, K.W., Vogelstein, B., and Zhang, L. (2003). PUMA mediates the apoptotic response to p53 in colorectal cancer cells. *PNAS* vol. 100 no. 4; 1931–1936.

Zambetti, G.P., J. Bargonetti, K. Walker, C. Prives, and A.J. Levine. 1992. Wild-type p53 mediates positive regulation of gene expression through a specific DNA sequence element. *Genes & Development* 6; 1143–1152.

Zhan, Q., Antinore, M.J., Wang, X.W., Carrier, F., Smith, M.L., Harris, C.C., and Fornace, Jr. A.J. (1999). Association with Cdc2 and inhibition of Cdc2/Cyclin B1 kinase activity by the p53-regulated protein Gadd45. *Oncogene* vol. 18; 2892–2900.

Zhang, J., Yan, W., and Chen, X. (2006). p53 is required for nerve growth factor-mediated differentiation of PC12 cells via regulation of TrkA levels. *Cell Death Differ.* 13; 2118–2128.

Zhang, X., Zhang, Z., Cheng, J., Li, M., Wang, W., Xu, W., Wang, H., and Zhang, R. (2012). Transcription Factor NFAT1 Activates the mdm2 Oncogene Independent of p53. *The Journal of Biological Chemistry* vol. 286 no. 36; 30468–30476.

Zhou, B.P., Liao, Y., Xia, W., Zou, Y., Spohn, B., Hung, M.-C., Zhou, B.P., Liao, Y., Xia, W., Zou, Y., et al. (2001). HER-2/neu induces p53 ubiquitination via Akt- mediated MDM2 phosphorylation, HER-2/neu induces p53 ubiquitination via Akt- mediated MDM2 phosphorylation. *Nat. Cell Biol.* 3; 973–982.

Zhukova, N., Ramaswamy, V., Remke, M., Pfaff, E., Shih, D.J.H., Martin, D.C., Castelo-Branco, P., Baskin, B., Ray, P.N., Bouffet, E., von Bueren, A.O., Jones, D.T.W., Northcott, P.A., Kool, M., Sturm, D., Pugh, T.J., Pomeroy, S.L., Cho, Y.K., Pietsch, T., Gessi, M., Rutkowski, S., Bognar, L., Klekner, A., Cho, B.K., Kim, S.K., Wang, K.C., Eberhart, C.G., Fevre-Montange, M., Fouladi, M., French, P.J., Kros, M., Grajkowska, W.A., Gupta, N., Weiss, W.A., Hauser, P., Jabado, N., Jouvett, A., Jung, S., Kumabe, T., Lach, B., Leonard, J.R., Rubin, J.B., Liau, L.M., Massimi, L., Pollack, I.F., Ra, Y.S., Van Meir, E.G., Zitterbart, K., Schuller, U., Hill, R.M., Lindsey, J.C., Schwalbe, Ed.C., Bailey, S., Ellison, D.W., Hawkins, C., Malkin, D., Clifford, S.C., Korshunov, A., Pfister, S., Taylor, M.D., and Tabor, U. (2013). Subgroup-Specific Prognostic Implications of TP53 Mutation in Medulloblastoma. *Journal of Clinical Oncology* vol. 31 no. 23; 2927–2937.

Zurawel, R.H., Chiappa, S.A., Allen, C., and Raffel, C. (1998). Sporadic medulloblastomas contain oncogenic beta-catenin mutations. *Cancer Research* 58; 896–899.

## VITA

Joselyn Cruz Cruz was born on November 20, 1989 in Humacao, Puerto Rico to Wanda Teresa Cruz Torres and Jose Luis Cruz Rivas. She attended University of Puerto Rico at Humacao completing her Bachelor of Science degree with honors in General Biology with a minor in Microbiology in May 2012. Then, she completed 1 year of research under the guidance of Dr. John Frelinger at University of Rochester, New York as part of the PREP program. Joselyn joined Purdue University Interdisciplinary Life Sciences (PULSe) program in August 2013 to pursue a doctorate degree in molecular signaling and cancer biology. She joined Dr. Mendrysa's lab in the Basic Medical Sciences department at the College of Veterinary Medicine in June 2014. Through the course of her graduate school years, Joselyn investigated the role of MDM2 and p53 pathway in cerebellar and embryonic development publishing her work at a peer-review journal under the mentorship of Dr. Mendrysa. Upon completion of her Ph.D., Joselyn will pursue a postdoctoral position and then transition into a scientist position in the pharmaceutical industry.